GISERA
Gas Industry Social and Environmental Research Alliance

Improving groundwater models to better represent coal seam gas extraction impacts in the Namoi region

Final report for Project W9
31 May 2019

Nicholas Lupton[1], Sreekanth Janardhanan[2], Luke Connell[1], Trevor Pickett[2]

[1] Onshore Gas, CSIRO Energy, Clayton, Victoria

[2]Groundwater and Resources, CSIRO Land and Water, Dutton Park, Queensland

CSIRO Report Number EP193251

GISERA, GPO Box 2583, Brisbane QLD 4001, Australia

Document control

Final report
31 May 2019

Version	Date	Description	Author	Approved
1	31/05/2019	Final Report	NL, SJ, LC, TP	Initials

Improving groundwater models to better represent coal seam gas extraction impacts in the Namoi region

ISBN (print): 978-1-4863-1281-8

ISBN (online): 978-1-4863-1282-5

The Gas Industry Social and Environmental Research Alliance (GISERA) undertakes publicly-reported research that addresses the socio-economic and environmental impacts of Australia's natural gas industries.
GISERA was co-founded by CSIRO and Australia Pacific LNG in July 2011. For further information visit gisera.csiro.au.

Citation

Lupton, N., Janardhanan, S., Connell, L.D., Pickett, T. (2019) Improving groundwater models to better represent coal seam gas extraction impacts in the Namoi region. May 2019. CSIRO, Canberra.

Copyright

© 2019 CSIRO To the extent permitted by law, all rights are reserved and no part of this publication covered by copyright may be reproduced or copied in any form or by any means except with the written permission of CSIRO.

Important Disclaimer

The partners in GISERA advise that the information contained in this publication comprises general statements based on scientific research. The reader is advised and needs to be aware that such information may be incomplete or unable to be used in any specific situation. No reliance or actions must therefore be made on that information without seeking prior expert professional, scientific and technical advice. To the extent permitted by law, GISERA (including its partners, employees and consultants) excludes all liability to any person for any consequences, including but not limited to all losses, damages, costs, expenses and any other compensation, arising directly or indirectly from using this publication (in part or in whole) and any information or material contained in it.

Contents

List of Tables

List of Figures

Acknowledgements

This report was supported by the Gas Industry Social and Environmental Research Alliance (GISERA). GISERA is a collaboration between CSIRO, Commonwealth and state governments and industry established to undertake publicly-reported independent research. The purpose of GISERA is to provide quality assured scientific research and information to communities living in gas development regions focusing on social and environmental topics including: groundwater and surface water, biodiversity, land management, the marine environment, and socio-economic impacts. The governance structure for GISERA is designed to provide for and protect research independence and transparency of research. Visit gisera.csiro.au for more information about GISERA's governance structure, projects and research findings.

The authors wish to thank Dennis Gonzalez for assistance providing updated mapping for the project.

Executive summary

Groundwater impact is a key issue of concern with coal seam gas (CSG) development. In the NSW CSG research interest GISERA stakeholder survey, groundwater levels were identified as the top ranked research topic. This document presents a report on GISERA project W9 "Improving groundwater models to better represent coal seam gas extraction impacts in the Namoi region." This project investigated the representation of the effects of CSG production in groundwater impact modelling of the Namoi region.

The project implemented an approach to improve the representation of CSG groundwater impacts into MODFLOW, the software package used for groundwater impact modelling in the Namoi sub-region. The methodology originally presented by Herckenrath et al. (2015) and applied to CSG related regional groundwater modelling of the Surat Basin was investigated and adapted for the site-specific conditions of the Namoi sub-region. The approach was based on CSG production scenarios specific to the Namoi sub-region, modelled using a reservoir simulator with detailed process descriptions. These detailed simulations were used to identify approximate relationships between key driving variables suitable for use with MODFLOW and its representation of unsaturated flow.

Simulations using the Namoi CSG model developed in the SIMED reservoir simulator explored the relationships between key driving variables of CSG production such as pressure, saturation and well rates. Simulations examined the impact of well pressure interference, size of the CSG well field, grid block size, and vertical and horizontal upscaling on these relationships, assessing their suitability for representing CSG reservoir flow behaviour in regional groundwater models. Based on these investigations, in a similar finding to Herckenrath et al. (2015), the intra-grid block water saturation versus pressure relationship (S_w vs P) was identified as the best approach for implementation into the MODFLOW model developed in the GISERA companion project W7 - Impacts of depressurisation on Great Artesian Basin (GAB) flux. The GAB flux groundwater model encompasses the areas of the Namoi sub-region proposed for future CSG development.

The S_w vs P relationship was modelled using the van Genuchten (1980) equation and implemented in a version of MODFLOW-USG with dual-phase functionality via the Richards equation and van Genuchten formulations. Multiple approaches were investigated for modelling S_w vs P data, and for implementation into MODFLOW. Prior to implementation in the GAB flux groundwater model, the approaches were compared for performance with respect to improving MODFLOW predictions of water production and pressure drawdown.

Single and dual-phase predictions were compared across identical CSG well field models constructed in MODFLOW and SIMED. After implementing dual-phase functionality in MODFLOW, comparisons demonstrated improvements over single-phase predictions of up to 77% for drawdown in the CSG target layer, and 63% for water production. However, predictions of water production are sensitive to simulation duration, upscaling and dual-phase property values. The results indicated it is important to include dual-phase functionality in all cells of the regional model that may experience desaturation. Importantly, implementing S_w vs P relationships derived from fine scale CSG reservoir simulations into spatially coarse MODFLOW models reduces the improved accuracy obtained from dual-phase functionality. When deploying into a vertically upscaled

MODFLOW model, use of van Genuchten parameters, derived only from CSG modelling of the target coal seam, provided the greatest improvement in predictive accuracy.

Modelling of dual-phase flow in Monte Carlo simulations completed on the MODFLOW GAB flux groundwater model did not result in significantly altered drawdown or flux change predictions for the main GAB aquifer of interest in the Namoi sub-region, the Pilliga Sandstone. The presence of aquitard layers between the CSG target and overlying aquifers may dampen the impact of modelling dual-phase flow, suggesting that for the region and aquifer of interest addressed in the GAB flux model, the single-phase model results are comparable. Within the Maules Creek layer, which contains the primary CSG production target, modelling dual-phase flow results in lower drawdown predictions and a more precise indication of the effects of well drawdown interference in the vicinity of the CSG well field. At a greater distance from the CSG wells there is no significant difference between the predictions of single and dual-phase model runs. Improvements to the accuracy of drawdown predictions in the CSG target layers establish the importance of utilising this approach in regions where geological conditions may imply greater communication between underlying and overlying strata.

1 Introduction

Coals seam gas production involves the extraction of water from a coal seam through CSG production wells in order to lower pore pressure in the coal. CSG developments proposed for the Namoi region involve the use of hundreds of CSG wells for undertaking gas production. The effect on groundwater levels in response to CSG development is the top ranked research topic identified in GISERA stakeholder surveys.

Groundwater modelling is used as a tool for predicting the impacts of groundwater extraction at a regional scale, estimating changes in groundwater heads and flux for aquifers of interest. Conventional regional groundwater models encompass extensive areas and, as a result, involve spatial scales that are considerably larger than used in CSG reservoir modelling, creating difficulties representing the reservoir flow processes that occur at small scales around CSG wells during gas production.

Gas production from coal seams is the result of a number of coupled reservoir processes that also determine the rate of water production. A key process is the two-phase flow of water and gas but the nature of gas storage in coal is also important. Gas in coal seams is stored through adsorption meaning that initially, before gas production starts, the porosity is water saturated. As the pore pressure decreases, gas is desorbed into the porosity and migrates through the coal towards producing wells. The rate of gas desorption is related to the adsorption isotherm and the change in pressure with time. This means that gas production is a series of coupled processes that operate at small scales around producing CSG wells. Representing these detailed processes is difficult when modelling large-scale regional groundwater impacts, and as a result for these problems groundwater models that only represent the water phase are used. The inability to represent detailed flow processes influences CSG groundwater assessments, and can lead to over-estimation of water extraction impacts.

The Queensland Office of Groundwater Impact Assessment (OGIA) developed a procedure to improve the representation of coal seam gas impacts in their groundwater modelling assessments of the Surat Basin (Herckenrath et al., 2015). This procedure was based on results from reservoir simulations of producing fields in the Surat Basin that modelled the detailed CSG reservoir flow processes that occur at small scales around producing wells in that basin. Simulation results were used to derive a relationship between water saturation and pressure that was implemented in a version of MODFLOW that represents unsaturated flow.

The objective of this GISERA project is to improve the representation of CSG impacts in groundwater modelling of the Namoi region. The methodology involves using a coal seam gas reservoir simulator to undertake detailed simulations of groundwater production as the basis to identifying simple relationships appropriate for implementation into regional MODFLOW models of Namoi. The detailed reservoir simulations include a range of reservoir processes and investigate various effects such as spatial grid block scales and boundary influences. In the final chapter the identified relationship is implemented in an existing MODFLOW model of the Namoi and the impacts evaluated.

The key project milestones are addressed in the following report chapters, which describe:

- Data collation and completion of a review of hydrogeology and CSG production scenarios in the Namoi sub-region.
- Construction of a detailed CSG reservoir model representing site-specific characteristics of CSG production in the Namoi sub-region.
- Completed CSG production simulations using the Namoi reservoir model that identify ways groundwater production is related to key driving variables of gas production; and identification of the most suitable relationships for implementation into MODFLOW groundwater flux models of the region.
- Investigation of vertical and spatial scale effects on derived relationships between key variables of gas and water production, and on the implementation of these relationships at the scale of the MODFLOW regional model.
- Implementation into MODFLOW of derived relationships capturing complex CSG well field influences, and assessment of the effect of the deployed relationships on predictions of drawdown and flux change.
- Deployment of the derived relationships into the MODFLOW model of the Namoi region developed in the GISERA companion project W7 - Impacts of depressurisation on Great Artesian Basin (GAB) flux, and updating of model regional drawdown predictions.

2 Review of OGIA modelling approach in Surat CMA

2.1 Representation of CSG well fields in groundwater models

Coal seam gas (CSG) production involves first extracting water from a coal seam through production wells in order to lower the pore pressure within the coal. Lowering the pore pressure allows methane gas to desorb from the coal surface, where it can then migrate as a free gas phase through the coal fractures towards the production well. The complex coupled reservoir flow processes that govern gas production from the coal seam will also affect the rate of water production over the CSG field life. These processes operate at relatively small scales around the producing wells, which makes them difficult to represent in the large scale regional groundwater models that are used to assess the impacts of coal seam gas water extraction.

Existing groundwater models do not represent the details of the actual flow processes in CSG well fields, and studies have shown that the inability to accurately represent these reservoir processes has a significant impact on CSG groundwater assessments (Commonwealth of Australia, 2014; Moore et al., 2015; Herckenrath et al., 2015). Instead, existing models rely on either simplified relationships or CSG water production estimates, and the conservative assumptions made in order to compensate for these inaccuracies can lead to over-estimation of the impacts of CSG water extraction.

A recent study by Moore et al. (2015) examined the possible effects of these complex reservoir processes on regional groundwater models, acknowledging that despite the significant upscaling that occurs in the construction of regional models and the possibility that impacts of CSG production may occur over large areas, the small scale near well conditions and processes cannot be ignored. Important reservoir processes identified by the authors include the heterogeneity of coal measures, as well two-phase flow processes that occur in CSG well fields due to gas desorption. For the study both a fine scale and a less detailed model were constructed to examine the depressurisation errors that occur due to upscaling. To explore the errors incurred by neglecting near well two-phase flow, single and dual-phase simulations were run in both a dual-phase reservoir simulator (ECLIPSE) and single-phase groundwater simulator (MODFLOW-USG). The fine scaled model was based on a stochastic realisation of coal and interburden lithologies, and hydraulic properties representative of the Walloon coal measures of Queensland's Surat Basin. In the dual-phase model adsorbed gas was represented using a uniform Langmuir isotherm across all coals, and the coals were modelled as a dual-porosity medium. To compare single-phase and dual-phase models, water production rates determined from the dual-phase simulation were assigned to the single-phase simulation, eliminating errors that would be incurred by the different model responses to well constraints.

Results from the single-phase MODFLOW-2005 and dual-phase ECLIPSE simulations indicated that despite assigning equivalent water production rates, the use of a single-phase simulator leads to overprediction of pressure drawdown (Moore et al., 2015). The disparities were largest at early times in the vicinity of the well field, showing up to 300m overprediction after one year of pumping. This overprediction decreased, but affected a larger reservoir volume after 20 years. The authors attribute the overprediction to the inability of the single-phase model to simulate both water production from pore storage and relative permeability effects due to gas desorption. Instead, in the single-phase model, water production occurs due to elastic storage. A similar overprediction of drawdown was recognised by Herckenrath et al. (2015) in their comparison of MODFLOW-USG and ECLIPSE simulations applied to simplified single layer and multi-layer coal seam models. As with Moore et al. (2015) the authors recognised that assigning ECLIPSE derived water production rates to a single-phase model still results in overprediction of pressure drawdown, and that further relationships governing two-phase flow in coal seams must be included. Similar results from De Vertuil et al. (2013) indicated that gas liberation in the near-well region plays a significant role in controlling drawdown in the liquid phase at larger distances.

In geologically complex reservoirs containing multiple interbedded lithologies, the level of heterogeneity normally captured in a fine scale coal seam gas reservoir model must be upscaled for incorporation into a coarse scale regional groundwater impact model. Comparison of depressurisation results from the fine-scale and upscaled models constructed by Moore et al. (2015) demonstrated that the vertical upscaling methodology chosen will affect the shape of pseudo relative permeability curves that govern two-phase flow in the upscaled model cell.

Vertically upscaling by amalgamating all coal and interburden fine-scaled layers into a single layer, and then averaging hydraulic properties across both coal and interburden, does not capture permeability contrasts, and subsequent plots of relative permeability versus saturation for the cells indicate that large changes in cell relative permeability do not correspond to changes in saturation. In contrast, first segregating coal and interburden layers into two separate upscaled layers of appropriate thickness, then averaging hydraulic properties within each upscaled layer, results in a plot of relative permeability versus saturation that more closely resembles the original relationship (Moore et al., 2015). Herckenrath et al. (2013) applied the segregation approach to compensate for errors due to upscaling, while Moore et al. (2015) suggest the use of a dual porosity representation of flow in an upscaled cell to compensate for the presence of permeability heterogeneity and anisotropy in a fine-scale reservoir model. This approach was applied to Queensland Office of Groundwater Impact Assessment (OGIA) (2016a) modelling of CSG groundwater impacts in the Surat Basin.

To compensate for the absence of desaturation and dual-phase flow within regional groundwater models, Commonwealth of Australia (2014) suggest two approaches for the representation of coal seam gas well fields. The first is to apply observed groundwater extraction rates to wells in the well field, as opposed to prescribing well hydraulic heads. However as discussed, the application of well rates to a single-phase model can still result in overprediction of drawdown (Moore et al., 2015; Commonwealth of Australia, 2014; Herckenrath et al., 2015). The second suggested approach is to use well field water table levels derived from reservoir models to define boundary conditions for the well field in a regional model. The authors suggest this would have the advantage of implicitly incorporating the effects of dual-phase flow and gas desorption into a single-phase model. Other methodologies for attempting to represent coal seam reservoir responses in regional models, such as using measured water levels in extraction bores are considered problematic, as water levels in extraction wells may not be representative of hydraulic heads beyond well casing (Commonwealth of Australia, 2014). In reality, the groundwater behaviour in response to production is a function of a range of conditions and processes that are unique to a given location and operating conditions. Models are required that can appropriately represent these effects in order to address the key questions related to groundwater levels and water production rates.

Other recent studies (Moore et al., 2013; Herckenrath et al., 2015) have examined methods for combining reservoir and regional models, specifically using a single-phase model to more accurately simulate multi-phase reservoir flow. The methodology described by Herckenrath et al. (2015) has been applied to CSG related regional groundwater modelling undertaken by OGIA on the Surat Basin.

2.2 OGIA Surat Basin modelling incorporating CSG field desaturation

In areas containing multiple adjacent gas fields the impacts of water extraction on groundwater pressure can overlap (OGIA, 2016a). This situation occurs in the Surat and southern Bowen basins, referred to collectively as the Surat Cumulative Management Area (CMA), where the coal seam gas industry operates. Groundwater impacts in this area were assessed by the OGIA using a groundwater model that incorporated a sub-model of the Talinga CSG wellfield area. In order to improve the representation of coal seam gas production impacts, the OGIA model included functionality to allow simulation of water desaturation in coal seams and around CSG wells. This unsaturated flow functionality was based on the approach documented by Herckenrath et al. (2015). The approach used in the OGIA groundwater impact modelling will approximate the approach to be taken for the Namoi region, and its methodology for representing the CSG well field flow processes for the Surat CMA region is described in some detail in this section.

An initial groundwater impact report was prepared by OGIA for the Surat CMA in 2012. Following publication of the first report, OGIA assessed new and existing geological, geophysical and hydrogeological data for the region, evaluated connectivity between reservoir formations, and reviewed additional water bore records. These new data, alongside new techniques to represent groundwater flow in coal seams were incorporated into the new groundwater flow model used to prepare the 2016 report (OGIA, 2016a).

2.2.1 Herckenrath et al. (2015) approach

A study undertaken by Herckenrath et al. (2015) examined errors in regional drawdown predictions that occur due to neglecting the process of gas desorption and the resulting presence of the gas-phase near CSG wells. It also proposed an approach for mitigating these errors in regional models by simulating desaturation near the wellbore using a modified Richards (1931) equation within the standard groundwater flow simulator.

Existing groundwater models used in regional groundwater impact assessments are not equipped to represent the details of flow processes in CSG well fields, instead relying on simplified relationships or on estimates of CSG water production as inputs. Neither approach adequately simulates CSG well field behaviour and in order to compensate, conservative assumptions are included to ensure groundwater impacts are not underestimated. This issue was recognised by both the U.S National Research Council (2010) and by the Commonwealth of Australia (2014). The former recommended that the uncertainties in groundwater modelling results be explicitly recognised when the results are used to make produced water management and regulatory decisions; the latter recommended that assessment of potential impacts should acknowledge uncertainty in the modelling, and that future research should address the influence of flow phenomena and geomechanical effects on coal seam dewatering. Herckenrath et al. (2015) proposed a methodology for incorporating the influence of some of these coal seam flow phenomena, in particular the presence of a near-well gas phase, into regional drawdown assessments made using single-phase groundwater modelling platforms.

Pressure drawdown predictions from a single-phase groundwater model differ to those from a two-phase model. One reason for this is that coal seam depressurisation leads to gas desorption from the coal matrix, and hence to the presence of free gas in the coal cleat system. Increases in the gas saturation within cleats leads to a reduction in the relative permeability of the water phase, which dampens the propagation of extraction induced pressure drawdown effects. In a two-phase model, this gas phase also contributes to occupation of the pore space previously occupied by previously extracted water, whereas a single-phase groundwater model relies on elastic storage to occupy the displaced volume.

The methodology for reconciling these differences proposed by Herckenrath et al. (2015) is based on ECLIPSE simulations of storage of gas and the two-phase flow of gas and water in coal seam reservoirs. These simulations include a range of gas storage and gas-water flow processes that operate during coal seam gas production. It was proposed that if the behaviour of two-phase systems under certain configurations and boundary conditions allow for expression of water saturation (S_w) as a function of P, then the equations governing horizontal two-phase flow in the reservoir may be decoupled and the water flow equation solved for pressure independent of the gas flow equation. This would then have application to regional groundwater models, where pressure drawdowns are often calculated far from areas where desaturation occurs.

Pressures and saturations induced by CSG production were calculated throughout the domains of two models, one constructed as a simple representation of a single coal seam, another as a representation of multiple seam and interburden layers. The ECLIPSE reservoir simulator and MODFLOW-USG groundwater flow simulator were employed for the study. The models described either a typical coal seam, or a sequence of coal and interburden layers, produced by a pattern of CSG wells over a period of 20 years, followed by a 20 year recovery period. The models constructed in MODFLOW-USG and ECLIPSE contained identical hydraulic properties and physical parameters, with no upscaling taking place.

Results from the ECLIPSE model were used to construct a scatter plot of S_w vs P at different times during CSG production containing all the cells which undergo desaturation. This plot allowed the authors to observe a relationship between S_w and P over time. The S_w vs P curve of all the desaturated model cells changes during CSG production, reaching an asymptote with increasing time, as well as increasing distance from wells, and tending towards a dynamic pseudo-equilibrium state. Within this dynamic pseudo-equilibrium state, with the exception of locations in the vicinity of producing wells, water saturation decreases as pressure falls.

Traditional groundwater modelling techniques apply the Richards equation to describe dual-phase flow of air and water in the vadose zone. The equation applies to the flow of the water phase alone, assuming gas flow occurs instantaneously and is in equilibrium with atmospheric pressure, therefore implying capillary pressure is the negative of the water pressure. When using this approach the relationship between S_w and P is described by the van Genuchten (1980) function:

$$S_e = \frac{S_w - S_r}{1 - S_r} = \left[1 + \{\alpha(h_b - h)\}^{\beta}\right]^{-\gamma} \qquad \text{for } (h_b - h) > 0 \tag{1}$$

Where

$$\gamma = 1 - \frac{1}{\beta} \quad \text{and} \quad h = \frac{p}{\rho_w^g}$$

In Equation 1 S_e and S_r represent equivalent and residual water saturation respectively, h represents water head, and h_b represents the bubble point pressure head, which in a CSG context refers to the height of a column of water that corresponds to the desorption pressure of the coal matrix. Parameters α and β are fitting parameters which define the S-shaped van Genuchten curve. In a groundwater model this equation is used to define a soil's capillary characteristics, while in the Herckenrath et al. (2015) study the authors used it to describe the time-asymptotic curve S_w vs P curve that emerges from CSG production. However, in using this equation they do not imply that the physical processes in the CSG and vadose zone contexts are equivalent.

The availability of the van Genuchten function and the Richards equation technique in MODFLOW-USG allowed the authors to simulate the effects of desaturation, which were traditionally neglected in groundwater flow models that include coal seams described by the single-phase MODFLOW-USG code. The procedure involves determining the time-asymptotic S_w vs P relationship for a given production scenario in a specific coal seam reservoir, using a detailed model of the reservoir and dual-phase simulator such as ECLIPSE. A plot of S_w vs P will asymptote towards a dynamic pseudo-equilibrium state as described above. The relationship in this state can then be modelled with the van Genuchten relationship, fitting for parameters α and β. These values are then included in a corresponding MODFLOW-USG model of the reservoir in all layers that contain coal seams, providing a methodology for simulating the effects of desaturation.

Herckenrath et al. (2015) evaluated this methodology through comparison of the results from a series of numerical experiments. They demonstrated that parameters for a van Genuchten function can be found that allow for the single-phase groundwater simulator to account for the presence of a gas phase reasonably well, and that the single-phase drawdown results appeared relatively insensitive to values assigned to the function parameters, although uncertainties in these parameters should still be taken account.

Some problems with the methodology were identified, such as the tendency of the modified Richards equation methodology to overpredict drawdown at early simulation times close to extraction wells. The authors suggest this response is due to high gas saturations that exist close to wells. In this situation water produced from the pore space is replaced with gas that desorbs from the coal matrix, providing a buffer against drawdown. The single-phase simulator does not replicate this behaviour because the dynamic pseudo-equilibrium condition underpinning the use of the S_w vs P relationship breaks down at early times and near well conditions. An additional problem concerns simulating drawdown during the pressure recovery phase, after well shut-in, as the modified Richards equation approach does not accurately approximate pressure recovery behaviour modelled by the dual-phase reservoir simulator. The observed time-asymptotic pseudo-equilibrium state between S_w and P does not manifest for the recovery period, thus undermining the theoretical basis for accounting for desaturation in a single-phase simulator during pressure recovery.

2.2.2 Surat CMA hydrogeology

The Surat CMA represented in the OGIA model consists of sections of three geologic basins: the Bowen, Surat, and Clarence-Morton. Each of the basins consists primarily of sandstone, siltstone and mudstone layers, and they are overlain by unconsolidated alluvial sediments and basaltic cover. Various parts of the three basins also comprise the GAB, designated a hydrogeological groundwater basin as opposed to a geologic basin, and examined herein.

The regional hydrostratigraphy of the Surat CMA can be divided into four primary systems: The Great Artesian Basin sediments, consisting of alternating aquitards and aquifers within the Surat and Bowen basins; the Bowen Basin sediments, comprising aquifers and aquitards of the Bowen Basin underlying the Surat Basin; the Basalt, a consolidated surficial aquifer mainly capping the Clarence-Morton Basin; and the Alluvium, consisting of the unconsolidated surficial aquifers of the Condamine and St. George Alluvium. Within the Surat CMA the most prominent of these systems are the GAB and Condamine Alluvium (OGIA, 2016b). The relevant hydrogeological units are presented in Figure 2-1.

The main sedimentary sequence of the GAB is almost 2500 m thick in the Mimosa Syncline, with individual formations ranging in thickness from 100 m to 600 m (OGIA, 2016c). The main sandstone aquifers within the GAB are typically laterally continuous, permeable, and have significant water storage. However they still contain significant proportions of siltstone and mudstone, and display the characteristics of aquitards in some areas (OGIA, 2016c). The major aquifers of the GAB within the Surat CMA include the Precipice, Hutton, Springbok, Gubberamunda, Mooga Sandstones and the Bungil Formation. The aquitards present in the GAB are typically dominated by low permeability siltstone, mudstone, shale, and occasional sandstone, and include the Evergreen, Westbourne, Orallo, Wallumbilla and Griman Creek Formations. The GAB sediments also comprise the Walloon Coal Measures, a target for CSG production in the Surat CMA.

The Bowen Basin sedimentary sequences include the Clematis Group aquifer, a quartzose sandstone dominated formation with interbedded silts and muds, and the aquitards of the Moolayember Formation, Rewan Group and Older Permian units. The aquitards host varying lithologies but consist of predominantly interbedded mudstones, siltstones and fine sands. The Bandanna Formation is the primary target of CSG production in the Bowen Basin, while the Cattle Creek Formation coals represent an emerging target.

The tertiary basalt sequence overlies the GAB sediments of the Hutton Sandstone and Walloon Coal Measures. It consists mainly of the Main Range Volcanics, a sequence of significant aquifers occurring at depths that range from 2 to 155 m (OGIA, 2016c). The aquifers respond to infiltration of rainfall, acting as unconfined to semi-confined aquifers at shallow depths and semi-confined to confined aquifers deeper (OGIA, 2016b). The Main Range Volcanics contribute to recharge of connected aquifers, including the Hutton sandstone and Walloon Coal Measures.

The alluvium of the tributaries of the Condamine River overlies the tertiary basalt sequence, and also directly overlies the Walloon Coal Measures and Springbok Sandstone. The aquifer is generally 30 to 60 m thick, and hosts groundwater developed for irrigation, stock and domestic use. The discrete channel sand and gravel aquifer beds within the alluvium are extensively interconnected (OGIA 2016c) with moderate permeability in the order of 2360 to 23600 md occurring in most of the formation. An extensive report by Queensland's OGIA (2016b) assessed the connectivity between the Condamine Alluvium and Walloon Coal Measures, concluding that impediments to flow, such as the clay-dominated transition zone and mudstones of the upper Walloon Coal Measures, exist between the formations, and that hydraulic conductivity between the formations is low.

The regional groundwater flow model constructed for the Surat CMA attempts to represent the regional hydrogeology using 32 layers. The Cenozoic sediments were combined into a single model layer referred to as the Condamine Alluvium and Main Range volcanics. A second layer combined the Griman Creek Formation and Surat Siltstone and also consisted of the sediments of the Condamine-Walloon transition zone. Single layers were assigned to each of the Bungil Formation, Mooga Sandstone, Orallo Formation, Gubberamunda Sandstone, and the Westbourne Formation. Two layers each were assigned to the Springbok Sandstone and Hutton Sandstone, and six to the Walloon Coal Measures. One layer each was assigned to Durabilla Formation, Evergreen Formation, Precipice Sandstone, Moolayember Formation, Clematis Group, and Rewan Group. The coal measures of the Bandanna Formation and Cattle Creek Formation are assigned three layers each, overlying and underlying the single layer of Undifferentiated Bowen Basin strata. The bottom model layer describes further Undifferentiated Bowen Basin strata.

Applying the Herckenrath et al. (2015) approach to representing unsaturated flow required comparison of a fine detail reservoir model of the coal seams with an upscaled hydrogeological model of the identical area. For the OGIA report, this was undertaken on a sub-model of the Talinga CSG well field, focusing on the Walloon coal measures and overlying and underlying units.

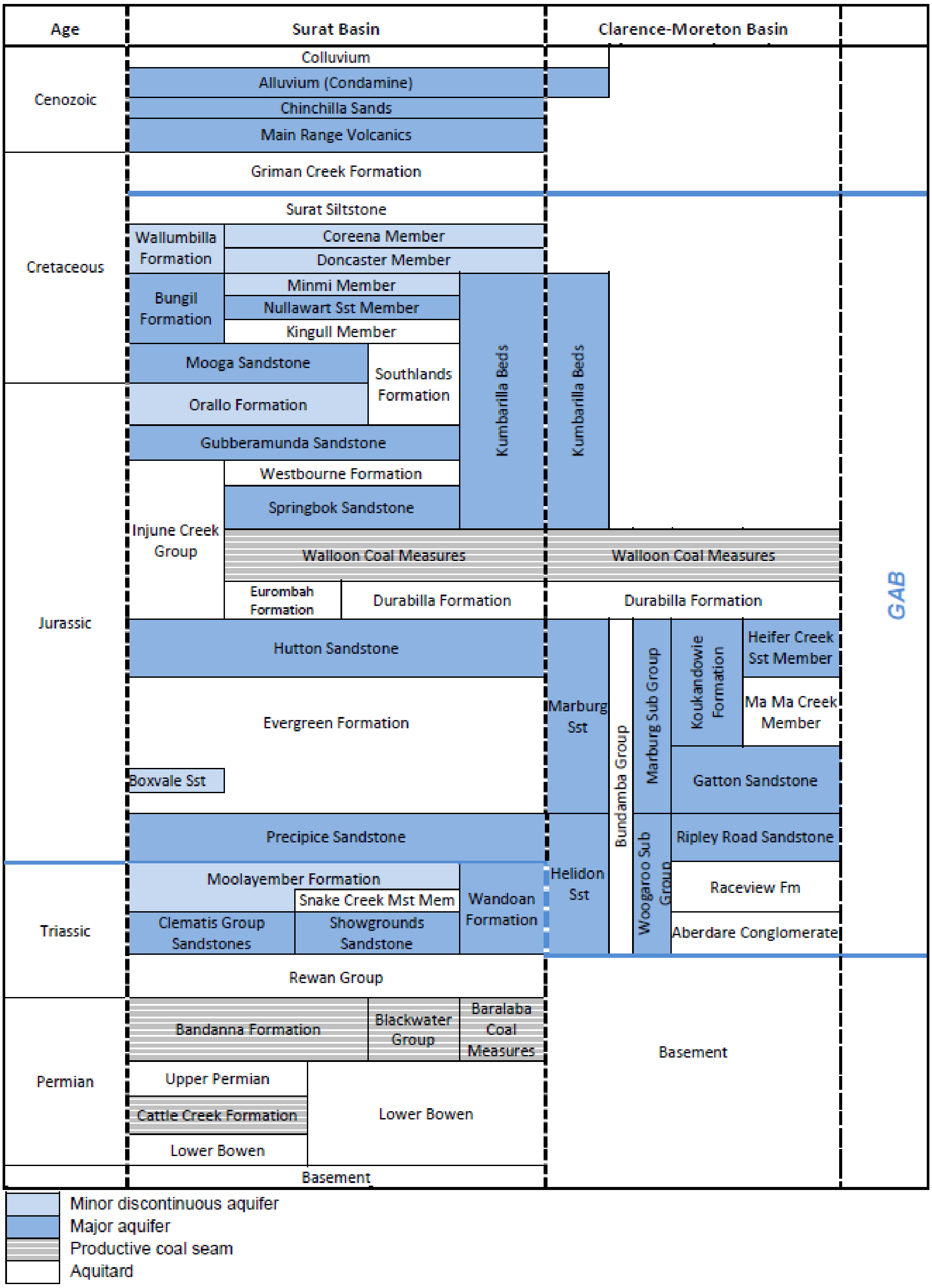

Figure 2-1 Regional hydrostratigraphy of the Surat CMA (OGIA, 2016c).

2.2.3 OGIA Surat CMA hydrogeological model development

A geological model describing the extent and thickness of the different geological units in the Surat CMA was redeveloped to incorporate revised modelled surfaces for geologic formations based on the new data, major geological faults, and better representation of surficial sediments such as the Condamine Alluvium. The revised surfaces and extents of geologic units in the updated geological model represented an important component of the Surat CMA groundwater flow model. The surficial sediments of the Condamine Alluvium were revised in the geological model as part of a study into connectivity (OGIA, 2016b) between this unit and the underlying Walloon Coal Measures, which contain the main CSG producing coals of the Surat Basin. In the regional groundwater model, geometry of coal seams that sub-crop beneath the Condamine alluvium, and unconformities due to erosion were represented. A one metre thick layer at the base of the alluvium represented the Condamine transition zone, which was ascribed spatially varying values of vertical conductivity that accommodated uncertainties associated with the barrier thickness and hydraulic properties. In reality the transition zone is thought to be non-continuous, with thicknesses ranging from 1 to 15 m. An additional study (OGIA, 2016b) provided a range of vertical hydraulic conductivities and concluded that vertical connectivity is generally low.

Geological units of the Surat and Bowen basins were modelled using a lithostratigraphic approach, whereby stratigraphic boundaries between geological units in the model were defined by the presence of geological unconformities, or by observable changes in the lithology resulting from changing depositional environments. A report by Green et al. (1997) assigned geophysical signatures to different stratigraphic units in the Surat and Bowen basins, which were then used by OGIA to interpret formation tops from wireline logs of hydrocarbon wells and water bores, which were then input into the geological model. The revised geological model contained 12 stratigraphic layers in the Surat Basin and 5 in the Bowen Basin, as well as 17 additional regional faults.

Development of the OGIA regional groundwater flow model for the Surat CMA involved 3 basic steps: translating the complex three-dimensional geological system and groundwater flow processes into an idealised conceptual model, conversion of the simple conceptual model into the groundwater flow model that mathematically represents the physical system and flow processes, and calibration of the groundwater flow model based on observed system behaviour. The calibrated model was then used to make predictions of water pressure and flow under different field development scenarios. Feedback from the performance of this model supplied additional input data to further revise and calibrate the model.

The extensive geological and hydraulic parameter data set available for the Surat CMA, including lithological data and hydraulic parameter estimates from well logs, allowed for an improved approach to initial parameterisation and calibration of the groundwater flow model. As opposed to previous regional modelling exercises, where initial parameters were derived from statistics (e.g. median) of available hydraulic conductivity data which were then varied during calibration, the OGIA 2016 model approach involved the following steps: Deriving initial values of hydraulic conductivity for 6 lithology types based on expert knowledge, literature, and petrophysical log data; calibration of these values using a stochastic permeability model to compare to available hydraulic parameter data; and use of the stochastic lithology and stochastic permeability models to derive spatially variable formation-scale horizontal and vertical hydraulic conductivity data for each stratigraphic unit. These lithology and permeability realisations corresponded to a larger scale "numerical permeameter" grid, whose individual 21 km x 21 km grid blocks correspond to a domain in the stochastic lithological model that comprises 105 x 105 grid cells, and between 30 and 357 vertical layers. Vertical and horizontal flow were simulated in the fine-scaled cells corresponding to each coarse-scale permeameter grid block in order to derive estimates of horizontal and vertical permeability. This process was repeated in each permeameter cell for different realisations of lithology and fine-scale permeability until a statistical value of the upscaled vertical and horizontal permeability was determined. The numerical permeameter model was used to assign hydraulic conductivity values to the final groundwater flow models, whose values for hydraulic conductivity in each of its 1.5 km x 1.5 km cells were determined by spatial interpolation. Layer depths for the permeameter and groundwater models were coincident. The final groundwater flow model was calibrated to match historical water production and drawdown data by adjusting the hydraulic conductivity values of “pilot points” in the groundwater model, whose initial values were assigned from the permeameter grid. Hydraulic conductivities for cells of the groundwater model were spatially interpolated from these adjusted pilot point values.

In the MODFLOW-USG regional groundwater flow model, the GAB sequence, Bowen sequence and alluvial formations in the Surat CMA were represented by 32 model layers in total, with six layers used to represent the Walloon Coal Measures and three layers each to represent the Bandanna and Cattle Creek Formations. This allowed a more accurate representation of unit geometry, and also better approximation of changes in lithology within certain hydrostratigraphic units. Using a minimum of three model layers allowed for the representation of vertical pressure gradients within the coal seams, which occur due to differences in head drawdowns between upper and lower layers subject to CBM extraction. Individual coal seams were not represented as separate layers as they often can not be correlated across the model area. Therefore, each of these layers in the groundwater flow model represented composite layers of high permeability thin coal seams separated by thicker, low permeability mudstone, siltstone and sandstones. In each of the coal formations the upper model layer was defied as “non-productive”, acting as a low permeability mudstone that does not contribute to CSG production.

In order to represent the vertical flow of water into thin, laterally discontinuous coal seams that are depressurised during CSG production, the coal model layers below the “non-productive” layer were assigned a dual porosity functionality in MODFLOW-USG. This approach helped avoid the difficulties associated with upscaling thin, discontinuous coal seams into a single regional model layer, whereby the water relative permeability curve can become distorted. In MODFLOW-USG the dual porosity formulation is configured such that coal is represented by a mobile domain, and an immobile domain represents silt and shale. The mobile domain fraction was equivalent to the percentage of coal in the model layer (varying from 1.6% to 16.8% in the Walloon Coal Measures). Upscaled horizontal permeability values that take into account the discontinuous nature of coal seams are ascribed to the mobile domain. The immobile domain remains saturated, and water may not undergo lateral flow. Water from the immobile domain transfers to the mobile domain as governed by a “dual domain flow transfer rate”, which in the model is used to represent vertical flow of water from an interburden material to the nearest coal seam connected to a well. The transfer rate is calculated from vertical interburden permeability and average spacing of coal seams within a model layer.

The model domain covered an area of approximately 460 km by 650 km and captured all CSG development areas within the Surat CMA. Each model layer was divided spatially into 1.5 km by 1.5 km model cells. CSG wells within the Surat CMA were modelled to first attain, and then operate at, a constant flowing bottom hole pressure of 240-830 kPa. The CSG wells were modelled in MODFLOW-USG using a ‘drain’ boundary condition. Multiple drains were assigned to each well; descending over time as pressures in the CSG well reduced. This approach is implemented because hydrostatic conditions which apply to multi-layer water extraction in groundwater models are not appropriate for simulation of gas extraction. Coalbed methane wells are not filled with water, but instead have a high and increasing gas content over time which approaches a uniform pressure within the well. The descending drain approach involved applying a MODFLOW-USG drain, governed by drain-specific head and conductance, to each model layer undergoing extraction. Elevation of the drains was equated to either water head in the top layer, or a pressure head equivalent to coal seam desorption pressure. After gas extraction commences, these drains descend at rates set by the modeller. The wells were switched on and off in the model according to the proposed timing of production commencement and cessation of CSG developments provided by the tenure holders.

The coal seam gas extraction wells are completed in coal seams which have a much higher permeability at the than the upscaled permeability that is assigned to the cell in the regional model. The transmissivity seen at a CSG extraction well is calculated as the sum of all intersected cell transmissivities, however in the regional model this value is much lower than the sum of coal seam transmissivities that would dominate the value in real life. To compensate for the effect the upscaled transmissivity has on drain conductance calculated using the Peaceman (1978) formula, supplemental functionality in the OGIA version of MODFLOW-USG substitutes the regional cell permeability with a higher value read in from an external file. This external value is calculated based on an average of hydraulic conductivities in the lithological model used prior to upscaling.

The groundwater flow model was first calibrated in steady state mode in order to replicate conditions in the aquifers prior to CSG production. In addition, the model was further calibrated by matching calculated monthly water production to values supplied by CSG operators in the area. The total modelled CSG water production over the period of 1995 to 2014 was within one percent of actual total over this time. Vertical pressure gradients within coal measures calculated by the MODFLOW-USG regional model were also compared to operator reservoir models simulated using the ECLIPSE reservoir simulator. Water levels for the Condamine Alluvium were imported into the regional model from a higher resolution sub-model of this unit previously developed for water resource planning purposes. Automated calibration of the model was undertaken using PEST software. Iterations were assessed quantitatively and qualitatively in line with the Australian Groundwater Modelling Guidelines (Barnett et al., 2012) to ensure consistency with expert knowledge of groundwater flows in the Surat CMA.

In order to make predictions using the calibrated regional model, it was set to make predictive runs from 1995 onwards. A base run without CSG extraction was compared to a run including CSG production. The difference in future water levels between these two runs provided the water pressure impact predictions expected from current and planned CSG production.

2.2.4 OGIA approach to representing desaturation in the Surat CMA modelling

A highly detailed sub-model comprising the Talinga CSG wellfield area was developed using the ECLIPSE reservoir modelling platform. Data derived from ECLIPSE simulation using the sub-model were then used as a basis for revising the MODFLOW-USG code to more accurately simulate the effects of CSG water extraction. The ECLIPSE sub-model contained 294 model layers with 200 m x 200 m grid size representing the Hutton Sandstone, Springbok Sandstone and Walloon Coal Measures, and results from the ECLIPSE model were compared to an upscaled MODFLOW-USG version of the same model which contained 8 layers at 1000 m x 1000 m grid size. The numerical permeameter approach discussed in section 2.2.3 was used to assign hydraulic properties to the upscaled model.

The Hutton Sandstone is the most extensive Jurassic aquifer in the GAB, ranging in thickness from 150 to 350 m. The unit displays significant heterogeneity, consisting of fine-medium grained, well-sorted sandstone with interbedded silts, shales, muds and coals. This is reflected in core and DST median permeability measurements ranging from 0.4 to 74 md in the Upper Hutton, and 0.07 to 15 md in the Lower Hutton. Median porosity is 0.12, and due to its location between two persistent aquitards interaction with other aquifer units is thought to be limited.

The deeper part of the Hutton Sandstone, in the region of CSG developments, acts as a confined aquifer. There are also extensive areas of known groundwater discharge to surface water, providing flow to a number of spring complexes. In the Surat CMA CSG development area interconnectivity between the Hutton Sandstone and the overlying Walloon Coal Measures is considered limited.

The Springbok Sandstone comprises an upper zone of fine-coarse grained sandstone interbedded with silts and muds with median permeability ranging from 0.8 to 7 md, and a lower zone comprising coarse-very coarse grained sandstone excluding significant silts or coals, with median permeability ranging from 1 to 2 md. The unit varies in thickness from 100 to nearly 250 m. It was deposited on the eroded surface of the Walloon Coal Measures and as such shows a high degree of variability (OGIA, 2016b). In the north-eastern Surat Basin the lower permeability upper layers of the Walloon Coal Measures were completely eroded prior to deposition of the Springbok Sandstone, leaving it in contact with productive coal seams, and therefore a higher degree of connectivity is expected. In confined areas near CSG production, there have been indications of potential impacts on groundwater levels from CSG development due to the presence of faults, however hydrochemistry data suggest limited connectivity across the broader formation (OGIA, 2016b).

The Walloon Coal Measures comprise highly heterogeneous and anisotropic deposits of siltstone, mudstone, fine-medium grain lithic sandstone and coals. They average 300 m in thickness, up to a maximum of 600 m in the Mimosa syncline. The coal seams occur in lenses up to 1 metre thick and with lateral extents of 500 to 3000 m (Ryan et al., 2012; Hamilton, Esterle & Sliwa, 2014). The coal seams are isolated by low permeability sequences of mudstone, siltstone and sandstone. High permeability contrasts exist between the coal layers and interburden. Median interburden permeability is approximately 0.12 md, while median coal permeability is 35 md and shows a decreasing trend with greater depth. This trend differs in area of higher than average permeability which correlate with higher fault density in the maximum horizontal stress direction.

Connectivity between the Walloon Coal Measures and the overlying and underlying formations is considered limited due to the highly heterogeneous and anisotropic properties of its strata, which results in low ratios of vertical to horizontal permeability. This is supported by hydrochemistry data which suggest limited connection to the overlying Springbok Sandstone, except in areas of local faulting. There is little evidence of even limited connectivity to the underlying Hutton Sandstone, consistent with the very low vertical permeability of the Durabilla Formation, considered the lowest unit of the Walloon Coal Measures.

Following the methodology documented by Herckenrath et al. (2015) values for α and β for the MODFLOW-USG model were obtained by fitting the van Genuchten curve to S_w vs P plots generated from the OGIA sub-model, as well as to ECLIPSE models constructed by gas companies. Results from the ECLIPSE and MODFLOW-USG sub-model comparisons confirmed that the upscaled MODFLOW-USG model was able to reasonably replicate stresses in overlying and underlying layers, pressure responses at moderate distances from the well, local relative permeability effects, and the slowing of lateral propagations of pressure reduction. This only occurred provided both models were endowed with the same values of S_{wr}, the same Brooks-Corey exponent and that h_b is equal to coal desorption pressure (OGIA, 2016a).

3 Development of Namoi CSG models

This section presents a summary of the estimation of the SIMED reservoir simulator, and the geological, hydraulic, mechanical and coal seam gas properties underpinning the development of the representative CSG model for the Namoi sub-region. The objective of producing the Namoi region coal seam gas model is to apply it to assess relationships between coal seam reservoir properties, likely well arrangements, and groundwater flow in order to improve current regional groundwater model representation of CSG production.

For effective design and parameterisation of the CSG model for the Namoi sub-region, appropriate geological, hydraulic and coal seam gas properties are required. These properties must be incorporated alongside estimates of possible production scenarios, which include data such as well types, well spacing and production rates.

3.1 Namoi sub-region geology and hydrogeology

The Namoi sub-region is underlain by two distinct basement geological elements: the Jurassic Surat Basin and the Permo-Triassic Gunnedah Basin (Welsh et al., 2014). It is also underlain by portions of the smaller Werrie Basin (Aryal et al., 2017a). These sediments in turn overlie early Permian and older meta-volcanic basement rocks (CDM Smith, 2014). Stratigraphy of the Gunnedah Basin and overlying Surat Basin is presented in Figure 3-1.

The stratigraphy of the Gunnedah Basin comprises up to 1200 m of marine and non-marine sediments overlying older basement rocks (CDM Smith, 2014). It is contiguous with the Bowen Basin and Sydney Basin, together forming the larger Permo-Triassic Bowen-Gunnedah-Sydney Basin system (Welsh et al., 2014). It also contains alluvial and deltaic coal bearing sequences within the Hoskissons Coal Member and Maules Creek Formation.

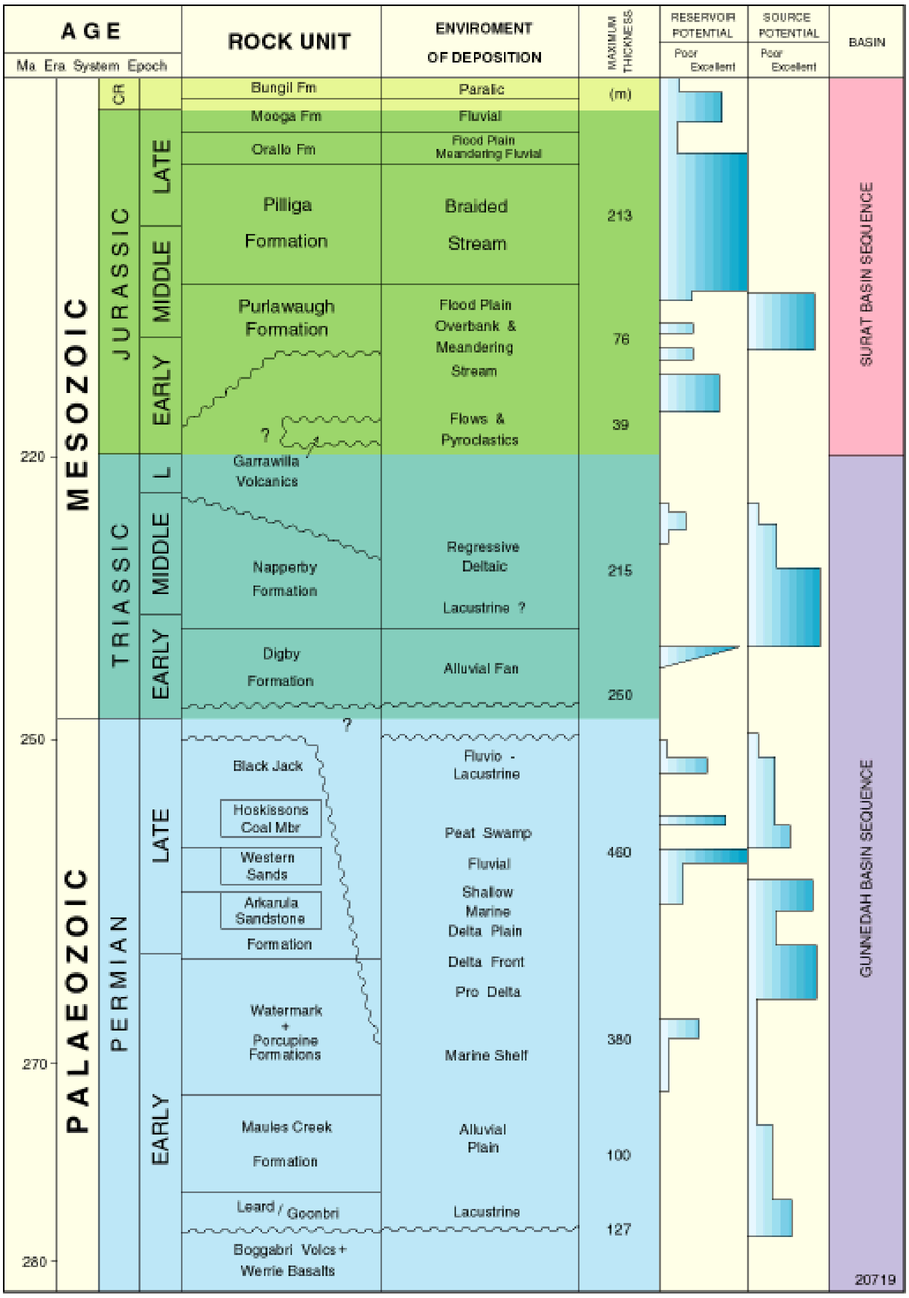

Figure 3-1 Stratigraphic column of Surat and Gunnedah basins (Welsh et al., 2014).

The Surat Basin sequence overlies the Gunnedah Basin in the western part of the Namoi catchment, and consists primarily of fluvial to marginal marine sedimentary deposits overlying the Garrawilla Volcanics, which are considered the base of the Surat Basin sequence in the Namoi subregion. Within the Namoi subregion the sediments of the Surat Basin are reported to have no economic value. (Welsh et al., 2014).

The regional hydrogeology of the Namoi subregion can be divided into four broad groups: The upper and lower Namoi alluvium comprising the Narrabri, Gunnedah and Cubbaroo Formations; the Surat Basin within the Coonamble embayment of the GAB, thought to be hydrogeologically isolated from the northern part of the Surat Basin and greater GAB (Herczeg, 2008; Radke et al., 2000); and the Jurassic sandstones and Permian Gunnedah sedimentary rocks; and the lower Permian volcanic rocks underlying the Gunnedah Basin and GAB deposits (Welsh et al., 2014).

Alluvial aquifers

The sediments of the upper and lower Namoi Alluvium consist of sand, gravel and clay and are divided into the Narrabri, Gunnedah and Cubbaroo Formations. The thickness of the formations is largely controlled by the bedrock topography (Barrett, 2012). The uppermost Narrabri Formation consists of extensive clays, with minor channel sands and gravel beds. Its depth from the surface ranges from 30 to 70 m. It is the water table aquifer, and is known to interact highly with the Namoi and Mooki rivers (Welsh et al., 2014).

The Narrabri Formation is underlain by the Gunnedah Formation, which acts as semi-confined to confined aquifer, containing up to 115 m of gravel and moderately well-sorted sands with minor clays (Welsh et al., 2014; CDM Smith, 2014). The Gunnedah Formation is considered the most extensive and productive aquifer in the subregion (Giambastiani et al., 2012). The hydraulic properties of the Narrabri and Gunnedah Formation are well documented but highly variable, with hydraulic conductivities ranging from 0.008 to 31 m/d, increasing both with depth and in the paleo-channel (Welsh et al., 2014).

The underlying Cubbaroo Formation is a confined aquifer consisting of carbonaceous sand and gravel with interbedded clays. It is present in the Lower Namoi Alluvium and is largely associated with coarser sediments of the main paleochannel (Welsh et al., 2014) which allow for higher groundwater extraction rates (Barrett, 2012). Hydraulic separation between the three formations of the Namoi alluvium is dependent on area, with the formations acting as a single aquifer in some far western and eastern parts of the subregion, whilst displaying minimal connectivity elsewhere (Welsh et al., 2014).

Great Artesian Basin sediments

Constituting a sub-unit within Coonamble embayment of the GAB, the aquifers and aquitards of the Surat Basin underlie the alluvium in the north and west of the Namoi sub region. The groundwater within these aquifers and aquitards is mostly under artesian conditions (CSIRO, 2012). The hydrostratigraphic units include the Pilliga Sandstone, Purlawaugh Formation, the Blythesdale Group, which itself contains the Orallo Formation, Mooga Sandstone and Bungil Formation, and the Rolling Downs Group (CDM Smith, 2014).

The Jurassic Pilliga sandstone is the main GAB aquifer in the Namoi subregion. It is a highly porous and permeable unit consisting of well-sorted medium to coarse grained quartzose sandstone, with minor interbeds of mudstone, siltstone and coal (CDM Smith, 2014). It averages over 100 m thickness extending to over 300 m in the south of the Coonamble Embayment (Tadros, 1993). Tests of hydraulic conductivity give results from 0.1 to 10 m/d with most tests at the lower end of this range (Welsh et al., 2014).

The Purlawaugh Formation underlies the Pilliga sandstone, outcropping in small areas in the south of the Namoi subregion. It is considered an aquiclude, suggesting limited vertical connectivity with underlying units (CSIRO, 2012). The formation consists of thinly interbedded carbonaceous claystone and siltstone, with minor interbedded thin coal seams (CDM Smith, 2014). The maximum recorded thickness is 152 m with an average of 100 m throughout the subregion. The hydraulic conductivity of the unit is considered to be generally quite low, ranging from 0.005 to 0.03 m/d (Welsh et al., 2014).

Overlying the Pilliga sandstone are the formations and sands of the Blythesdale Group, consisting of coarse-grained, cross-bedded, well-sorted, porous sandstone and conglomerate, interbedded with minor shale, siltstone, and coal. The group has a total average thickness of 30 to 50 m (CDM Smith, 2014). Across the Coonamble embayment these sediments are considered to range from confined partial aquifers to leaky aquitards (CSIRO, 2012). They are overlain by the sediments of the Rolling Downs group, whose Wallumbilla Formation acts as the main Cretaceous aquitard (CSIRO, 2012).

Gunnedah Basin rocks

The sedimentary and volcanic rocks of the Gunnedah Basin underlie the eastern portion of the Namoi subregion, and comprise up to 1200 m of sandstone and siltstone of marine and non-marine origin with interbedded coals (Welsh et al., 2014). The basin also contains the principal targets of CSG extraction, including the Hoskissons Coal Member and the Bohena Seam within the Maules Creek Formation (Welsh et al., 2014). The main sedimentary sequences include the Triassic Napperby, Deriah and Digby Formations, the hydrostratigraphic units of the Black Jack Group, the Watermark and Porcupine Formations of the Middle Permian Millie Group, and the Early Permian aquifers and aquitards of the Bellata Group, including the coals of the Maules Creek Formation.

The lower unit of the Deriah Formation consists of coarse granule-bearing sandstone at the base fining upward to medium grained lithic sandstone with occasional siltstone and claystone beds. The upper unit comprises sandstone and mudstone with minor coal layers (Welsh et al., 2014). The widely distribute sediments of the Napperby Formation consist of three units. The lowest a fine-laminated siltstone 18 to 45 m thick, the middle a sandstone siltstone laminate and the upper a siltstone with minor interbedded claystone and fine sands (Welsh et al., 2014). The lithic and quartz conglomerate, sandstone, and minor fine-grained sedimentary rocks of the Digby Formation range in thickness from 20 to 200 m (Welsh et al., 2014), and it unconformably truncates rocks of the Black Jack Group.

The Black Jack group contains the Hoskissons Coal Member, a CSG extraction target (Welsh et al., 2014). Overlying the Hoskissons Coal Member are the sedimentary sequences of the Coogal and Nea subgroups. The Nea subgroup contains the Trinkey Formation, a sequence up to 258 m thick consisting of finely bedded claystone, siltstone and fine-grained sandstone, with some coal seams. This unit overlies the Wallala Formation, a 55 metre thick unit consisting of conglomerate, sandstone, siltstone, claystone and coal. Like most units in the Black Jack group, these units are not considered to have significant transmissibility, with horizontal hydraulic conductivity of 0.0002 – 0.0004 m/d (CDM Smith, 2014). The Coogal subgroup contains the Clare Sandstone, a sequence of medium-coarse grained quartzose sandstones and quartzose conglomerates ranging in thickness from a few m to 95 m, and the only unit aside from the Hoskissons Coal Member thought to contain significant transmissibility (CDM Smith, 2014). The remainder of the subgroup consists of the minor Breeza and Howes Hill Coals, the Hoskissons Coals Member, and the Benalabri Formation. The Benalabri Formation averages 20 to 30 m thickness and consists of organic-rich mudstone, siltstone and sandstone. Schlumberger water services ascribed horizontal hydraulic conductivity of 0.01 m/d to the upper Black Jack Formation units (SWS, 2012), however Welsh et al. (2014) assume hydraulic conductivities of the upper Black Jack Group and Digby Formation to be one to two orders of magnitude lower than the coal seams, and are thus considered to act as aquitards.

The Hoskissons Coal Measure consists of inertinite-rich coal interbedded with fine-grained sandstone, carbonaceous siltstone and claystone (Welsh et al., 2014). It ranges in thickness from 1 to 18 m and is split by the Clare sandstone in the western margin of the sub-basin (Welsh et al., 2014). It is laterally continuous over a wide area (SWS, 2012). Drill stem tests estimate the hydraulic conductivity of the unit at 0.33 to 3.3 m/d, although smaller values of 0.0082-0.02 m/d were obtained at Narrabri Mine (Welsh et al., 2014). Investigations by Eastern Star Gas suggest that the hydraulic conductivity is fracture controlled rather than cleat controlled (CDM Smith, 2016). The vitrinite reflectance values of the coal range from 0.5-0.7%, indicating that thermogenic gas generation has likely taken place (Northey et al., 2014). Gas content of the Black Jack group coals has been measured at around 9.1 m^3/t (Decker, 1999), while for the Hoskissons Coal Member, Gurba et al. (2009) reported gas content of 4 to 7 m^3/t. An average Langmuir volume and pressure of 17.8 m^3/t and 4.2 MPa respectively have been measured for the Black Jack group coals.

Underlying the Hoskissons Coal Member is the Brothers subgroup, containing the Brigalow, Arkarula and Pamboola Formations, and the Melvilles Coal Member. The Arkarula/Brigalow Formation underlies the Hoskissons Coal Member over the Mullaley sub-basin, ranging in thickness from 22 to 51 m. It is characterised by medium grained sandstone at the base and finely interbedded sandstones and siltstones at the top (Welsh et al., 2014) with an estimated hydraulic conductivity ranging from 0.0015 to 0.047 m/d (SWS, 2012). These units overlie the Melvilles Coal Member, a 2.5 to 3.5 metre thick high-vitrinite coal with layers of fine-grained sandstone, carbonaceous siltstone and claystone (Tadros, 1995). This unit in turn overlies the Pamboola Formation, an 89 to >206 metre thick sequence consisting of lithic sandstone, siltstone, claystone, conglomerate and intercalated coal (Welsh et al., 2014) with an estimated hydraulic conductivity ranging from 0.0015 to 0.047 m/d (SWS, 2012). All units of the Brothers subgroup are considered to act as probable non-transmissive units (CDM Smith, 2014).

The Watermark and Porcupine Formations of the Middle Permian Millie Group act as an aquitard underlying the units of the Black Jack group (SWS, 2012). The Watermark Formation is a sequence of sandy siltstone, siltstone and claystone with a maximum recorded thickness of 230 m (Welsh et al., 2014). CDM Smith (2016) estimated the horizontal hydraulic conductivity from geological analogues to range from 1.0e-6 to 1.0e-2 m/d. The underlying Porcupine Formation is an upward-fining sequence of pebble conglomerate through to sandstone, shale and siltstone that ranges in thickness from 10 m along western margin of the Mullaley sub-basin to 186 m in the south-east (Welsh et al., 2014). CDM Smith (2014) estimated the unit's hydraulic properties were to be similar to the overlying Watermark Formation.

The sandstone, siltstone and coal sediments of the Bellata Group, underlie the Millie group and make up the deepest units before the regional basement. The Bellata Group contains the coals of the Maules Creek Formation, whose Rutley, Namoi, Parkes and Bohena Seams are CSG targets in the Namoi sub-region (CDM Smith, 2014). The Upper Maules Creek Formation overlying the coal and interburden sequences, is assumed to act as an aquitard, alongside the overlying Porcupine and Watermark Formations, and consists of sandstone, conglomerates, siltstone, mudstone and coal (CDM Smith, 2014). The complete Maules Creek Formation ranges from <100 m thick in sub-basins west of the Boggabri Ridge to >800 m thickness in the Maules Creek sub-basin adjacent to the Hunter-Mooki Thrust System. It contains coal seams of up to 8 m thickness (Welsh et al., 2014) which display horizontal hydraulic conductivity estimated to range from 0.054 to 3.3 m/d (CDM Smith, 2014). The main CSG target for the Namoi subregion, the Bohena Seam has measured gas content of the ranging from 4.1 to 19 m^3/t (Gurba et al., 2009) with an average value of approximately 12 m^3/t. Numerous CH_4 adsorption isotherms have been measured on core samples extracted from pilot wells in the Namoi region. These measurements were reported in well logs and report average Langmuir volume and pressure of 22 m^3/t and 4.9 MPa for Maules Creek coals.

The underlying Goonbri and Leard Formations represent the deepest units of the Gunnedah Basin sedimentary sequence, resting unconformably on the weathered volcanic basement (Welsh et al., 2014). The Lear Formation averages 12 to 18 m thickness of claystone, conglomerate, sandstone and siltstone, while in the Maules Creek sub-basin the Goonbri Formation averages >125 m thickness and consists of layers of organic-rich siltstone, coal, sandstone and siltstone-claystone laminate (Welsh et al., 2014). In combination with the Lower Maules Creek Formation (underlying the coal measures) these units are considered to act as an aquitard (CDM Smith, 2014). Underlying the Bellata Group, the weathered volcanic basement in the Namoi sub-region consists of the Werrie Basalt and Boggabri Volcanics.

Namoi sub-region aquifer hydrogeology

Within the Namoi sub-region exist unconfined groundwater resources in the alluvial aquifers and confined and unconfined groundwater resources in the aquifers and aquitards of the GAB and Gunnedah Basin (Santos, 2016). In shallow unconfined aquifer the drawdown represents a decrease in water table elevation, whereas in deeper confined aquifers it represents a drop in hydraulic head for that aquifer. Within the sub-region the shallow and deep aquifers are separated by aquitards, and potential interaction is largely limited to areas where aquifers sub-crop at the base of the alluvium (Santos, 2016), for example within the Hoskissons Coal Member where it subcrops beneath the Coocooboonah Creek alluvium (Aryal et al., 2017b). Recharge to the Gunnedah Basin strata is likely to occur to the far east and far south of areas targeted for CSG extraction, and as such these strata are considered confined in the extraction areas (CDM Smith, 2014).

3.2 SIMED reservoir simulator

When compared to conventional gas reservoirs, there are several additional reservoir processes that occur during CSG production, including the relationship between coal permeability and effective stress, and the influence on permeability of matrix shrinkage that occurs during gas desorption. Both these processes can influence the extent to which CSG production will impact groundwater drawdown levels. These processes were not modelled in the ECLIPSE simulations undertaken by Herckenrath et al. (2015), however the SIMED reservoir simulator captures them in its representation of coalbed methane reservoir fluid storage and transport behaviour.

The model relating coal permeability to effective stress is derived from the conceptualisation of coal seam physical geometry as a vertical bundle of matchsticks (Figure 3-2), as per the model utilised by Reiss (1980), Seidle et al. (1992), Shi and Durucan (2004) and others. In this model the matchsticks represents the coal matrix porosity, while the space between matchsticks represents the coal cleat porosity. SIMED utilises the model developed by Shi and Durucan (2004) to account for permeability alteration due to both effective stress changes, and to matrix shrinkage resulting from gas desorption. The equation takes the form:

$$k = k_0 e^{-3C_f(\sigma^e - \sigma_0^e)}$$

Where k_0 is the reference permeability, C_f is the cleat compressibility, and σ^e is the effective stress, and:

$$\sigma^e - \sigma_0^e = -\frac{\nu}{1-\nu}(P - P_0) + \frac{E}{3(1-\nu)}[\varepsilon^s(C_{tot}) - \varepsilon^s(C_{tot0})]$$

Where ν is the coal Poisson's ratio, E is the Young's modulus, C_{tot} is the total gas content, and:

$$\varepsilon^s = \varepsilon_{max}^s C_{tot}/VLmax$$

Where ε^s is the dimensionless volumetric sorption strain and V_{Lmax} is the maximum Langmuir volume for the coal.

Inclusion of these relationships in the dual-phase modelling of the Namoi CSG reservoir will provide a more accurate representation of the coal seam fluid production and pressure drawdown behaviour during gas production. This will improve the representation of saturation and pressure behaviour which is then modelled in the approach of Herckenrath et al. (2015) to account for the presence of a gas phase in single-phase groundwater flow models.

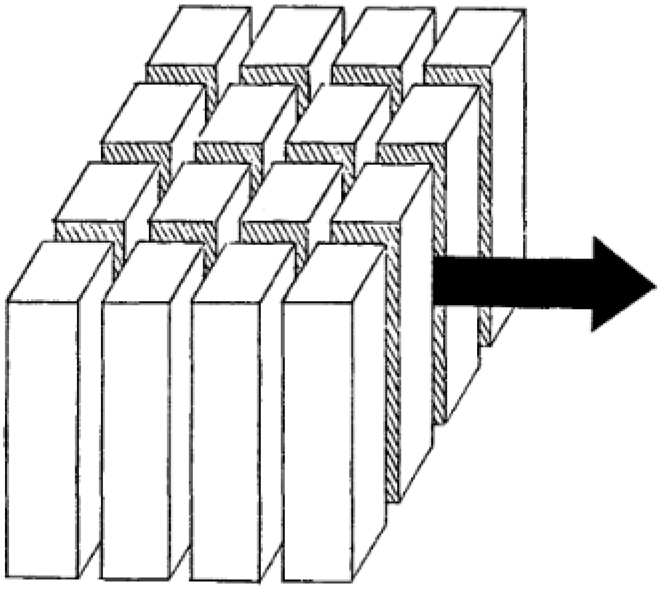

Figure 3-2 Coal matchstick geometry conceptualisation (Seidle, 1992).

3.3 Model geometry and lithology

The detailed stratigraphy and hydrostratigraphy of the Namoi sub-region are presented in Section 3.1 of the report. Previous groundwater flow models of the Namoi sub-region were constructed by CDM Smith (2014) for the Santos Narrabri Gas Project Groundwater Impact assessment, Schlumberger Water Services (SWS) for the Namoi Catchment Water Study (NCWS, 2012) and by CSIRO for the Bioregional Assessments (BA). These models combined stratigraphic units into model layers, using between 9 and 20 layers to represent the hydrostratigraphy of the sub-region. CDM Smith (2014) classified the stratigraphic layers as Significant Transmissive Units (STU), Less Significant Transmissive Units (LSTU), Probable Negligibly Transmissive Units (PNTU) and Negligibly Transmissive Units (NTU). These models did not attempt to represent the CSG production behaviour using the methodology developed by OGIA. The CSIRO Namoi CSG model constructed in SIMED utilised the discrete stratigraphic units and grouped hydrostratigraphic units described in the existing groundwater flow models, alongside their hydrogeological classifications as a basis for determining preliminary model layers and their associated stratigraphic units. Further data on lithology of the stratigraphic units, as well as representative formation depths and thicknesses within the Namoi sub-region were obtained from examination of well completions reports and well logs from exploration and pilot studies in the proposed Narrabri Gas project area. These formation depths were used to construct the representative model of the CSG project area.

Similar to the hydrogeological classification approach in the CDM Smith (2014) model, the stratigraphic units and layers in the Namoi CSG model can be broadly classified as either aquifer units, aquitard units or CSG target units. The depths to the stratigraphic unit tops used in the Namoi CSG model were based on depths provided in well completion reports for the wells utilised in the Bibblewindi 9-spot production pilot, and on reported thicknesses in the well completion reports for specific lithologies such as coals. The predominant lithologies in each of the stratigraphic and hydrostratigraphic units were determined based on literature and on data from selected well logs in the CSG project area. Each layer in the Namoi CSG model was then classified hydrogeologically based on data from existing groundwater models and the predominant lithology types. For each unit, the hydrogeologic classification, reported hydraulic parameters and thickness were compared in order to inform the amalgamation of stratigraphic units into a reduced number of model layers that would assist in improving model CPU time.

3.4 Model hydraulic parameters

Namoi sub-region groundwater modelling studies have attempted to collate hydraulic conductivity and specific storage data from numerous possible sources (e.g. colliery planning applications, Environmental Impact Statements), however they acknowledge that limited data are available and they are often applicable to small areas, whilst other published reports use generic values for different lithologies in their estimations (SWS, 2012). Initial estimates for hydraulic conductivity in the previous groundwater flow models often range over one to two orders of magnitude, but suggest that an order of magnitude estimation is still useful given the large range of possible hydraulic conductivities (CDM Smith, 2014).

Previous groundwater models have used different approaches for the configuration of hydraulic properties for individual model layers. The OGIA (2016) sub-model of the Talinga CSG field used realisations of a stochastic lithological model, combined with stochastic permeability/porosity models for each lithology type. Lithology/permeability/porosity realisations were upscaled and used to generate a probability distribution of permeabilities and porosities at the groundwater model grid scale. Initial values taken from these probability distributions were adjusted as part of the calibration process to well field production data. The SWS (2012) model chose the most representative hydraulic parameter values based on a range of calibrated values from the Lower Namoi Groundwater Flow Model (Merrick, 2001) which were then assumed to be homogeneous throughout all layers except the Namoi alluvium. These initial values were then varied during model calibration to match measured groundwater production and hydraulic head data. The BA model plotted permeability against depth for alluvium, interburden and coal-bearing layer categories, and modelled this relationship exponentially. This model was then used to populate the groundwater flow model with hydraulic conductivity values. These initial values were used as part of a probabilistic approach to the modelling, running the model with a range of conductivity and storativity values to explore sensitivity. The CDM Smith (2014) groundwater flow model for the proposed Santos Narrabri Gas Project adopted values of hydraulic conductivity and storativity based on physical characteristics of rock types (i.e. literature values) and hydrogeological information relating to the Gunnedah Basin, including existing modelling studies and their related investigations. For aquitard units, hydraulic conductivity values at the low end of estimated ranges were chosen in order to correspond with literature values for shale, mudstone and siltstone. Due to size of the model grid, production and pilot test data were not used to calibrate the model, instead varying values of hydraulic conductivity were adopted as part of a sensitivity and uncertainty analysis.

For the CSG model developed in this present study of the Namoi sub-region permeability and porosity data were collated from groundwater modelling studies, from pilot well drill string test (DST) results, and from permeability and porosity measurements on core collected in the project area. Permeability and porosity values from the literature for the general lithologies encountered in the project area were also considered.

The objective of the Namoi CSG model is to derive and model relationships between the key driving variables of gas and water production in order to improve the predictive capability of the CSIRO BA Namoi regional groundwater model. As such, in order to preserve correspondence between models, the values for hydraulic conductivity from the BA model were utilised as the basis for permeability values assigned to the Namoi CSG model. To do this, the relationships between hydraulic conductivity and depth for coal-bearing and non coal-bearing lithologies derived for the BA model were used to calculate and assign permeability values based on the depth and lithology of layers in the Namoi model. Differences in the number of model layers between the Namoi CSG and BA models meant that firstly, this approach was applied to all layers that comprised identical stratigraphic units between models, and secondly, to all layers that were not modelled explicitly as dual-porosity CSG targets (e.g. Bohena Seam and Hoskissons coal). The Upper Maules Creek Formation contains multiple interbedded coal and non-coal lithologies whose thicknesses are known in the Bibblewindi pilot area. In order to represent this in the Namoi CSG model as a single layer overlaying the Bohena Seam, the coal and non-coal lithologies were assigned permeabilities based on the derived BA relationships, and then the values were upscaled to a single layer using thickness-weighted averaging. The permeability of the Bohena Seam, the primary target for CSG extraction in the Namoi sub-region, is assigned from values of permeability derived from a drill string test (DST) performed in Bibblewindi 1. The DST results provide the most scale appropriate direct measurement for permeability available in the literature.

Data on horizontal to vertical permeability ratios were also collated from existing groundwater modelling studies and values were selected for each of the model layers based on the predominant lithology type and hydrogeological classification of the layer. Relative permeability curves were chosen for the layers likely to experience desaturation based on literature values and assigned for the different hydrogeological classification in the model.

The reported ranges for formation permeability based on previous modelling and literature values were used to inform the porosity of each layer, applying a lithology based porosity-permeability relationship derived from core data, and the porosity-depth relationship observed in the Bibblewindi pilot area. The cleat porosity of the Bohena CSG target seam was assigned from literature values, a value of 1.3% was assigned. The cleat porosity value represents only a portion of the total effective porosity of the coal seam, however the dual-porosity conceptualisation of coal limits the storage and flow of formation water to the cleat porosity only.

3.5 Model coal seam gas parameters and properties

The SIMED coal seam gas reservoir simulation software used in the CSIRO Namoi sub-model allows for representation of reservoir processes during CSG production not captured in traditional groundwater models. This includes relative permeability effects, the relationship between permeability and effective stress, and the influence on permeability of matrix shrinkage that occurs during gas desorption. All these processes can influence the extent to which CSG production will impact groundwater drawdown levels. Correct application of this functionality requires parameters which describe the physical properties of the coal in the CSG target intervals, this includes the coal gas content and composition, the gas adsorption and diffusion behaviour of the coal and the coal mechanical properties. The most prospective target coal seam for CSG production in the Namoi sub-basin is the Bohena Seam of the deeper Maules Creek Formation, which is expected to account for approximately 94% of water production (CDM Smith, 2014). Gas content and composition data, as well as Langmuir isotherm values for the Bohena Seam coal (Maules Creek Formation) and the Hoskissons Coal (Black Jack Group) were collated from a report that examines the CO_2 storage potential of the Namoi sub-region (Gurba et al., 2009), as well as from laboratory measurements on core extracted from exploration pilot wells in the project area. The CSIRO model used these data to derive average values of the gas content and coal adsorption properties for the coals of the Black Jack Group and the Maules Creek Formation. The produced gas consists of predominantly CH_4 and the model assumes 3 percent consists of CO_2 which is the maximum allowable CO_2 content to meet surface pipe specifications. Measured values of CO_2 content display spatial variability, ranging from negligible to 66% in the sub-basin (Gurba et al., 2009), the SIMED model assumes CSG production occurring in a low CO_2 content area. The values for coal gas content, composition and adsorption parameters are presented in Table 3-1 and Table 3-2.

Table 3-1 Prescribed gas content and composition of coals in Namoi CSG model.

CSG TARGET	GAS CONTENT (M^3/T)	ADSORBED GAS COMPOSITION (%CH_4 / %CO_2)	DESORPTION TIME (DAYS)
Black Jack Group	7.8	97/3	0.2
Maules Creek Fm	12.4	97/3	0.2

Table 3-2 Prescribed Langmuir properties of coals in Namoi CSG model.

CSG TARGET	LANGMUIR VOLUME (M3/T)		LANGMUIR PRESSURE (MPA)	
	CH_4	CO_2	CH_4	CO_2
Black Jack Group	17.8	38.2	4.2	2.3
Maules Creek Fm	22.6	41.5	5.3	2.9

The desorption time is a parameter describing the rate of gas diffusion from the coal matrix into the coal cleat porosity as gas is desorbed during CSG production. This value is not measured for any of the data collated from well reports and was therefore estimated from the literature (Crosdale et al., 1998; Laxminarayana & Crosdale, 1999), alongside other relevant coal properties such as cleat compressibility (Seidle, 2011).

3.6 Model mechanical parameters

The reservoir simulator requires estimates of mechanical properties for the different rock types present in the model. Depending on the model for stress-dependent permeability chosen, the required inputs may include Young's modulus, Poisson's ration and formation compressibility. Previous groundwater models use the specific storage parameter to represent groundwater storage in the formation porosity, which includes a previously assumed value for formation compressibility. The SIMED reservoir simulator requires a separate input for formation compressibility however this value, alongside other mechanical properties, was not encountered in any literature specific to the Namoi project area. Thus values for these properties have been assumed from wider literature for similar rock types. The model mechanical parameters are presented in Table 3-3.

Table 3-3 Mechanical parameter inputs for Namoi CSG model layer types.

LAYER TYPE	YOUNG'S MODULUS (kPa)	POISSON'S RATIO	FORMATION COMPRESSIBILITY (1/kPa)
Coal	2960	0.27	7.8e-05
Aquifer	n/a	n/a	1.0e-05
Aquitard	n/a	n/a	1.5e-05

3.7 SIMED preliminary model construction

A comparison of the spatial geometry and production parameters of the preliminary SIMED Namoi CSG model and the OGIA Talinga sub-model used for the derivation of saturation versus pressure relationships is presented in Table 3-4. The initial steps undertaken to develop the appropriate CSG model in SIMED included:

- An assessment of the role of the model boundary. SIMED implements a no-flow condition at the model boundary that could affect the predicted drawdown; this must be either quantified or mitigated by extending the boundary distance.
- Determining the effect of total number of grid blocks on simulation run time and CPU requirements.
- Examining drawdown and water production from model layers and assessing options for model streamlining to reduce CPU run time.

Taking into account the aforementioned steps, the final configuration consisted of a 15 layer, ¼ well symmetry model, whose output was then compared against expected water and gas production reported in the Santos Environmental Impact Statement (EIS) (Santos, 2016). Further details of this model and the subsequent calibration and simulations are provided in the following chapter.

Table 3-4 Comparison of OGIA (2014) and preliminary Namoi CSG model parameters.

MODEL PROPERTY	OGIA TALINGA SUB-MODEL	CSIRO NAMOI CSG MODEL
Grid block size	200 m	25 – 40 m
No. of layers	294	15
Hydraulic parameters	stochastic lithology model	after BA Namoi groundwater model
Production life	25 years (50 recovery)	20 years
Calibration	previous gas and water production	Expected gas and water production based on Namoi CSG EIS (Santos, 2016)

4 Relationships between groundwater pressure and production rate in the CSG field

The coal seam gas simulation component of the project was undertaken to identify how groundwater production is related to water table level or other key reservoir variables. Utilising the representative Namoi CSG model, simulation results were compiled to investigate the potential for developing simple relationships between the key driving variables operating in CSG reservoirs and groundwater production, in a similar manner to that used in the OGIA modelling described by Herckenrath et al. (2015). The intent was to derive relationships for the Namoi sub-region suitable for incorporation into the regional groundwater models produce in MODFLOW.

4.1 Coal seam gas model properties

This section provides a summary of the values assigned to parameters of the representative Namoi sub-regional model used in CSG production simulations using the SIMED reservoir simulator. Chapter 3 provides a more detailed discussion of the methodology used to derive the geological, hydraulic, mechanical and CSG gas content and desorption properties used in the model. The model represented the production from a single vertical well situated within the CSG field boundary. A 1/4 well symmetry model was used to improve simulation run times, consisting of a 20 x 20 grid block spatial grid with exponential grid refinement in the near well region. The model covered an area of 265 x 265 m; the spatial dimensions of the model were based on minimum well spacing proposed in the EIS for the Narrabri Gas Project (Santos, 2016). The spatial grid of the Namoi CSG model is presented in Figure 4-1.

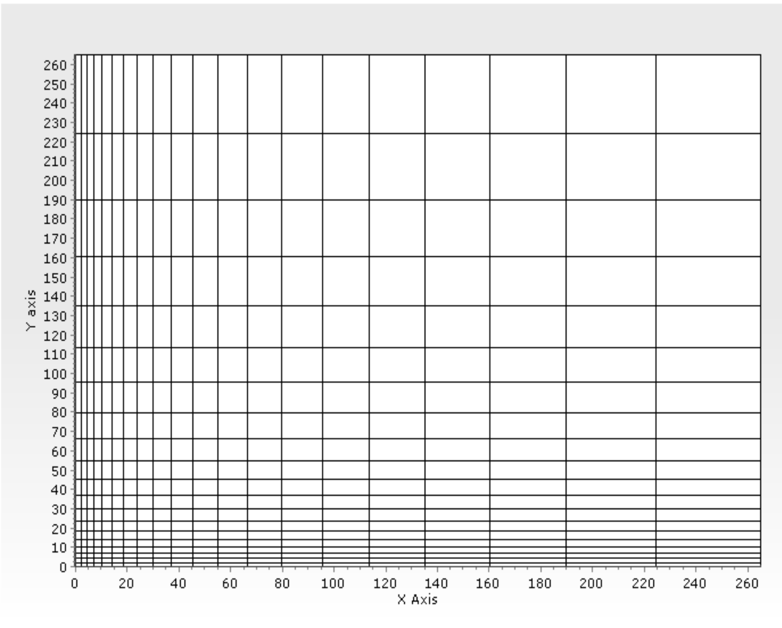

Figure 4-1 Spatial dimensions of the Namoi CSG model.

In a CSG field development, well interference is utilised to effect regional pressure drawdown, in order to promote methane desorption from the coal surface. The desorbed gas then flows as free gas through the coal cleat porosity toward the producing well. The boundaries of a symmetry model represent the no flow condition imposed by interference from adjacent producing wells in a wider CSG field. The 265 x 265 m dimensions of the Namoi CSG model therefore represented a regular vertical well spacing of 530 m. Regional groundwater flow models such as those created for the Surat CMA often employ grid block sizes of around 1.5 x 1.5 km. Across the Namoi region it is possible that such grid blocks will be located entirely within the boundaries of a producing CSG field, where well interference behaviour is dominant, and the influence of adjacent aquifers, such as at a field boundary is not present. The symmetry model thus investigated the reservoir fluid flow processes unique to CSG production where they are likely to be most influential. The influence of adjacent aquifer flow such as at the boundary of the field development was examined as part of the chapter investigating scale dependency of the impact of CSG production on regional groundwater flow models.

The model consisted of 15 vertical layers representing the varying lithology of formations in the Narrabri Gas Project target area. CSG production was modelled from the Bohena Seam of the Maules Creek Formation only, as this is predicted to represent 94% of water production (CDM Smith, 2014). The formation depths, thicknesses and selected reservoir properties are presented in Table 4-1. Vertical permeability of non-coal layers was set to 10% of horizontal permeability, and for coal layer at 1% of horizontal permeability. Further discussion of the derivation of model properties can be found in Chapter 3.

Table 4-1: Layer properties for Namoi CSG model.

GEOLOGICAL UNITS	LAYER	DEPTH TO TOP (M)	THICKNESS (M)	PERMEABILITY (MD)	POROSITY (%)
Narrabri Formation (Fm)	15	0	89.5	2.6	20.5
Gunnedah Fm					
Cubbaroo Fm					
Warrumbungle Volcanics					
Liverpool Range Volcanics					
Bungil Fm	14	89.5	21.5	0.74	13
Mooga Sandstone					
Orallo Fm					
Pilliga Sandstone (upper)	13	111	172	0.34	12
Pilliga Sandstone (lower)					
Purlawaugh Fm	12	283	30	0.15	9
Garrawilla Volcanics (upper)	11	313	211	0.06	8.8
Garrawilla Volcanics (lower)					
Deriah Fm					
Napperby Fm					
Napperby Fm (basal)					
Digby Fm (Ulinda Ss)	10	524	40	0.023	12

Digby Fm					
Digby Fm (Bomera Congl.)					
Trinkey Fm	9	564	68.4	0.02	5.6
Wallala Fm					
Breeza Coal					
Clare Sandstone					
Hows Hill Coal					
Benalabri Fm					
Hoskissons Coal	8	632.4	9.6	0.15	9
Brigalow Fm	7	642	50.6	0.009	7
Arkarula Fm					
Melvilles Coal Member					
Pamboola Fm					
Watermark Fm	6	692.6	138.9	0.004	2.1
Porcupine Fm					
Upper Maules Creek Fm	5	831.5	51.7	0.03	7.4
Rutley Seam					
Interburden					
Namoi Seam					
Interburden					
Parkes Seam					
Interburden					
Bohena Seam	4	883.2	8.3	18.9	1.3
Lower Maules Creek Fm	3	891.5	39.1	0.001	12
Goonbri Fm	2	930.6	121	0.0007	10
Leard Fm					
Werrie Basalt And Boggabri Volcanics (Basement)	1	1051.6	148.4	0.00025	2

The model layers were assigned hydrostatic pressure at initial conditions, and the coal seam gas related properties including Langmuir constants, desorption pressure, and gas desorption times were as described in Table 3-1 and Table 3-2. Well and production data are presented in Table 4-2. Initial water production rates were calculated based on the regional peak water production rates and regional cumulative water production values specified in the Narrabri Gas Project EIS (Santos, 2016). The specified bottom hole pressure is based on literature values for typical CSG production scenarios.

Table 4-2 Well and production data for Namoi CSG model.

SIMULATION PARAMETER	VALUE	UNIT

Surface water rate	55	m^3/day
Bottom hole Pressure	250	kPa
Production period	20	years
Well radius	0.114	m
Completion interval	Bohena Seam	n/a
Production period	20	years

4.2 Performance of symmetry model

Simulations of the previously described CSG production scenario were undertaken on the SIMED Namoi CSG model. The outputs from the production simulation were compared to predicted water and gas production data provided in the Narrabri Gas Project EIS (Santos, 2016) and Eastern Star Gas (Eastern Star, 2007; Eastern Star, 2011). The symmetry model showed broad agreement with the predicted cumulative gas and water production, peak gas and water production rates, and average gas and water production rates for an individual well in the Narrabri Gas Project. Details of the model performance are presented in herein.

Table 4-3 Comparison of Namoi CSG model output and estimated average reported values.

OUTPUT	NAMOI CSG MODEL OUTPUT	ESTIMATED AVERAGE REPORTED VALUE	SOURCE
Peak water production rate (per well)	55 m^3/day	51 m^3/day	Narrabri GAS Project EIS base case (CDM Smith, 2016)
Average water production rate (per well over field life)	4.3 m^3/day	4.6 m^3/day	Narrabri GAS Project EIS base case (CDM Smith, 2016)
Cumulative water production (per well)	31.4 ML	41.8 ML	Narrabri GAS Project EIS base case (CDM Smith, 2016)
Peak gas production rate (per well)	703 mscf/d	730 – 1040 mscf/d	Well average based on Bibblewindi 9-spot modelled production (Eastern Star, 2007)
Cumulative gas production (per well)	0.99 bcf	1.6 bcf	Well average based on 1520 PJ 2P reserves estimate (Eastern Star, 2011)

Comparison of the output from the Namoi CSG model to estimated average reported values is presented in Table 4-3. The comparison demonstrates that production simulations using the Namoi CSG model produce similar values for gas and water production to those estimated by operators from environmental impact statements, CSG modelling and production pilots. The estimated average reported values for cumulative gas were derived from the overall 2P reserve estimate for the gas project (Eastern Star, 2011) and the expected number of wells (Santos, 2016). The values for cumulative water are based on the base case for total extracted water volume and number of wells (CDM Smith, 2016). Cumulative values for water and gas production from the simulation are sensitive to the thickness of the target interval, which is fixed in the Namoi CSG symmetry model, but can vary across the project area from 6.5 to 15 m (Gastar, 2006).

The estimated average reported values for peak gas production rate were based on modelled peak gas rates for the Bibblewindi 9-spot production pilot (Eastern Star, 2007) converted to a per well estimate. For average and peak water production values were based on the maximum rates supplied in the CDM Smith (2016) base case adjusted to a per well basis. Peak water and gas production rates, and average water production per well over the life of the field show agreement between simulations using the CSG model and reported values.

Pressure drawdown within the symmetry model is affected by the model boundary and thus represents a theoretical pressure drawdown due to well interference in a specific field development grid pattern. In addition, the SIMED reservoir simulator applies a no-flow condition at the model boundaries and cannot represent potential recharge of the model layers due to lateral groundwater influx. Both these limitations affect drawdown values, which will likely differ to those generated by specialised regional groundwater modelling packages. The maximum pressure drawdown in each layer of the Namoi CSG model for the described simulation scenario is presented in Figure 4-2. As expected the results indicate significant drawdown in the target coal seam and adjacent formations, with negligible drawdown occurring in the shallower layers. As mentioned, these values must be interpreted in the context of the symmetry model being used.

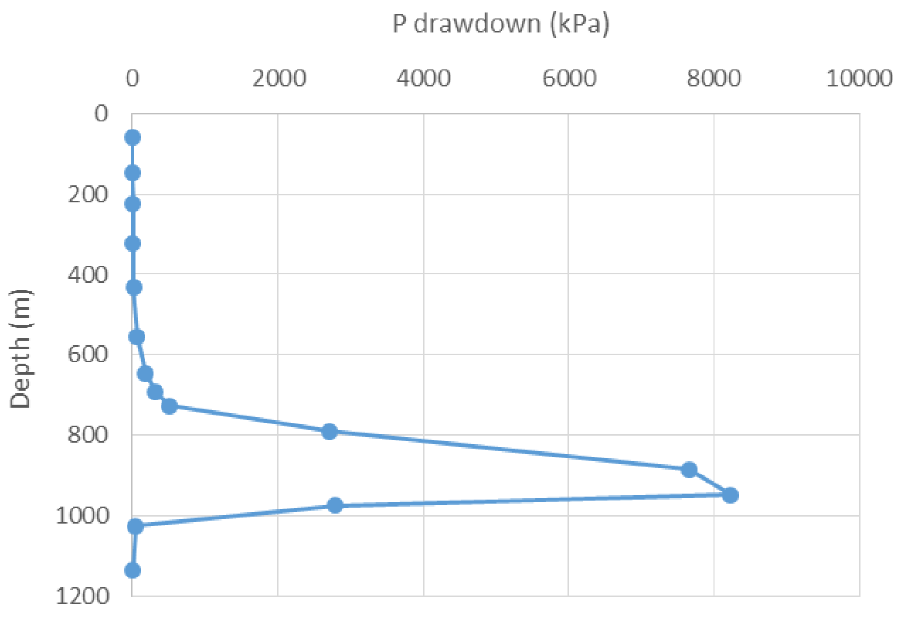

Figure 4-2 Pressure drawdown vs depth for simulated production scenario in Namoi CSG model.

A calibrated model that can simulate expected water and gas production behaviour for the specific field (in this case the Narrabri Gas Project) is a necessary requirement for further investigations between key driving variables of CSG production in that field. The Namoi CSG model developed for SIMED utilised broad data relating to stratigraphy, reservoir properties, and production scenarios for the Namoi sub-region to produce simulations that reflect the measured and expected behaviour of producing CSG wells in the project area, suggesting a suitable basis for further investigation of variables of CSG production.

4.3 Relationships between driving variables in CSG production

SIMED reservoir simulations of CSG production using the Namoi CSG model create a suite of well-specific, regionally averaged, and spatially varying data for specified times throughout the production and recovery period. Simulations were run to include gas and water production for a period of 20 years.

Well-specific data include cumulative gas and water production, surface gas and water rates, bottom hole flowing pressure, gas-water ratios and individual gas component rates. The SIMED well model allowed for constant surface water rate control, switching to constant bottom hole pressure control once a specified bottom hole pressure was reached. No well skin or permeability alteration was assigned to the well.

Regionally averaged data are averaged over all grid cells in the model domain, or over a user-specified area of the model. For these simulations averaged data were collected for the entire model and for a subsection of the model consisting of grid blocks in the target layer (Bohena Seam of the Maules Creek Formation). The simulation results for this production scenario and model indicated that this is the only layer to undergo desaturation. The regional averages are derived from the spatially varying data, which are calculated for every model layer at specified time points. Regionally averaged and spatially varying data include: pressure, water saturation, porosity, pore volumes, coal cleat and coal matrix specific variables, individual component material balance data, and gas content.

4.3.1 Internal grid-block relationships between grid distributed variables

Relationships that occur between key driving variables within each individual grid block were investigated. At each specified time point during a simulation, an array of values for pressure, saturation etc. for each individual grid block are generated. The values vary temporally and spatially, and can be investigated within this framework to assess if relationships between the variables exist. Such relationships will differ for different model geometries, reservoir properties and production scenarios, therefore results are specific to the Namoi CSG model. An example of investigating internal grid block relationships as they vary spatially and temporally is the Herckenrath et al. (2015) determination of a time-asymptotic pressure-saturation relationship in single layer and six layer CSG models.

Figure 4-3 presents the relationship between water saturation and pressure at different production times for all the grid blocks in the model that experience desaturation during CSG production. The model results indicated that desaturation was confined to the targeted Bohena Seam in the Maules Creek Formation.

Unlike results from the model used by Herckenrath et al. (2015) the relationships displayed from the Namoi CSG symmetry model do not show a time-asymptotic behaviour. This result is expected given the different intended scale of the two models; the former representing a complete well field in a significantly larger region, and the latter representing single well interference within the boundaries of a producing CSG field. The relationship between S_w and P in the grid blocks that experience desaturation alters with increasing production time. This could occur as flow in the CSG model progresses from a pressure transient regime to a boundary dominated flow regime, and as all grid blocks within the target interval experience significant pressure drawdown and gas desorption into the cleat porosity. This results in a different S_w vs P curve shape between the early time data and the late stage production data.

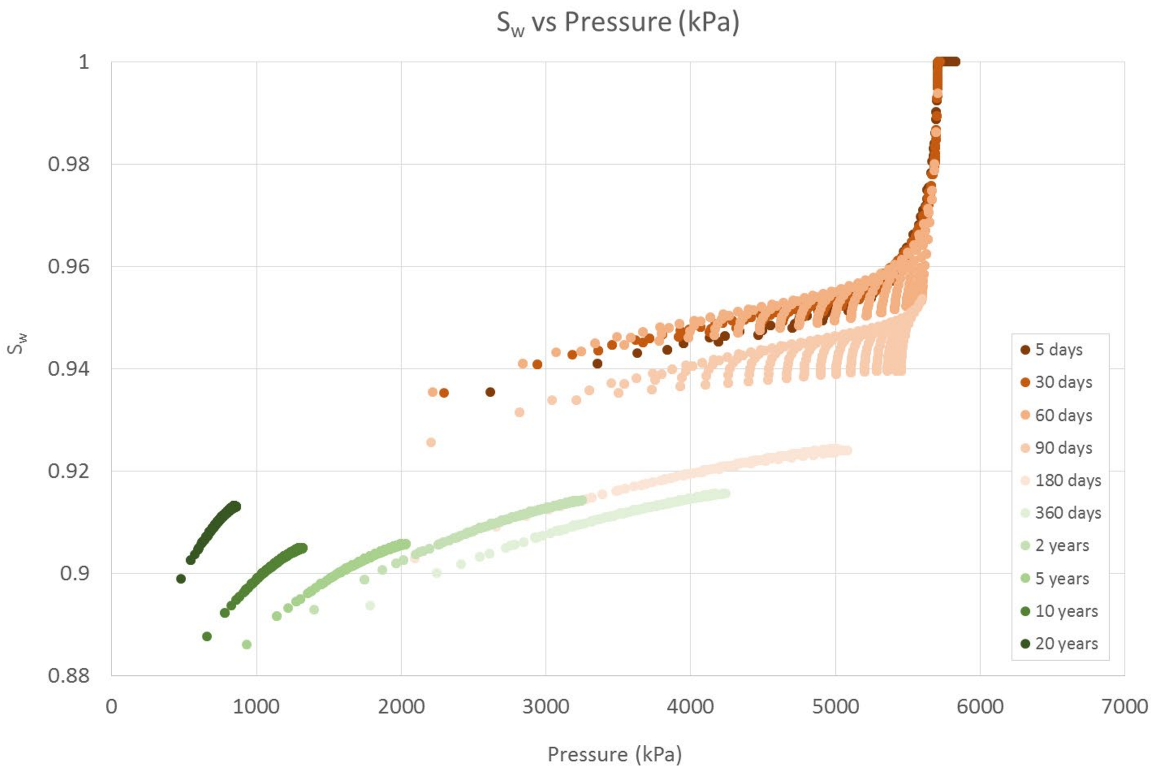

Figure 4-3 Plot of S_W vs P for grid distributed variables that experience desaturation.

Early time data in the pressure transient flow regime displayed larger spreads of pressures and saturations (Figure 4-3). This early data also showed closer resemblance to the relationship approximated by Herckenrath et al (2015) using the van Genuchten (1980) unsaturated flow relationship. As expected, the complex saturation and pressure relationship resulting from changing fluid flow regimes propagates through other relationships, and is dominant in the relationship between grid block effective permeability to water and pressure displayed in Figure 4-4. This relationship is also affected by the effect of matrix shrinkage due to gas desorption, and by the relative permeability behaviour of the coal, which is often difficult to measure due to the heterogeneity, low porosity and stress-dependent permeability (Meaney and Paterson, 1996).

The absolute permeability of the target formation in the Namoi CSG model displays the effect of stress-dependent permeability in the very early stages of production (Figure 4-5). Similarly, the matrix shrinkage effect due to gas desorption is indicated by the increase in absolute permeability for grid cells at later stages when pressure (and thus gas content) decrease. The curve shape simply reflects the derivation from the conceptualisation of coal seam permeability alteration given by Shi and Durucan (2004).

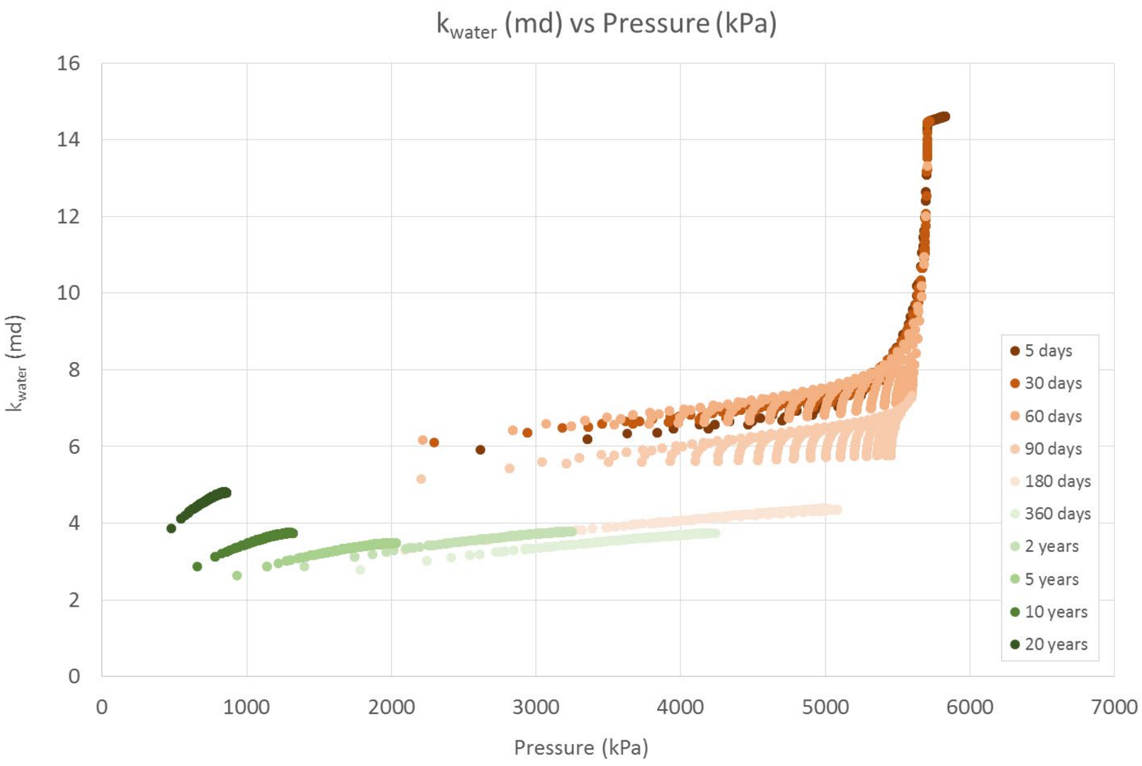

Figure 4-4 Plot of effective permeability to water vs pressure for grid cells within target seam.

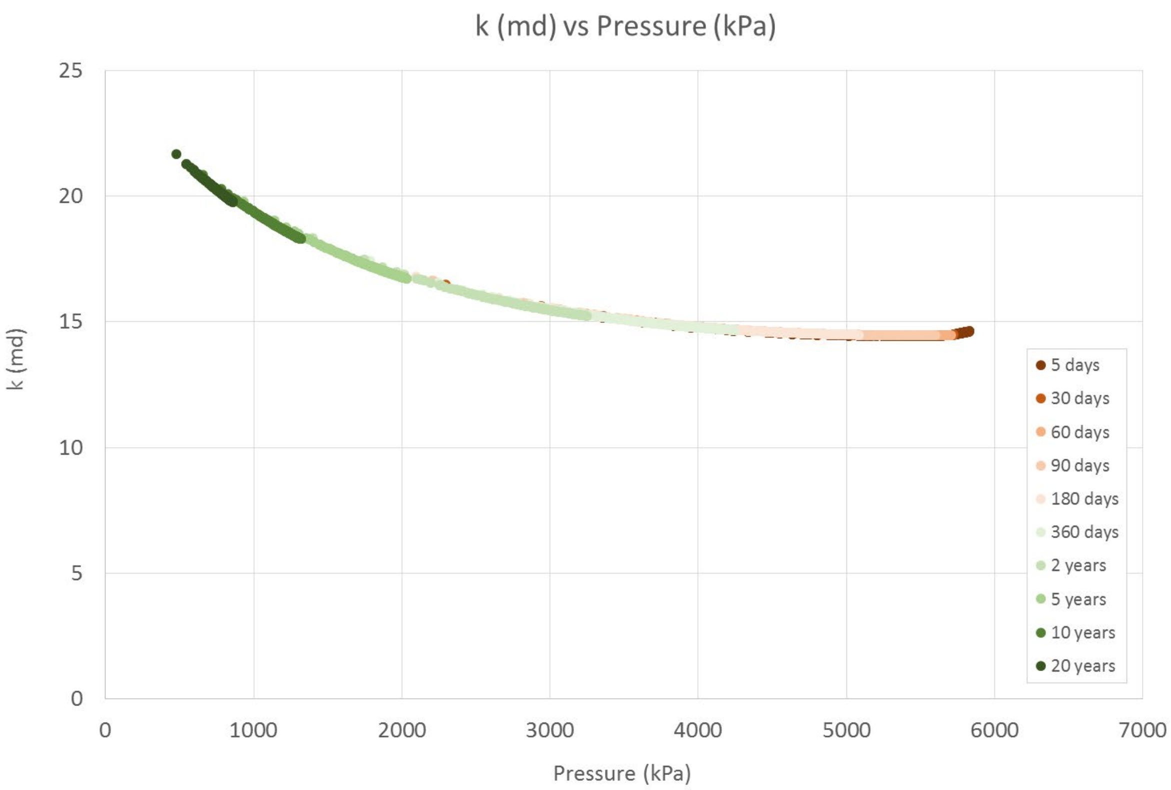

Figure 4-5 Plot of absolute permeability vs pressure for grid cells within target seam.

4.3.2 Relationships averaged across the target layer

The production simulation using the Namoi CSG model generates outputs that are averaged for user pre-defined subdomains of the model. For the production simulations, averaged outputs were collected for both the entire model domain, and for the Bohena Seam target layer. These averaged outputs represent a rudimentary arithmetic averaging method for upscaling of production and reservoir properties to a coarser scale. SIMED does not export averaged permeability values for specified subdomains. Upscaled values for horizontal permeability in the Bohena Seam target layer were calculated separately using volume-weighted averaging methods.

Figure 4-6 presents the average saturation across all grid cells of the target layer against the average pressure for the target layer. These data are presented superimposed against the grid distributed data previously derived. The plot indicates that comparing layer averaged saturation and pressure values produces a curve shape that can be approximated by the van Genuchten (1980) relationship. Comparison of the averaged data with the temporally varying grid distributed data reveals that the averaged relationship cannot sufficiently approximate the spatial distribution of S_W vs P behaviour in all grid cells at all times during CSG production. Early time production experiences less desaturation in low pressure grid blocks than would be predicted using the average, whilst later stage production shows greater desaturation in low pressure grid blocks than would be predicted using the layer average.

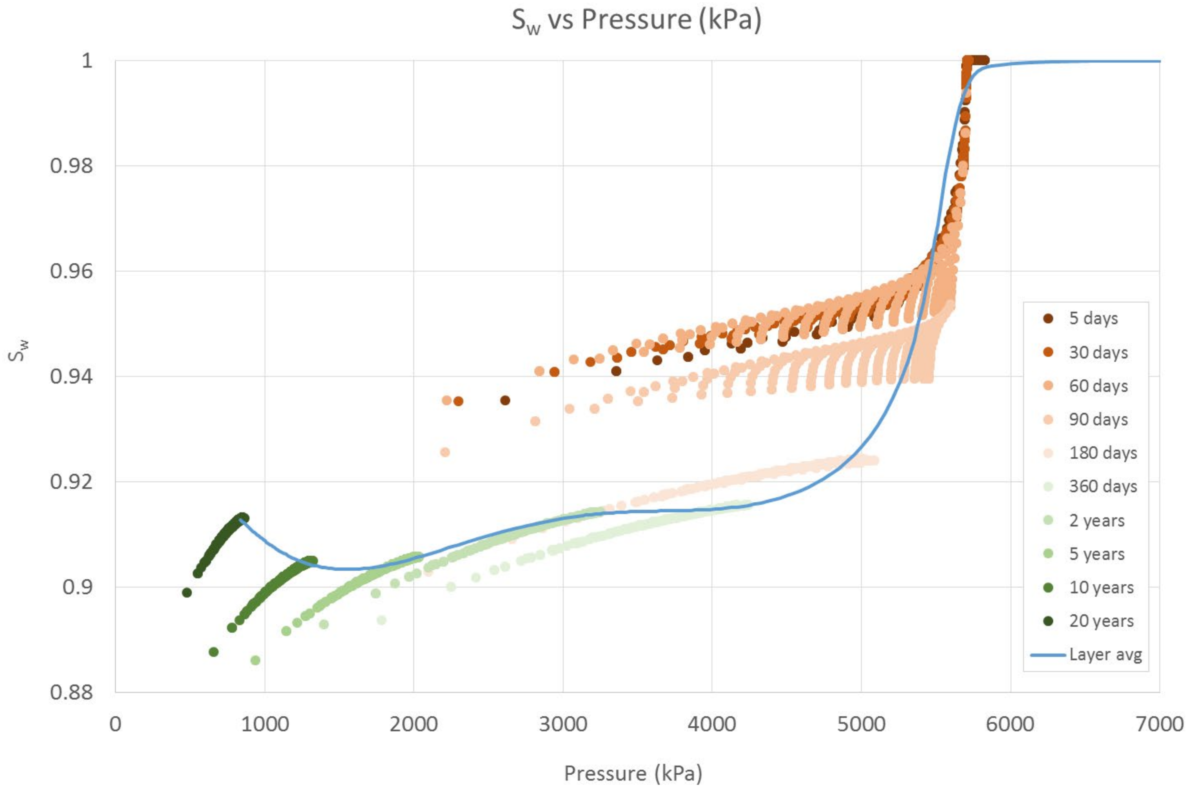

Figure 4-6 Plot of average saturation vs average pressure for the entire model target layer, superimposed against grid distributed data.

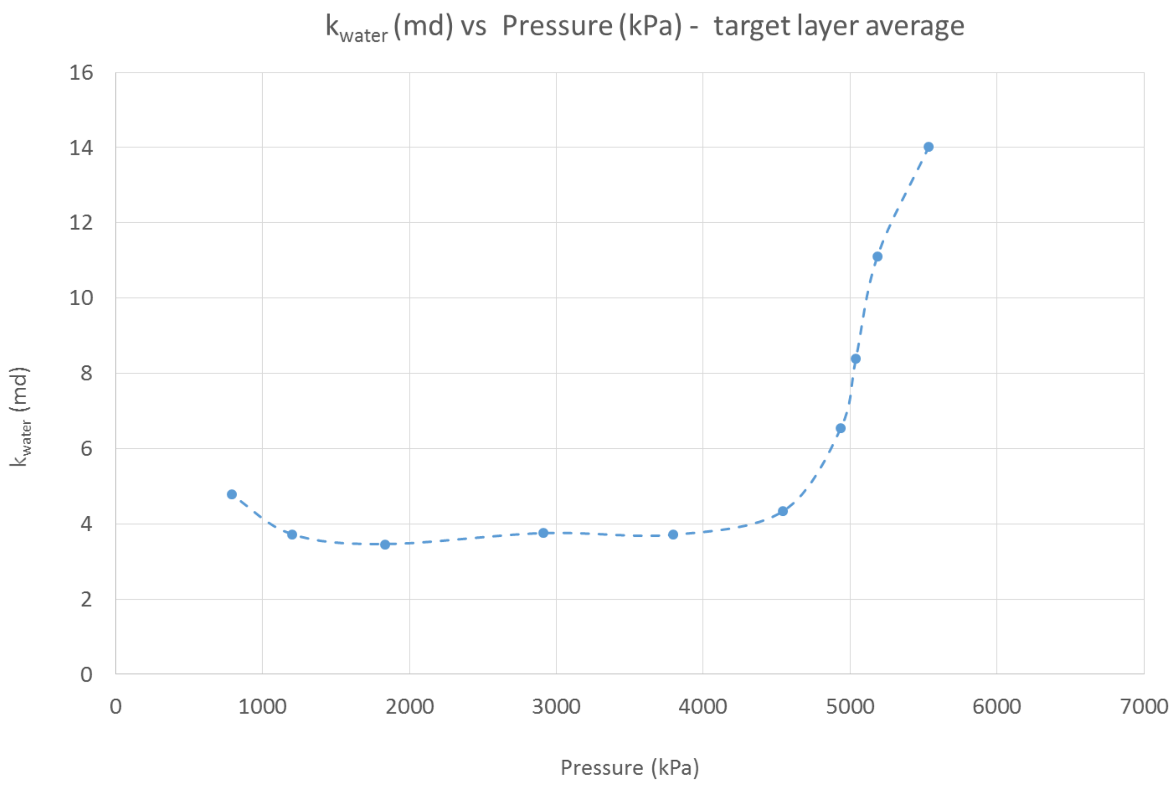

Figure 4-7 Upscaled effective permeability to water vs average pressure for the model target layer.

Figure 4-7 presents the upscaled horizontal effective permeability for the entire model layer versus the average pressure. At a selection of times during the field life a single upscaled value for layer pressure and saturation were calculated. The plot confirms that, as with the grid distributed data, averaged relationships between any saturation dependent variables are strongly influenced through propagation of the saturation behaviour. These results indicate that, alongside the behaviour seen in individual grid blocks, the averaged saturation-pressure relationship across the target layer will be sensitive to the relative permeability curve used for the target formation.

4.3.3 Wellbore data relationships

The production simulation produces well-specific outputs that vary with time, including water and gas production rates and cumulative amounts, bottom hole pressure, gas-water ratio, and component specific production rates. Figure 4-8 and Figure 4-9 present the gas and water production rates and cumulative production for the production simulation. Both the production rates and cumulative production are converted to the total well drainage area, by multiplying the symmetry model result by four. The initial spike in gas rate is due to desorption in the near wellbore area, while the wider effects of gas desorbing into coal cleat porosity across the entire model domain are visible in the production rate results from approximately 60 days as the water rates fall and gas rates rise. Figure 4-9 shows the cumulative gas production levelling off at a greater rate than the water production.

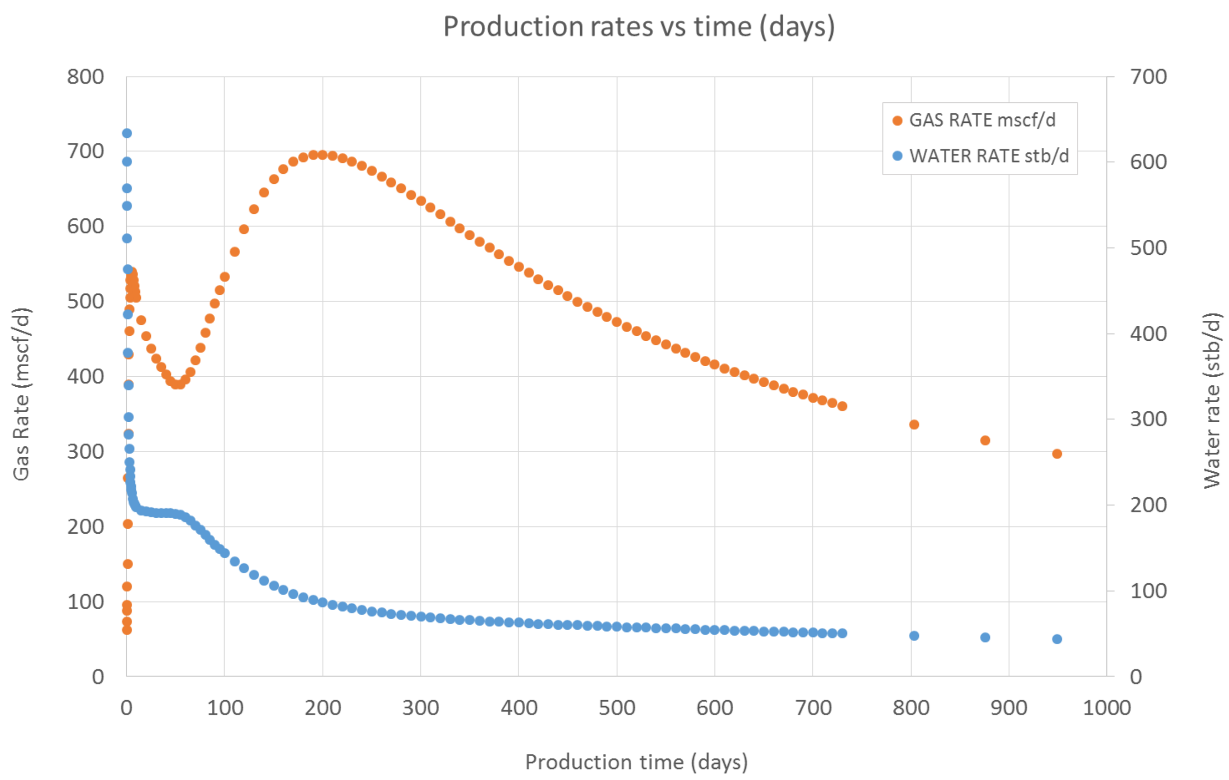

Figure 4-8 Production rate vs time for the Namoi CSG model.

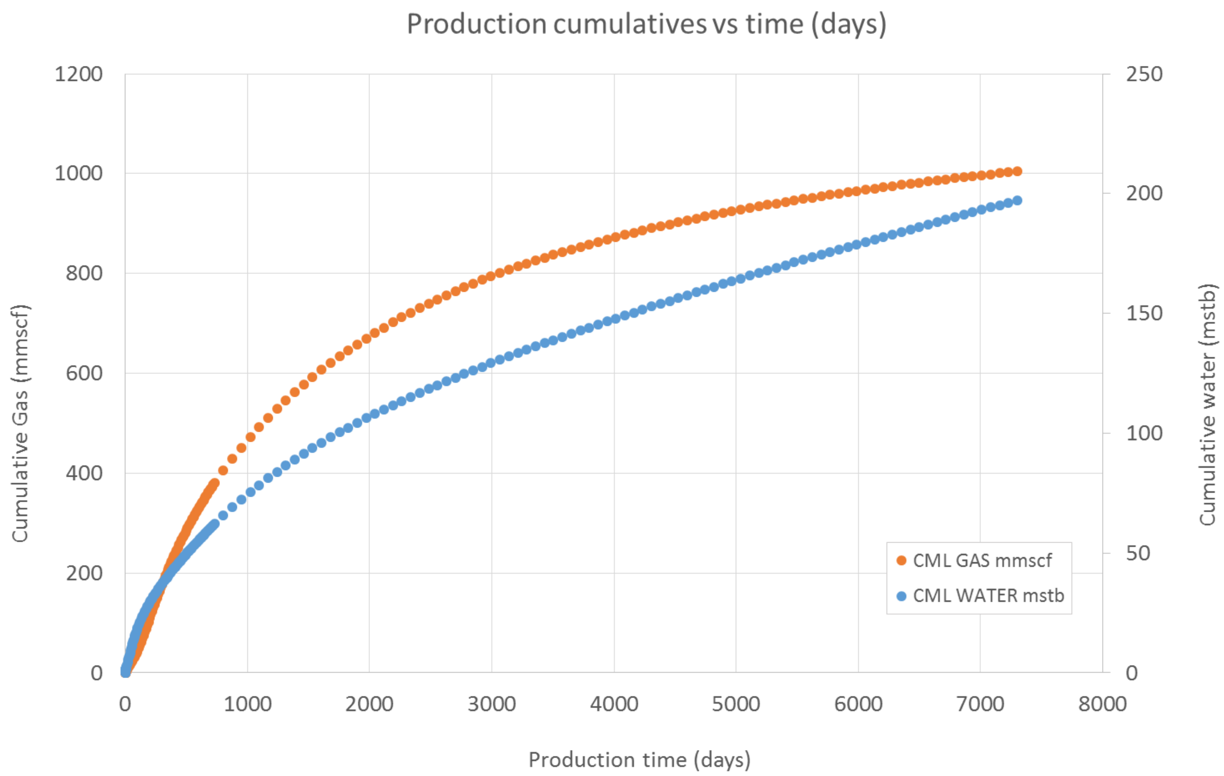

Figure 4-9 Cumulative rates vs time for the Namoi CSG model.

Of the wellbore based outputs produced by SIMED, the water production rate can be compared to a groundwater abstraction rate that may be assigned in a MODFLOW regional groundwater model. Comparison of selected sub-domain averaged values to the water production rate may yield relationships amenable to inclusion in a regional groundwater model. The average pressure in the Bohena Seam target layer versus production water rate is plotted in Figure 4-10. It displays an increasing monotonic relationship between the variables, while a noticeable change in water production rate occurs across the desorption pressure for the coal seam.

Figure 4-11 presents a plot of the average target layer saturation versus water production rate. The saturation relationship displays a similar relationship to water production rate as it does to averaged and individual grid block pressure. This is expected due to the increasing monotonic relationship between water production rate and pressure (Figure 4-10). A plot of upscaled target layer horizontal permeability versus water rate presented in Figure 4-12 also displays a similar characteristic shape as when plotted against pressure (Figure 4-7), again resulting from the monotonic relationship demonstrated in Figure 4-10.

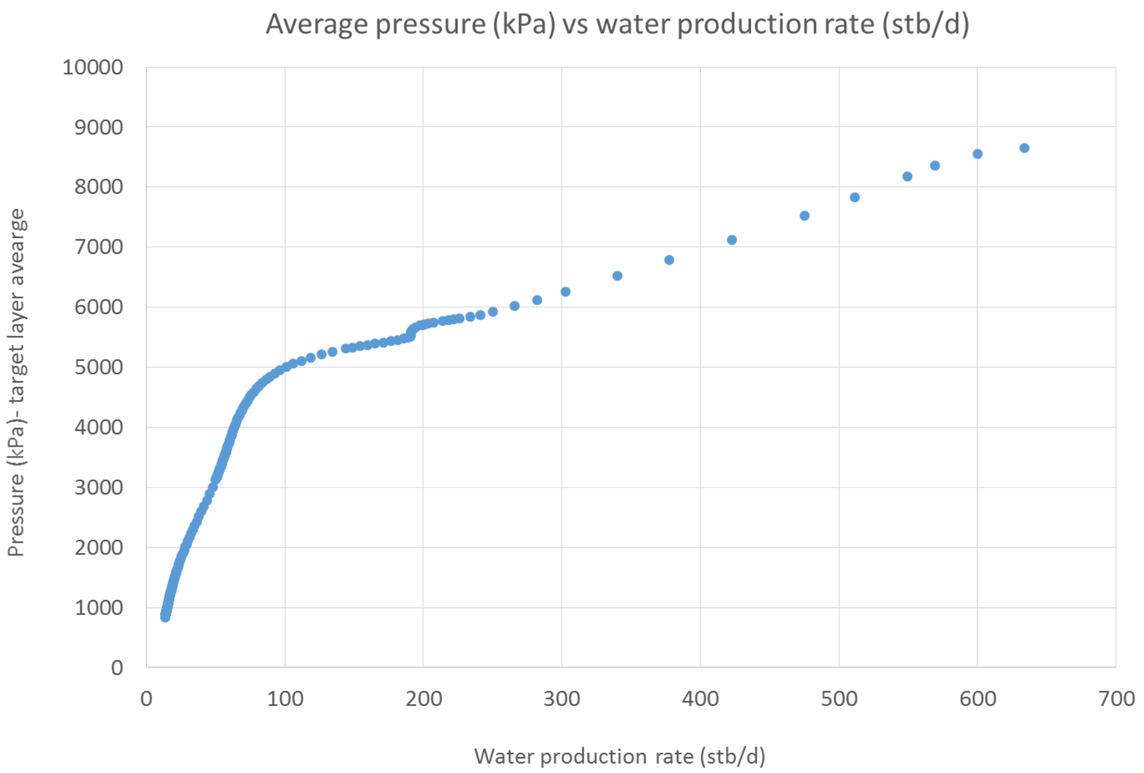

Figure 4-10 Target layer average pressure vs well water production rate.

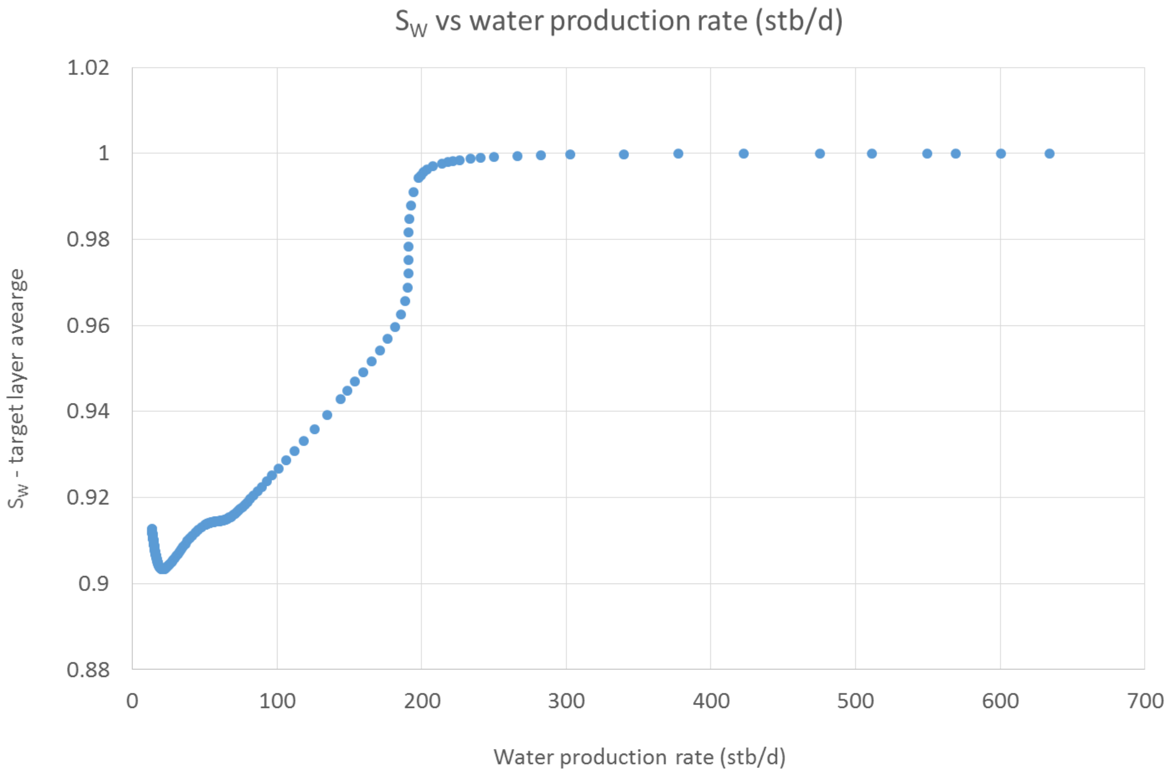

Figure 4-11 Target layer average saturation vs well water production rate.

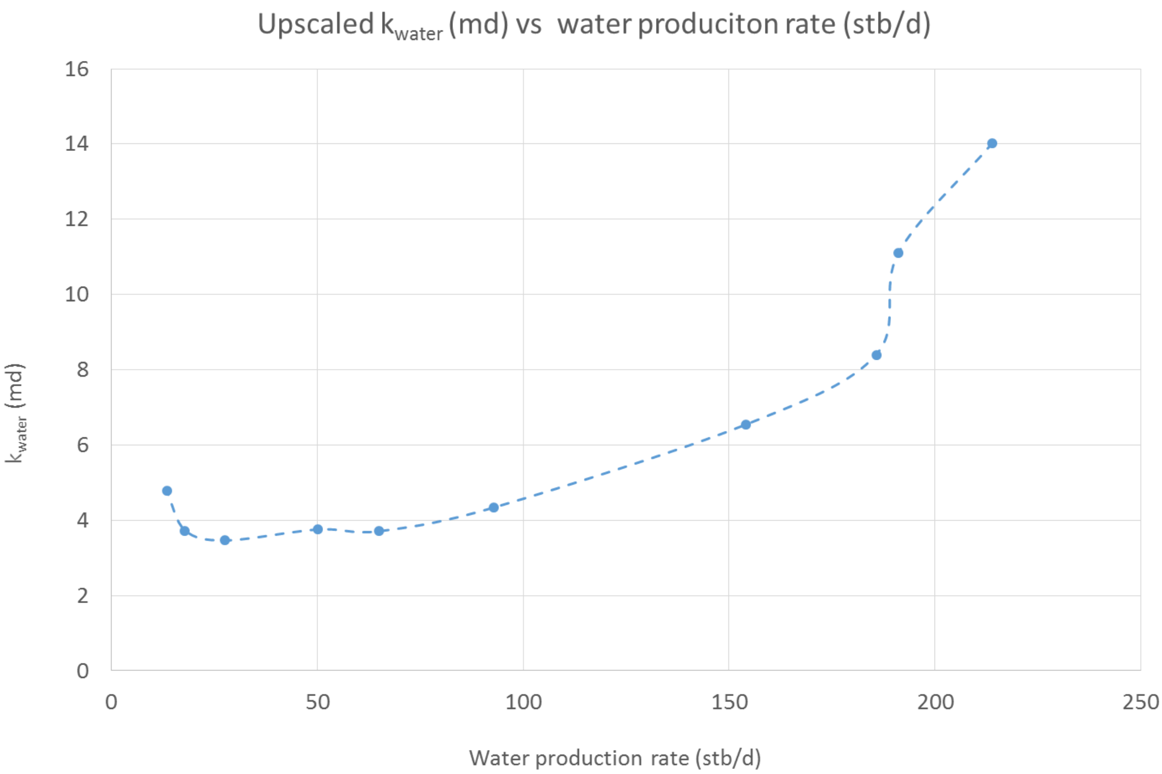

Figure 4-12 Upscaled target layer horizontal permeability vs water production rate.

4.4 Production and groundwater relationships derived for within the CSG field

Simulations undertaken on the Namoi CSG well-symmetry model were used to explore relationships between key driving variables operating in the reservoir during CSG production. The results were specific to a portion of the producing reservoir contained within the boundary of the CSG well field, where pressure interference between adjacent producing wells results in higher levels of pressure drawdown and gas desorption.

Examination of intra-grid block relationships, such as grid block saturation versus pressure (Figure 4-3) and grid block permeability versus pressure (Figure 4-4), indicate that while observable relationships occur between the variables at a given production time, a time-asymptotic pseudo-steady state behaviour is not likely to occur in a subset of grid blocks contained entirely within the boundaries of the CSG well field. This is due to the large reduction in pressure seen by all the grid blocks of interest over the production life of the field, and indicates that for a time-asymptotic relationship to be identified, it may only be possible across a set of grid blocks that also includes those that do not see a significant reduction in pressure during production. Consequently, the distribution of grid blocks in this set will affect the derivation of averaged relationships, which may not as closely approximate grid-block relationships, as shown in Figure 4-6.

Implementation into regional groundwater models of any relationships between the driving variables of gas and water production will require understanding of the effects introduced by the particular set of grid-block and simulation data used to describe the relationships. In the case of intra-grid block relationships, the number of cells and their proximity to the producing field will need to be examined. In the case of relationships based on well production rate (Figure 4-10 to Figure 4-12) the influence of adjacent wells and proximity to field boundary would also need to be examined to develop a relationship suitable for implementation. These considerations are addressed as part of the following chapter examining the effects of regional model spatial scale.

5 Approaches to representing coal seam gas groundwater impacts at the spatial scale of the MODFLOW grid

The grid scale utilised in regional groundwater modelling is coarser than what is often employed for modelling subsurface behaviour and production of gas and water in coal seam gas well fields. Studies have demonstrated that the complex coupled reservoir flow processes captured in fine-scale CSG reservoir models affect drawdown behaviour at regional scale (Moore et al., 2015). To effectively represent these processes at the scale of a regional scale groundwater flow model may require significant upscaling, depending on the region being modelled. The previously developed Namoi CSG model was expanded to investigate the role of the spatial scale on the relationships between key variables of CSG production. In addition, the influence of boundary conditions and the contribution of shallower layers to water drawdown and production were examined. Potential approaches were assessed for upscaling the CSG well field simulations to larger scales, amenable to the grid block sizes used in regional MODFLOW groundwater modelling.

This chapter first discusses the expansion of the Namoi CSG model, required for examination of the impact of lateral boundaries and spatial upscaling. Prior to its expansion into a partial field model the applicability of vertical upscaling techniques is assessed, such as those employed Moore et al. (2015), as well as the possibility of simplifying the model by removing individual model layers that do not contribute to groundwater production and drawdown. The simplified model is then used as a basis for building the partial field model.

5.1 Lithological segregation after Moore et al. (2015)

Moore et al. (2015) compared two techniques for upscaling stacks of adjacent coal and interburden layers, observing that the upscaling methodology used affects the shape of pseudo relative permeability curves governing two-phase flow in the upscaled model cell. The first technique amalgamates all coal and interburden fine-scaled layers into a single layer, and then averages hydraulic properties across both coal and interburden. This approach did not capture permeability contrasts, and a subsequent plot of relative permeability versus saturation in the upscaled model cells indicated that large changes in cell relative permeability did not correspond to changes in saturation.

A second technique involves first segregating individual coal and interburden layers into two separate upscaled layers of appropriate net thickness, and then averaging the fine layer hydraulic properties across each of these two upscaled layers. For a reservoir model constructed by Moore et al. (2015) this resulted in a plot of relative permeability versus saturation for the upscaled model cells that more closely resembles the original relative permeability relationship.

The suitability of the segregation approach for upscaling complex reservoirs with multiple coal and interburden layers was demonstrated by the OGIA (2016) when modelling CSG groundwater impacts in the Surat Basin. CSG production in the Surat Basin targets the 300 to 600 metre thick Walloon Coal Measures, where a large number of coal seams occur in lenses up to 1 metre thick and with lateral extents of 500 to 3000 m (Ryan et al., 2012; Hamilton, Esterle & Sliwa, 2014). The coal seams are isolated by low permeability sequences of mudstone, siltstone and sandstone and a high permeability contrasts exist between the coal layers and interburden. In contrast, as described in Chapter 1, gas production from the Namoi subregion will predominantly target the thick individual coals seams of the Bohena Seam in the Maules Creek Formation, and to a lesser extent the Hoskissons Coal Member in the Black Jack Formation. The absence of a large number of thin discontinuous coal layers, such as with the Walloon Coal Measures suggests that the segregation approach used by Moore et al. (2015) would not be required for any vertical upscaling that might be undertaken on the Namoi CSG model.

5.2 Spatial model development

As initially described in Chapters 3 and 4, the Namoi CSG model incorporated data from well logs, published reports, well tests and existing groundwater models into a 15 layer model representing gas and groundwater production behaviour on a single well within the boundaries of a representative CSG well field. To calibrate the model, gas and groundwater production was compared to averaged values derived from data presented in the Narrabri Gas Project EIS base case (CDM Smith, 2016) and pilot production? studies conducted by Eastern Star Gas (Eastern Star, 2011).

5.2.1 Simplification of the model grid in the vertical direction

In Chapter 4 reservoir simulations were run on the calibrated single well symmetry model to determine relationships between key driving variables of CSG production. The simulations identified desaturation as occurring within the target formation only, and identified inter and intra-grid block relationships between pressure, saturation, permeability and production parameters in the target interval within the CSG field boundary. For model layers distant to the target interval of the Bohena Seam, the contribution to coupled reservoir flow processes, such as two-phase flow, is largely limited to the contribution of any groundwater within that layer to overall production.

Within the 15 layer model produced in Chapter 4 the upper six layers and base layer contribute less than 1% to the total water production from the well, an insignificant amount compared to adjacent layers, and likely to have minimal effect on the relationships between driving variables of CSG production being investigated. The percentage of original water in place (OWIP) that is produced from each of the formations during the 20 year production simulation is presented in Table 5-1.

Based on these findings, the upper 6 layers and base layer were removed to simplify the model and decrease CPU time. As presented in Table 5-1, the removal of the layers leads to a slight increase in the production of water from the Hoskissons coal and its overlying and underlying formations. The contribution of these layers to overall water production from the model increased by less than 1%, therefore in the context of this assessment, a small change in water production from these layers does not contribute significantly to the relationships between coupled reservoir flow processes that occur in the target formation during CSG production.

Table 5-1 Water production from the individual layers of the 15 layer and 8-layer symmetry models.

GEOLOGICAL UNITS	MODEL LAYERS		WATER PRODUCTION (%OWIP)	
	15 LAYER	8-LAYER	15 LAYER	8-LAYER
Narrabri Formation (Fm) / Gunnedah Fm / Cubbaroo Fm / Warrrumbungle Volcanics (Vol) / Liverpool Range Vol	15	N/A	0.000044	
Bungil Fm / Mooga Sandstone (Ss) / Orallo Fm	14	N/A	0.000079	
Pilliga Sandstone (upper & lower)	13	N/A	0.000155	
Purlawaugh Fm	12	N/A	0.001345	
Garrawilla Vol (upper & lower) / Deriah Fm / Napperby Fm (upper & basal)	11	N/A	0.001811	
Digby Fm (Ulinda Ss) Digby Fm / Digby Fm (Bomera Congl.)	10	N/A	0.013839	
Trinkey Fm / Wallala Fm / Breeza Coal / Clare Sandstone / Hows Hill Coal / Benalabri Fm	9	8	0.026635	0.044511
Hoskissons Coal	8	7	0.04776	0.060115
Brigalow Fm / Arkarula Fm / Melvilles Coal Member / Pamboola Fm	7	6	0.077615	0.084642
Watermark Fm / Porcupine Fm	6	5	0.656337	0.657553
Upper Maules Creek Fm / Rutley Seam / Interburden / Namoi Seam / Interburden / Parkes Seam / Interburden	5	4	1.169006	1.169042
Bohena Seam	4	3	9.922283	9.92321
Lower Maules Creek Fm	3	2	0.667926	0.667926
Goonbri Fm / Leard Fm	2	1	0.009586	0.009604
Werrie Basalt And Boggabri Vol (Basement)	1	N/A	0.000072	

Table 5-2 presents the cumulative gas and water production, and gas and water production rates from the 15-layer and 8-layer models. Results indicate that the simplified model produces identical water production for the life of the field and comparable cumulative and peak gas production, indicating it is a suitable model for investigation into reservoir processes affecting water production and drawdown in the target formation during CSG production.

Table 5-2 Comparison of Namoi CSG model output and estimated average reported values.

OUTPUT	15 LAYER MODEL	8-LAYER MODEL
Peak water production rate (per well)	55 m^3/day	55 m^3/day
Average water production rate (per well over field life)	4.3 m^3/day	4.3 m^3/day
Cumulative water production (per well)	31.35 ML	31.35 ML
Peak gas production rate (per well)	703 mscf/d	695 mscf/d
Cumulative gas production (per well)	0.99 bcf	1.00 bcf

5.2.2 Model spatial boundary extension

In order to investigate the influence of scale on the relationships between reservoir process that occur during CSG production, the Namoi CSG model needed to be extended to a size that is suitable for both upscaling to MODFLOW scale grid blocks, and for representing flow processes in varying proximity to the field boundary. The process of creating a representative field model had three main steps:

- increasing the model boundary to a distance where it does not affect production output
- including a greater number of wells to simulate part of a larger well field, and to enable investigation of coupled reservoir processes both inside and outside the boundary of the CSG well field
- calibrating the field scale model to ensure that overall water production and gas production match reported values from sources reported in Chapter 3.

The number of wells in the model was increased to 9 in order to create a one quarter field symmetry model for a well field containing 25 CSG wells in a square pattern (Figure 5-1). The well spacing was maintained at 530 m as per the minimum spacing calculated from the Narrabri Gas Project EIS (CDM Smith, 2016) and the well production parameters, completion interval, model layers and reservoir properties were maintained from the 8-layer single well symmetry model.

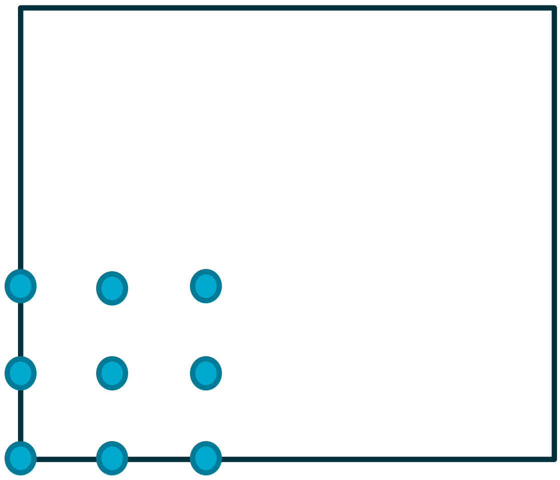

Figure 5-1 Well layout of field symmetry model (not to scale).

The SIMED reservoir simulator imposes a no-flow condition at the boundaries of the model, which has the potential to introduce artefacts into the simulations, particularly if the boundary is too close to the producing wells. The influence of the boundary condition will also depend on total simulation time, with short time simulations not requiring as distant model boundaries. When determining the effect of model boundary on the CSG field production, the variation due to boundary distance in production values (water and gas production rates and cumulative production) is of key interest. In addition, the pressure drawdown in grid blocks at the model boundary will indicate if it is influencing the flow behaviour.

As the distance to the model boundary increases, the pressure drawdown at the boundary due to gas production tends towards zero, meaning beyond a certain distance further increases in model dimensions will have no effect on production data. The production data for the 9 well field symmetry model described above is presented in Table 5-3 for various distances to the field boundary. These data indicate that extending the field boundary beyond 12.9 km produced little effect on the production properties. As a result, the 12,945 m model boundary was chosen for the spatial model used in the following simulations. In this model, no drawdown in pressure was observed at the model boundaries after 20 years of production.

Table 5-3 Production data changes with varying distance to model boundary.

MODEL BOUNDARY	2650 M	6355 M	12945 M	19535 M
Cumulative water production (average per well, ML)	77.82	129.8	133	133
Peak gas production rate (average per well, mscf/d)	614.7	614.8	612	613.8
Cumulative gas production (average per well, bcf)	1.47	0.9	0.88	0.88

In the multi-well extended boundary model, CSG production wells adjacent to the aquifer saw a larger amount of water production than wells that were located within the well field boundary, whose production was affected by well interference. This latter condition was represented in the well symmetry model of Chapter 4.

The increased water production from field boundary wells led to a much larger cumulative water production when averaged on a per well basis. Similarly, compared to the single well model, differences in gas production between wells within the field boundary and wells adjacent to the aquifer resulted in altered cumulative and peak gas production averaged on a per well basis. In order to maintain production outputs consistent with the reported values from sources in Chapter 3, the extended Namoi CSG model required recalibration for field performance in addition to individual well performance. This recalibration was completed using a series of steps:

- A reservoir simulation was run on the extended boundary multi-well model using identical reservoir and production parameters as the single-well interference model.
- A relationship was derived between cumulative water production from a given well and the well location. This relationship was then calibrated using cumulative water production from the single-well interference model to produce a relationship between increased water production from a well and its distance from an interference-dominated well within the field boundary. Further models were derived for the relationship between cumulative gas production and cumulative water production per well, and maximum gas rate and water production.
- A simplified field model consisting of 841 wells in square grid pattern was constructed, and the modelled relationships between production parameters applied to produce values of cumulative water production, cumulative gas production and peak gas rate for each well dependent on its location in the field, and thus total production for the field. These values were then averaged on a per well basis to produce values for comparison to the original source data.

- Calibration was undertaken by adjusting reservoir parameters in the extended boundary multi-well model, completing CSG production simulation, deriving the relationships between production outputs and well locations, and applying these relationships to the simplified square grid field model to determine production averages on a per well basis. The reservoir parameters were adjusted and this process repeated until a level of agreement between averages and reported predicted values was reached.

Examples of the derived relationships between production outputs used for calibration of the field model are presented in Figure 5-2. The production data relationship approach allowed for use of a smaller, less computationally intense model for calibration of the reservoir parameters, however the use of a simplified square field geometry may limit its applicability to more complex field development patterns.

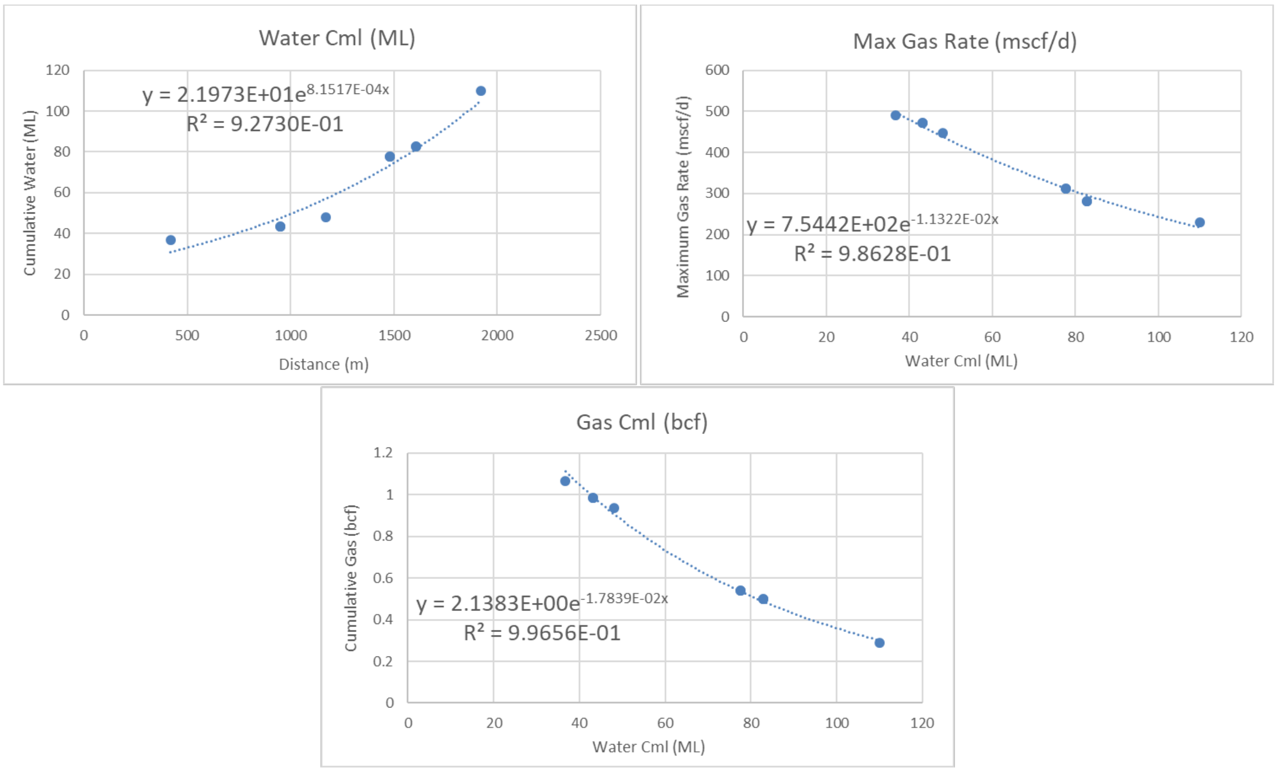

Figure 5-2 Relationships between production outputs used to calibrate the field model.

Production parameters, such as water rates and flowing bottom hole pressure were maintained from the single well interference model. The majority of reservoir parameters were retained from the single-well model, however, certain reservoir parameters were adjusted to produce field scale estimations of gas and water production that were consistent with the averaged values derived from data presented in the Narrabri Gas Project EIS base case (CDM Smith, 2016) and Eastern Star Gas pilot production? studies (Eastern Star, 2011). The calibrated reservoir parameters were still consistent with the expected ranges for values presented in the relevant literature, and are presented in Table 5-4. The calibrated and extended 9 well model was used to investigate the relationships between key driving variable of gas production at field scale, and continues to be referred to herein as the Namoi CSG model.

Table 5-4 Calibrated reservoir parameters for extended boundary field symmetry model.

RESERVOIR PARAMETER	VALUE	UNIT
Bohena Seam target layer thickness	9.7	m
Bohena Seam horizontal permeability	5	md
Coal relative permeability	vs. S_W	-
Coal cleat compressibility	0.000044	Pa^{-1}
Coal desorption time	0.2	days
Maules Ck coal/interburden layer permeability	0.009	md

5.3 Relationships between key variables at field scale

The relationships between key driving variables examined in the well symmetry model differ at field scale, where the presence of a significant laterally adjacent aquifer affects water and gas production from CSG wells. For comparison, Figure 5-3 and Figure 5-4 present the S_w vs P relationship for grid cells in the target layer of the symmetry model, and the field model respectively.

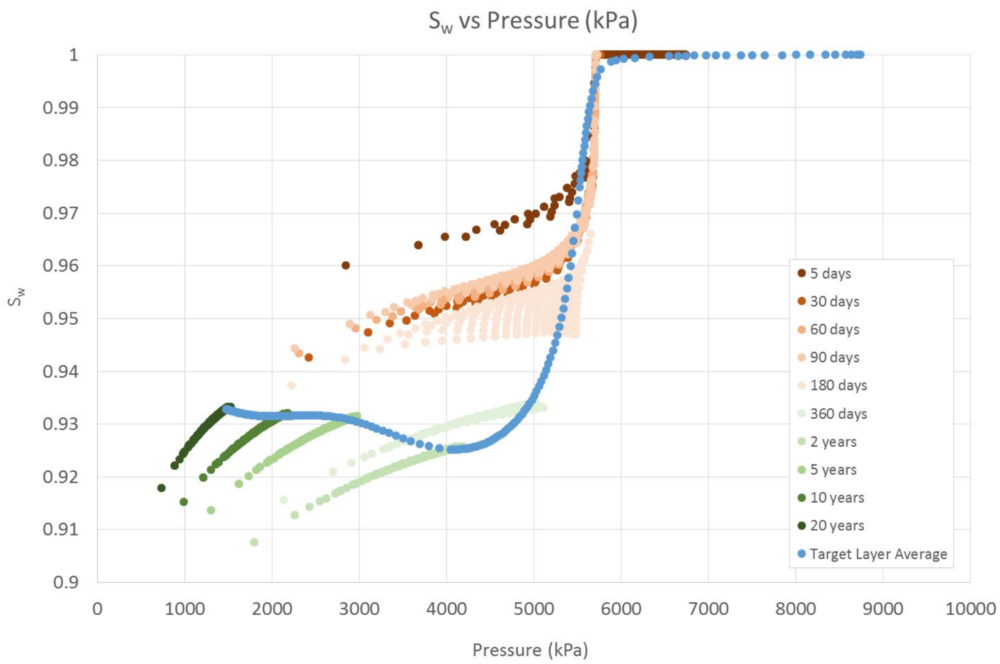

Figure 5-3 S_W vs P relationship for grid cells in the target formation in the Namoi single well symmetry model.

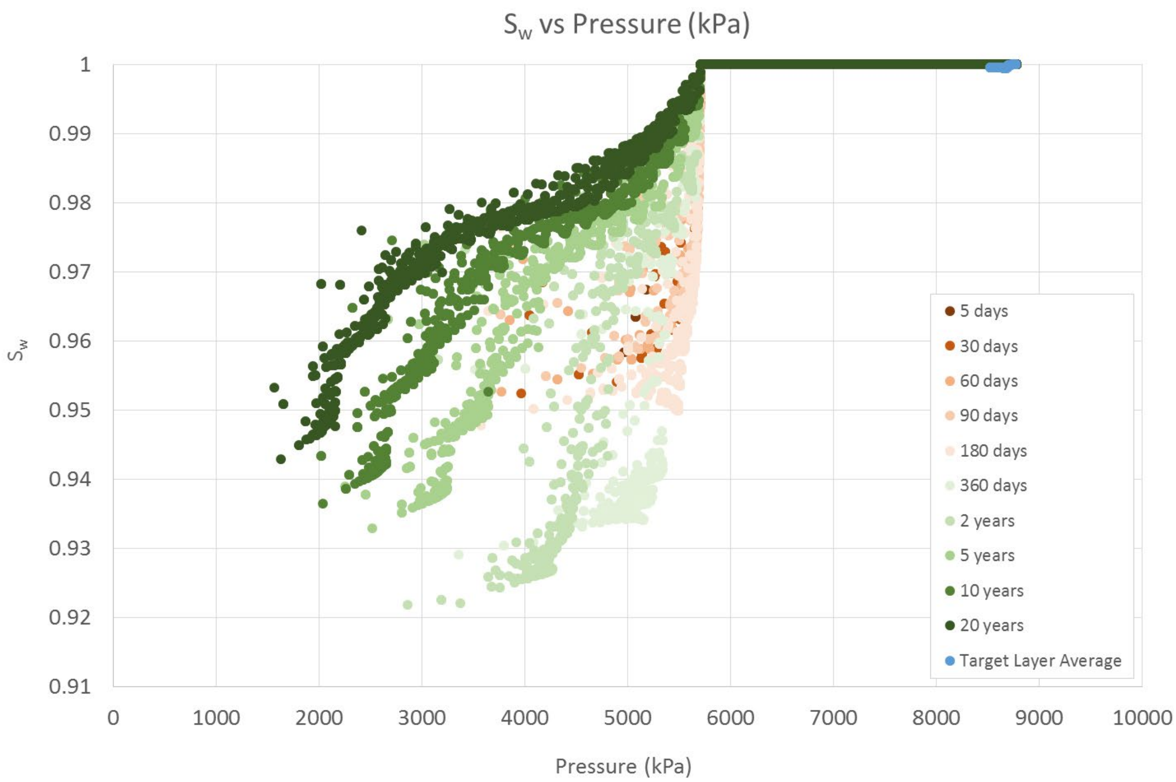

Figure 5-4 S_W vs P relationship for grid cells in the target formation of the Namoi field model.

The influence of the adjacent aquifer in the field model results in a larger range of saturations and pressures at a given production time across grid cells of the target formation. The S_w and pressure data also approach a time-asymptotic pseudo steady state relationship, however not to the extent described in previous literature (Herckenrath et al., 2015). This is potentially the result of the specific reservoir and production parameters derived for the Namoi CSG model. A less well-defined time-asymptotic relationship may impact the accuracy of using a single van Genuchten S_w vs P model to represent desaturation behaviour in the single-phase MODFLOW groundwater model.

As expected, averages of saturation and pressure across the target layer are dominated by the large number of grid blocks that remain fully saturated, therefore unlike in the symmetry model (Figure 5-3), the layer averaged data (shown in blue on Figure 5-4) do not approximate the intra-grid block relationships. This may have potential to lead to inaccuracies if averaged relationships are implemented into the regional groundwater flow model.

This influence of saturated grid blocks on averaging also applies to the plot of water effective permeability and pressure in the Bohena Seam presented in Figure 5-5. Although here, as with the well symmetry model, propagation of the effect of the complex saturation versus pressure relationship for the grid cells can still be observed in the permeability data.

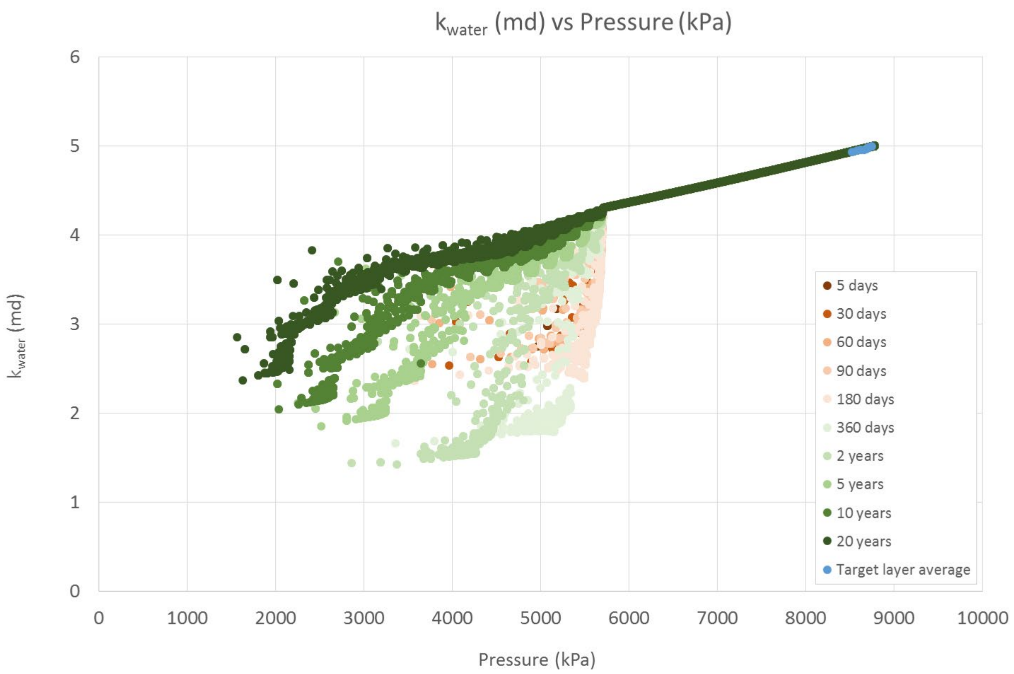

Figure 5-5 k_{water} vs P relationship for grid cells in the target formation of the Namoi CSG field model.

As with the well symmetry model used in Chapter 4, well-specific outputs that vary with time were collected from the Namoi CSG field model, including water and gas production rates and cumulative volumes, bottom hole pressure, gas-water-ratio, and component specific production rates. Of these outputs, the water production rate can be compared to a groundwater abstraction rate that may be assigned in a MODFLOW regional groundwater model. The averages of pressure, saturation and upscaled permeability across the target layer for the Namoi field model were plotted against the production rate and presented in Figure 5-6 and Figure 5-7. These plots demonstrate the effect that the large number of distal grid blocks has on the average values. As with the previous plots (Figure 5-4 and Figure 5-5), the change in average saturation, pressure, and permeability is extremely small compared to the changes actually occurring within the field. There is potential that this large difference between layer averaged and in-field values may reduce the suitability of using layer averaged relationships in the regional model. When determining a relationship between a reservoir variable and the production data (i.e. well rate or cumulative production) it is necessary to undertake some form of averaging of the reservoir parameter over a set of grid blocks. This requirement may also reduce the suitability of implementing relationships that operate as a function of production data into the regional groundwater model.

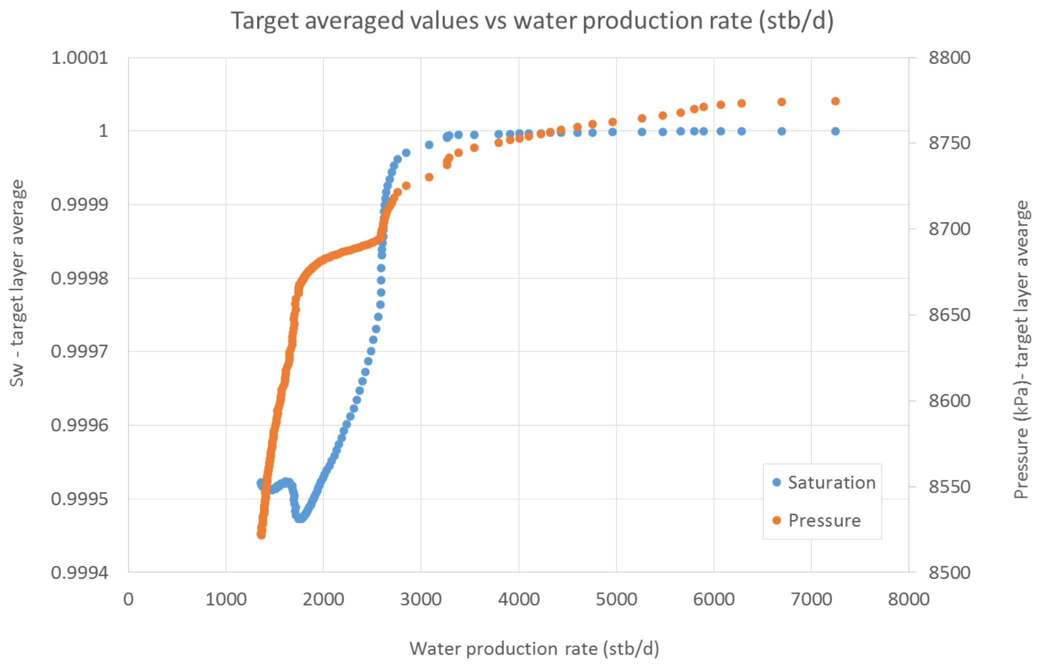

Figure 5-6 Target layer averaged pressure and saturation vs production rate for the Namoi field model.

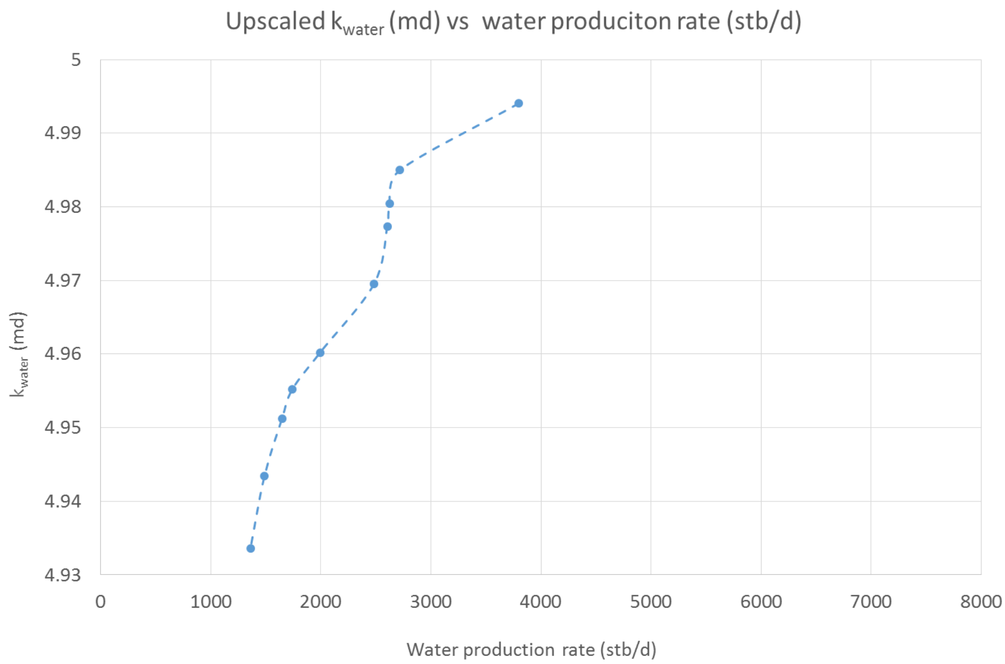

Figure 5-7 Target layer upscaled permeability vs production rate for the Namoi field model.

5.4 Effect of grid block size on the S_w vs P relationship

The minimum grid block size employed in regional groundwater flow models is commonly around 300 x 300 m, considerably larger than what is utilised for coal seam gas reservoir models, particularly in the near wellbore region. The smaller grid block size is required for CSG reservoir models in order to capture complex dual-phase near-wellbore flow processes, however it is too computationally intensive to implement this grid block size in extensive regional models. Illustrating the importance of having a small grid block scale to derive relationships between grid distributed variables, Figure 5-8 and Figure 5-9 present the previous S_w vs P relationship derived from the CSG model, but using 106 x 106 metre grid blocks and 265 x 265 metre grid blocks. As can be observed from the two plots, increasing the grid block size significantly reduces the information available, and the resolution of any derived relationship between grid distributed variables. It is also apparent that the 300 metre grid block size used in regional groundwater modelling would provide insufficient detail if used in a CSG model to determine these near-wellbore relationships.

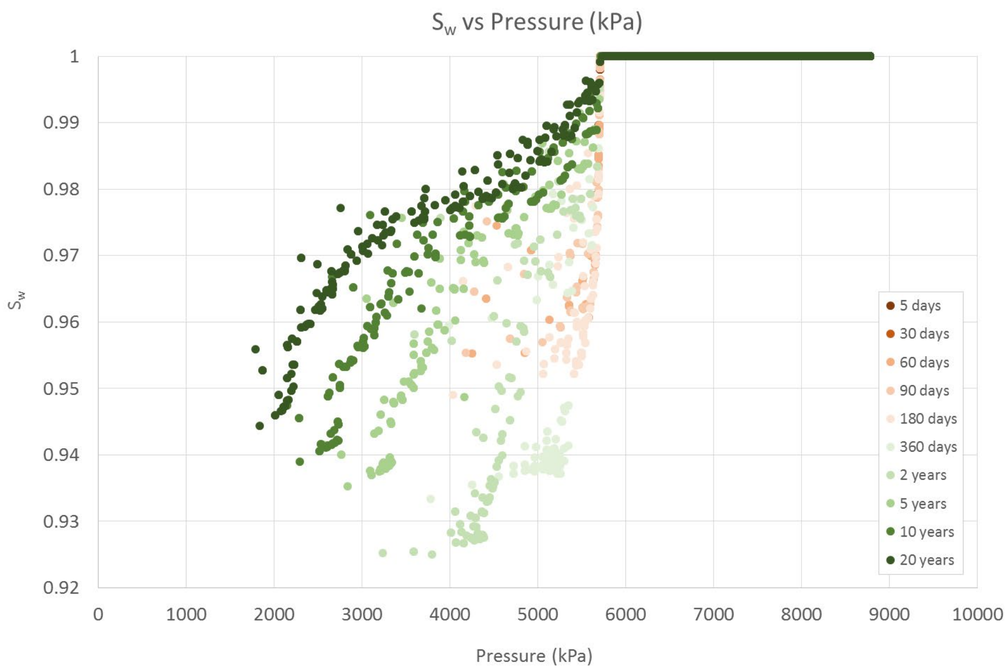

Figure 5-8 S_W vs P relationship using 106 x 106 m grid cells in the target formation.

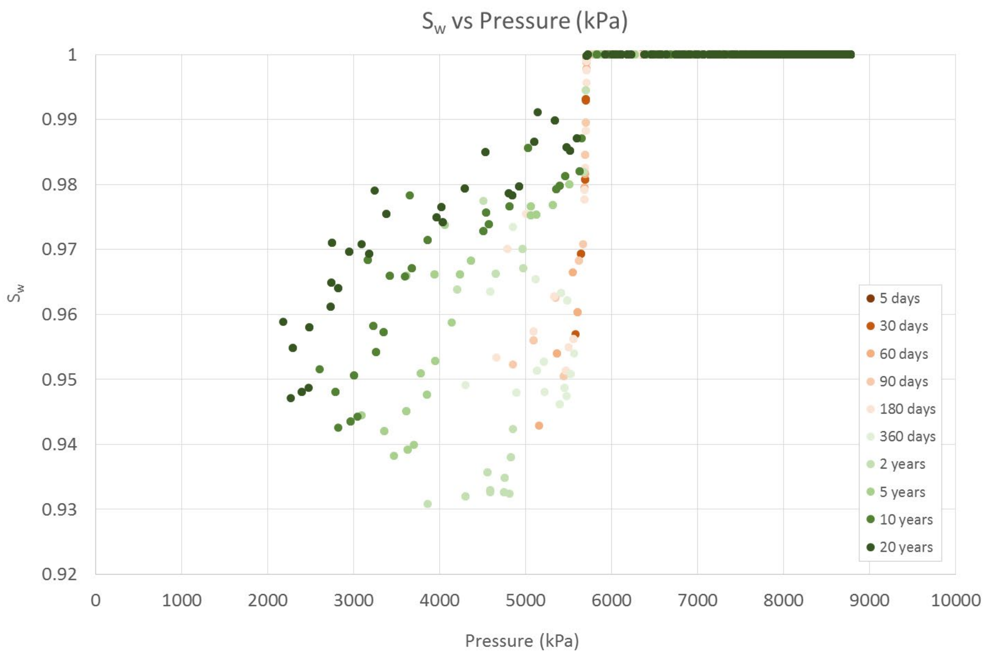

Figure 5-9 S_W vs P relationship for 265 x 265 m grid cells in the target formation.

5.5 Spatial upscaling of the S_w vs P relationship

Due to the large spatial extent of regional groundwater models, the computational requirements are too high with a small grid block size such as applied in the near-wellbore region of a CSG field model. To overcome this issue, methods exist for upscaling the data from a number of small grid blocks to single large grid block that occupies the same volume and location. The upscaling methods are intended to preserve the physical behaviour of the set of small grid blocks at the larger scale. Arithmetic methods were applied by Moore et al. (2015) to upscaling in the vertical direction which are also applicable to spatial upscaling examined here. The method utilised for saturation and pressure upscaling was grid cell volume weighted arithmetic mean, which is appropriate for spatial upscaling within a single model layer. Figure 5-10 presents the S_w vs P relationship at 60 days, 180 days, 5 years and 20 years and shows the upscaled relationship against the original fine-scale relationship. The size of the grid blocks that are represented by the upscaled data ranged from between 318 m to approximately 4 km square. These values are similar to the spatial dimensions of cells used in regional groundwater modelling.

Results indicate that upscaled saturation vs pressure relationships provide a good match to fine-scaled relationships, particularly at the later stages of production. During early production times, the number of desaturated cells is fewer, supplying less data to adequately match the upscaled relationship to the original. The close curve approximation at later stages of production, closer to the time-asymptotic behaviour described by Herckenrath et al. (2015) indicates potential for applying this approach to upscaling the Namoi CSG well field for regional scale MODFLOW models. Whilst the S_w vs P relationship may not be altered significantly when upscaled from SIMED data, the effect on water production and drawdown behaviour due to the implementation of the relationship into an upscaled regional groundwater model grid block will still need to be investigated.

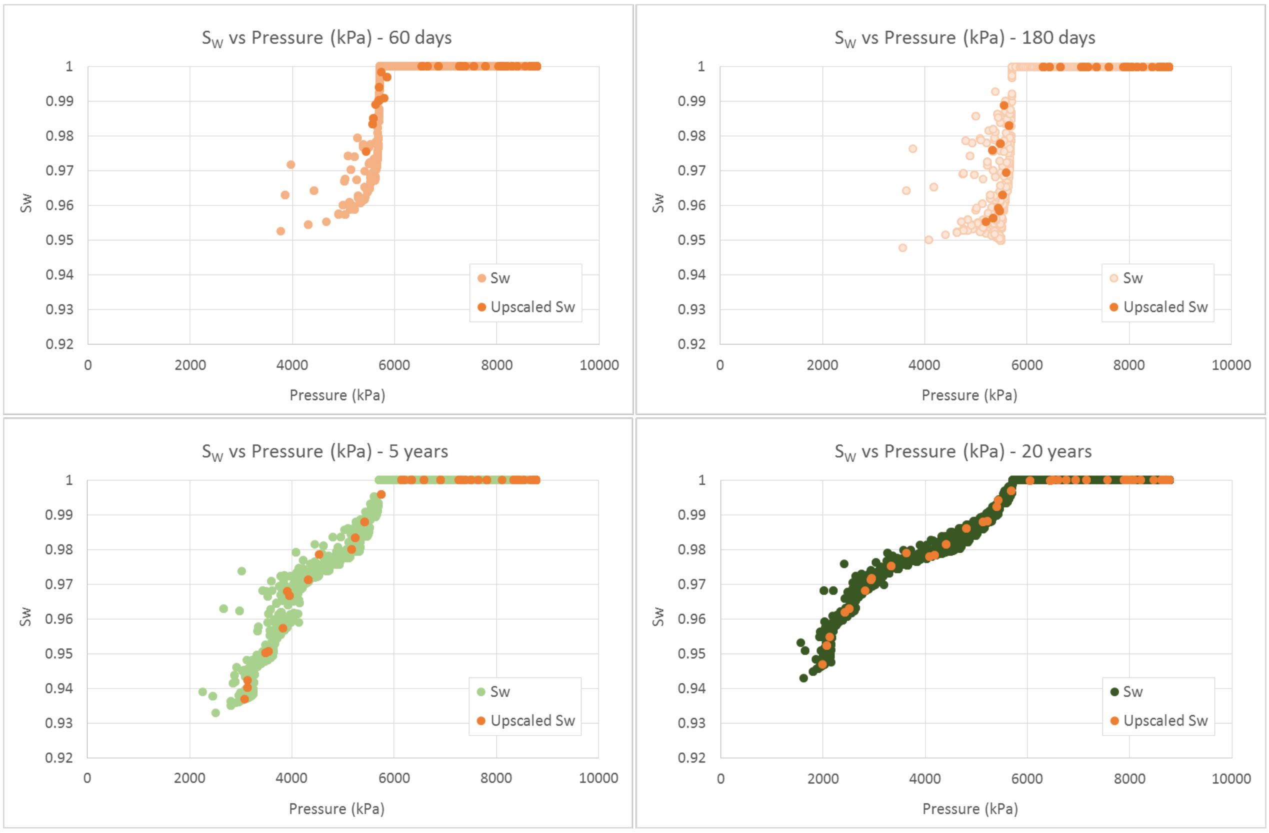

Figure 5-10 Upscaled S_w vs P relationship presented with fine-scale data.

5.6 Field boundary effect on key variable relationships

Simulations using the Namoi CSG field model investigated the role of field size and field boundary on the intra-grid cell relationships between saturation and pressure. Figure 5-11 depicts the change in the S_w vs P relationship across the Bohena Seam after 20 years of production for field sizes of 3 x 3 through to 6 x 6 wells. The overall model dimensions remained unchanged for the different scenarios. The same relationships are depicted overlayed in

Figure 5-12. In these data the saturation versus pressure relationship appears to follow the a similar shape for different field sizes, suggesting it may be possible to apply the same van Genuchten desaturation equation for large-scale grid blocks that have different proportions of CSG field coverage occurring with the grid block boundary. Results also indicate that as the size of the field increases as a proportion of the model area, the number grid blocks with low saturation increases. The subsequent effect on the saturation versus pressure relationship is fewer data at the higher saturation portion of the curve, and extension of the curve to lower overall saturations. For example, the 6 x 6 well field minimum grid block saturations approach 0.92 after 20 years, whilst the 3 x 3 well field minimum saturation remains above 0.94. This result is not unexpected, but it highlights that if S_w vs P relationships and relative permeability behaviour are to be incorporated into specific grid blocks or regions of the large-scale MODFLOW model, attention should be paid to the proportion of well field coverage that occurs within the equivalent larger scale grid block. Accordingly, the proposed relationships must be suitable for representing the full range of desaturation behaviour expected to be encountered in the grid block during production; a greater range for grid blocks containing a greater CSG field proportion.

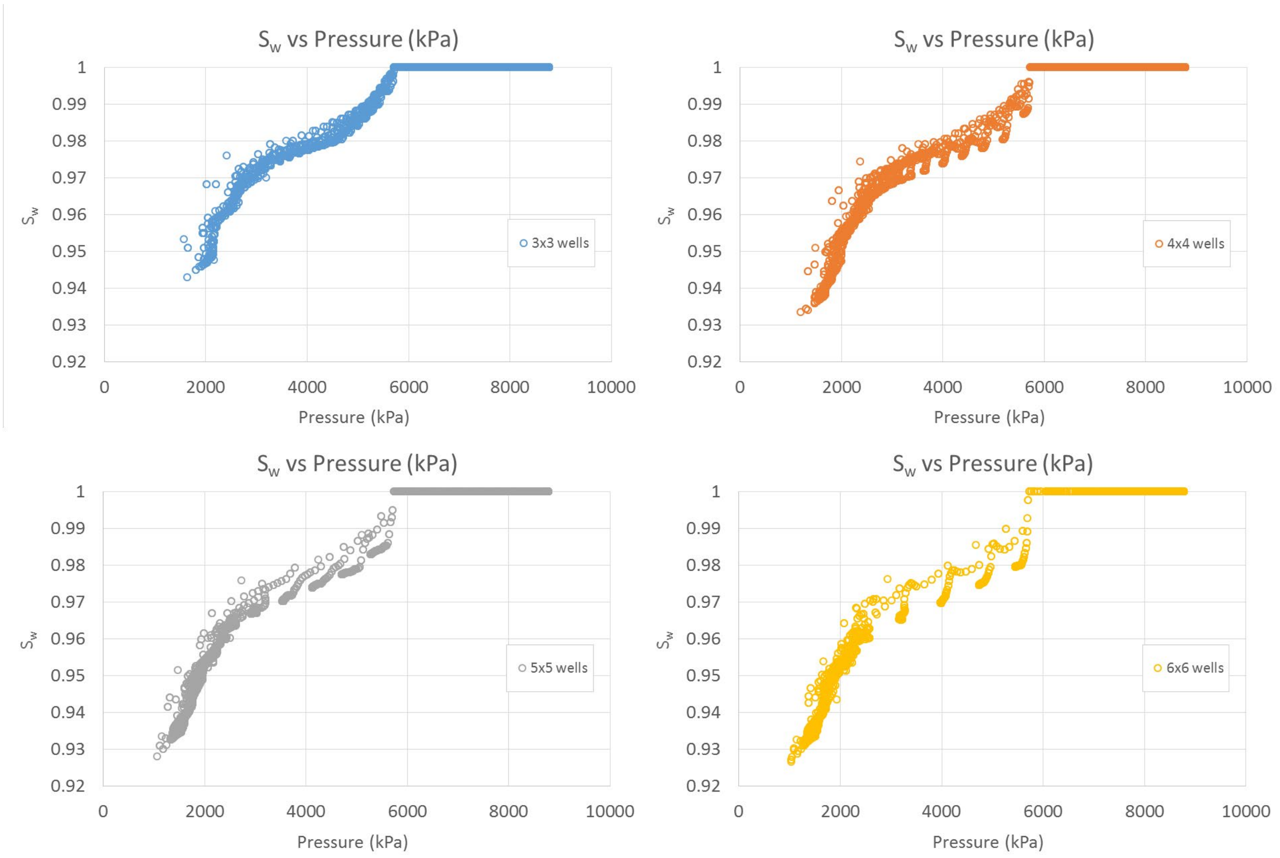

Figure 5-11 S_w vs P relationship across the Namoi CSG field model for different well field sizes.

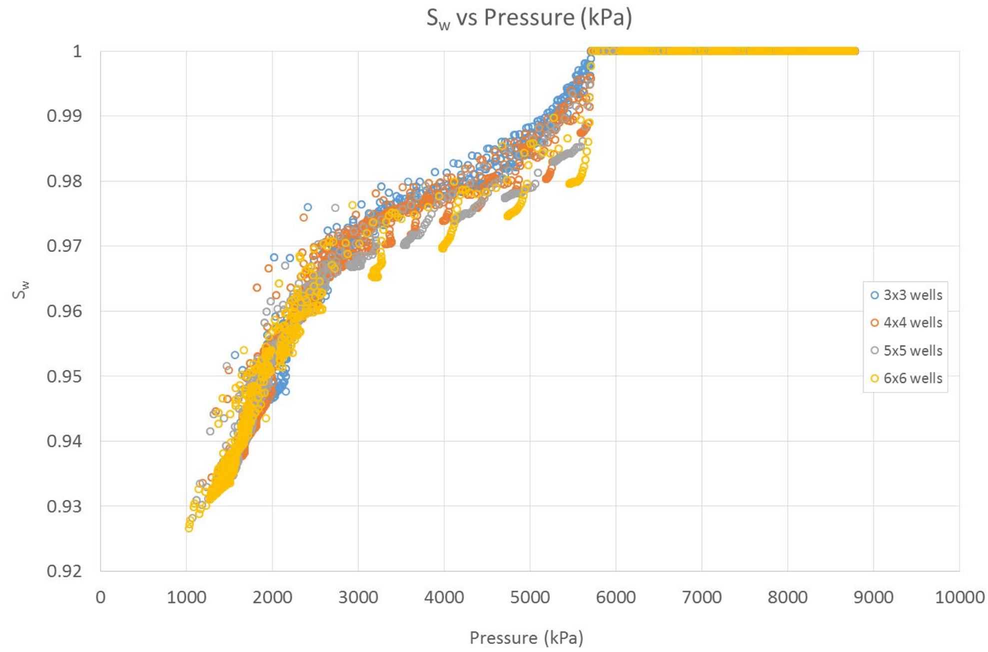

Figure 5-12 Overlayed S_w vs P relationships at 20 years production for differing field sizes in the Namoi CSG model.

5.7 Vertical upscaling to approximate regional model layering

The regional groundwater flow model of the Namoi subregion produced in MODFLOW for the Bioregional Assessments uses a total of nine layers to represent Gunnedah Basin hydrostratigraphic units. In this model a single layer is assigned to the Hoskissons coal member, a potential target formation for CSG production in the region. The primary CSG target, the Bohena Seam, is modelled as part of a layer that combines all geological units of the Maules Creek Formation. These include the Upper Maules Creek Formation, the Rutley, Namoi, Parkers and Bohena Seams and their associated interburden, and the Lower Maules Creek Formation.

The Namoi CSG model uses a different layering approach to represent the stratigraphy of the Gunnedah Basin target formations. The Hoskissons coal member, as in the BA model, is represented by a single layer, the Bohena Seam is also represented with an individual layer and the remainder of the overlying Maules Creek Formation is combined into a single layer. The Lower Maules Creek Formation is also assigned its own individual layer (Table 5-1). This layering approach is required in the CSG model to adequately represent the coupled reservoir flow processes occurring at a fine-scale in the vicinity of the well field. Accurately representing these processes in the MODFLOW regional groundwater model may require implementation of relationships that apply to the entire upscaled Maules Creek Formation model layer it employs. This means relationships that are derived solely for the Bohena Seam may need to be vertically upscaled so that they incorporate behaviour of the adjacent formations.

The Namoi CSG model layer representing the Maules Creek Formation above the target Bohena Seam incorporates three other thin coal seams and their associated interburden layers. Few data exist to establish the exact desorption pressure for these coal seams, and results of simulations using the Namoi CSG model suggested that interburden formations present a sufficiently impermeable barrier to prevent pressure drawdown equivalent to desorption pressure in the target seams. Consequently, it is assumed that during the production period unsaturated flow does not occur in the Namoi CSG model layer containing these stratigraphic units. The saturation versus pressure relationship, vertically upscaled to match the layering used in the Namoi BA regional groundwater flow model is presented in Figure 5-13, and the upscaled effective permeability to water versus pressure is presented in Figure 5-14.

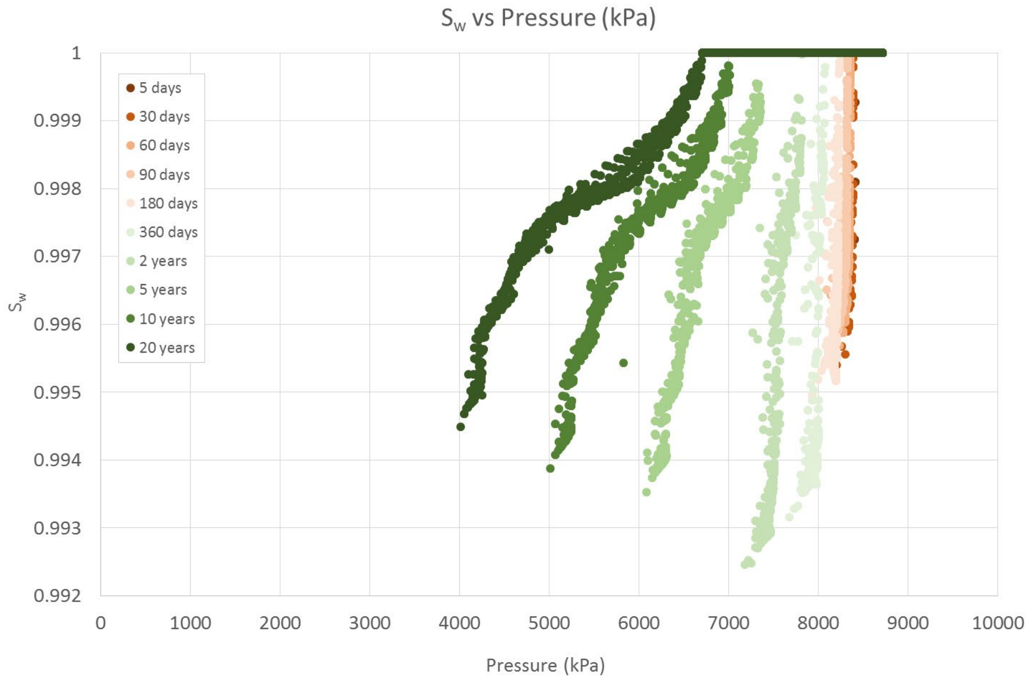

Figure 5-13 Upscaled S_w vs P relationship based on simulation results from the Namoi CSG model.

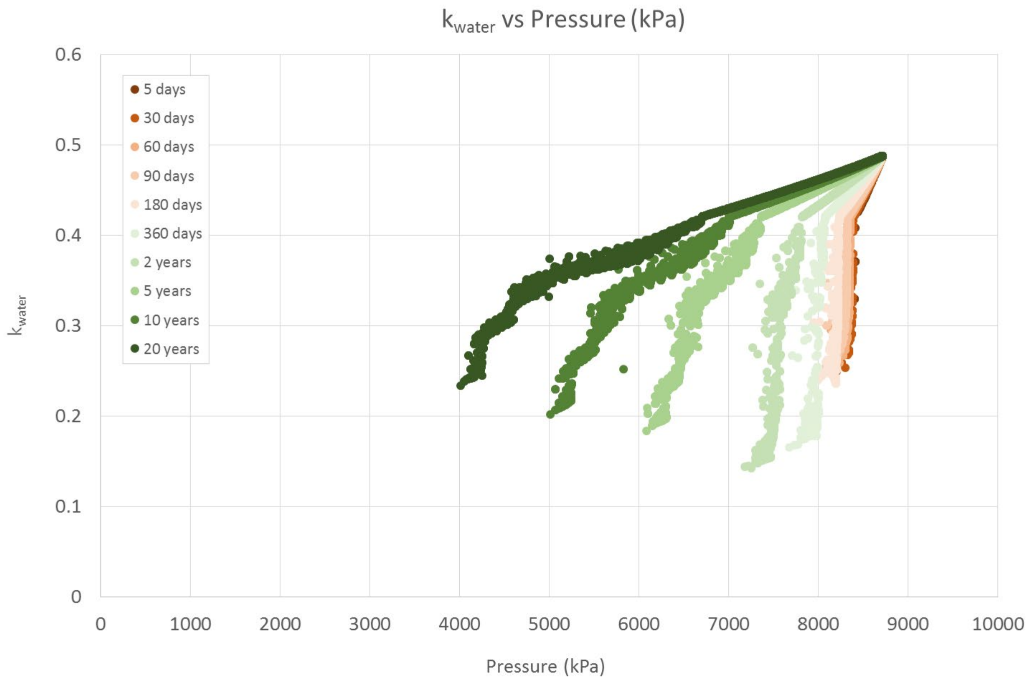

Figure 5-14 Upscaled k_{water} vs P relationship based on simulation results from the Namoi CSG model.

These figures clearly demonstrate the impact of undertaking vertical upscaling to include the overlying and underlying Gunnedah Basin strata. The basic curve shape is similar at late production times to the curve produced for the Bohena Seam only, using the full field Namoi CSG model (Figure 5-4). However, the relationships for the Bohena Seam only, regardless of production time, begin to show desaturation at the seam desorption pressure (see Figure 5-4). In the upscaled relationships, the desaturation portion of the curve occurs at gradually lower pressures in later stages of production. This is due to the influence of the large volumes of overlying and underlying formation on the upscaled pressure value: early time desaturation occurs in the target formation when the desorption pressure is reached, while at the same time pressure in the adjacent formations is still higher due to low vertical permeability. As production time increases, more distal grid blocks in the target formation reach desorption pressure and gas is produced, and during this period the average pressure in adjacent formations has decreased, therefore reducing the upscaled pressure at the beginning of the desaturation curve. This may pose difficulties if attempting to model the relationship using the van Genuchten (1980) function as per Herckenrath et al. (2015), as desaturation no longer begins at the single desorption pressure of the target coal but rather at a range of upscaled pressures. The effect of this saturation versus pressure behaviour also propagates into the upscaled permeability versus pressure relationship in Figure 5-14.

The horizontal propagation of desaturation in the target layer means a large proportion of upscaled grid blocks show a small amount of desaturation despite limited pressure drawdown. This is reflected in the near vertical relationships between saturation and pressure in the first 2 years of production. The extent of desaturation experienced by the upscaled grid blocks is an order of magnitude smaller than that of the target seam only. This is due to the incorporation of the S_w vs P relationship of the large adjacent formations, which remain fully saturated throughout the entire life of the field.

If implementing the upscaled S_w vs P relationship into grid blocks of the regional groundwater flow model, the relative permeability relationship for the upscaled layer also needs to be recalculated to provide a suitable reduction in relative permeability to match the small changes in saturation. The resulting pseudo-relative permeability curve for the upscaled layer is presented in Figure 5-15. It was calculated using the approach documented by Moore et al. (2015) using thickness-weighted upscaling of permeability and saturation values.

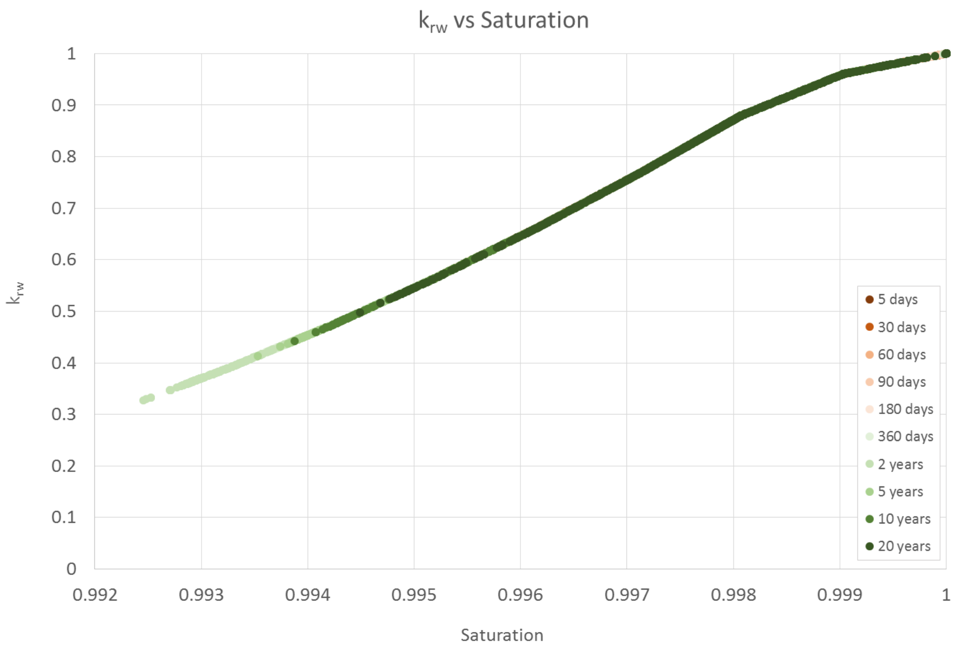

Figure 5-15 Pseudo relative permeability curve, based on upscaled data from the Namoi CSG model.

6 Implementing the results of Chapters 4 and 5 in MODFLOW to represent CSG well field influences

In this chapter the outcomes described in Chapters 4 and 5 are implemented in the version of MODFLOW used for groundwater assessment work performed under GISERA. Earlier tasks investigated the potential for developing simple relationships between the key reservoir variables operating during CSG production, and established the effect of upscaling and spatial scale on these relationships. Here, the derived relationships were modelled and implemented into MODFLOW-USG, the software used for Namoi groundwater flux predictions. The effect that the implementation has on water production and drawdown predictions using MODFLOW was assessed, and the output compared to similar predictions made using the CSG reservoir simulator SIMED. The comparison investigated a number of modelling and implementation approaches and scenarios in order to establish which approach provides the most appropriate representation of CSG well field influences in groundwater models for the Namoi region.

6.1 MODFLOW-USG model development

MODFLOW is an open-source hydrologic model produced by the United States Geological Survey (USGS) for groundwater simulation. The version MODFLOW-USG allows for the construction of models with unstructured grids (USG), and has been used for the OGIA model of the Surat Basin Cumulative Management Area, and the Namoi model developed for the GISERA GAB flux project.

Compared to CSG reservoir simulators, MODFLOW provides only limited functionality for representing dual-phase fluid transport and the complex coupled flow behaviour associated with gas production from CSG reservoirs. In an attempt to compensate, existing MODFLOW models encompassing CSG production have relied on simplified relationships or use of CSG water production estimates as inputs. It has been demonstrated that these approaches, as well as the conservative assumptions made in order to compensate for these inaccuracies, can lead to over-estimation of the impacts of CSG water extraction (Moore et al., 2015).

Using data produced for the Namoi region in Chapters 4 and 5, the approach documented by Herckenrath et al. (2015) to representing CSG impacts in MODFLOW was implemented in a groundwater flow model of a representative Namoi CSG field development. This approach has been demonstrated to account for the presence of a gas phase reasonably well (Herckenrath et al., 2015). The implementation documented in this chapter used a modified version of MODFLOW-USG, supplied to CSIRO by the package’s original developer, that allowed for modelling of desaturated flow behaviour in the groundwater simulation. The modified version is referred to herein as MODFLOW.

6.1.1 Verification of MODFLOW and SIMED single-phase model results

In order to demonstrate agreement in the results produced by MODFLOW and SIMED modelling packages, single-phase groundwater flow models were first developed in each package, and the water production and drawdown predictions from production simulations compared. The single-phase groundwater model was constructed in MODFLOW using the identical geometry and reservoir parameters as the Namoi CSG field symmetry model produced in SIMED for Chapter 5. However, not all reservoir parameters defined in SIMED are available to be represented in MODFLOW. Table 6-1 presents relevant SIMED reservoir parameters and their associated parameters in the MODFLOW single-phase groundwater flow model. This initial MODFLOW model included 9 wells modelled using the drain condition, a constant head method also used in the GISERA GAB flux groundwater models that provides the nearest approximation to constant bottom-hole pressure production from a CSG well.

Table 6-1 Selected SIMED reservoir parameters and equivalent MODFLOW single-phase reservoir parameters.

SIMED RESERVOIR PARAMETERS	ASSOCIATED SINGLE-PHASE MODFLOW RESERVOIR PARAMETERS
Permeability	Hydraulic conductivity
Cleat compressibility	n/a
Young’s modulus	n/a
Poisson’s ratio	n/a
Porosity	Specific storage
Formation compressibility	Specific storage
Water relative permeability	n/a
Gas relative permeability	n/a
Langmuir adsorption model	n/a
Desorption pressure	n/a
Desorption time	n/a

The Namoi CSG field symmetry model was modified for single-phase water production only. This involved removing the reservoir parameters that are not able to be reproduced in the MODFLOW model, and modifying the CSG production condition to a constant bottomhole pressure, as opposed to a constant water production rate that monitors and switches to constant BHP control. The well productivity index was calculated from a production simulation in the single-flow SIMED model and then used to calculate the drain conductance for the equivalent MODFLOW model.

Water production and pressure drawdown from the single-phase MODFLOW model was compared to the results of the single-phase SIMED model in order to verify results from each package under identical simulation conditions. Drawdown profiles for the Bohena Seam target layer and prediction error after 20 years of production are presented in Figure 6-1 and show that the drawdown in head after 20 years differs by a maximum of 1.26 m between the two models, which constitutes an error of approximately 0.36% in that region of the model. The predicted water production differed 0.5% between the MODFLOW and SIMED models. The heat map presented in Figure 6-2 shows the distribution throughout the producing layer of the error in drawdown head after 20 years production. The heat map indicates that the greatest difference in predicted drawdown between the models is concentrated in the region around the CSG field boundary.

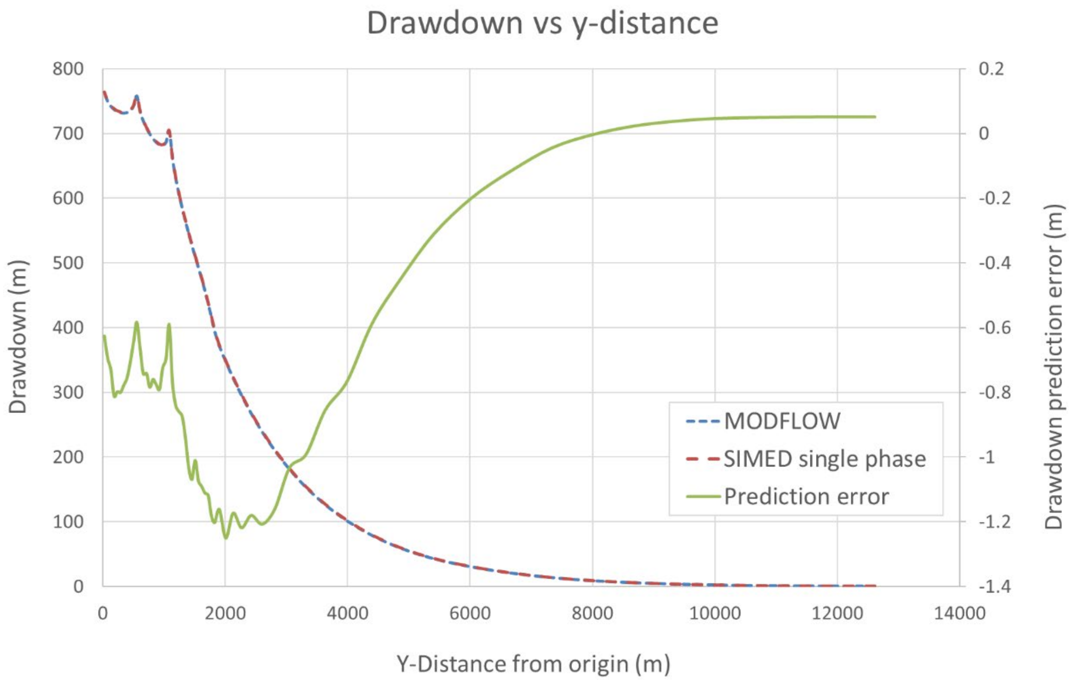

Figure 6-1 Bohena Seam drawdown profiles in horizontal distance from origin for single-phase MODFLOW and single-phase SIMED.

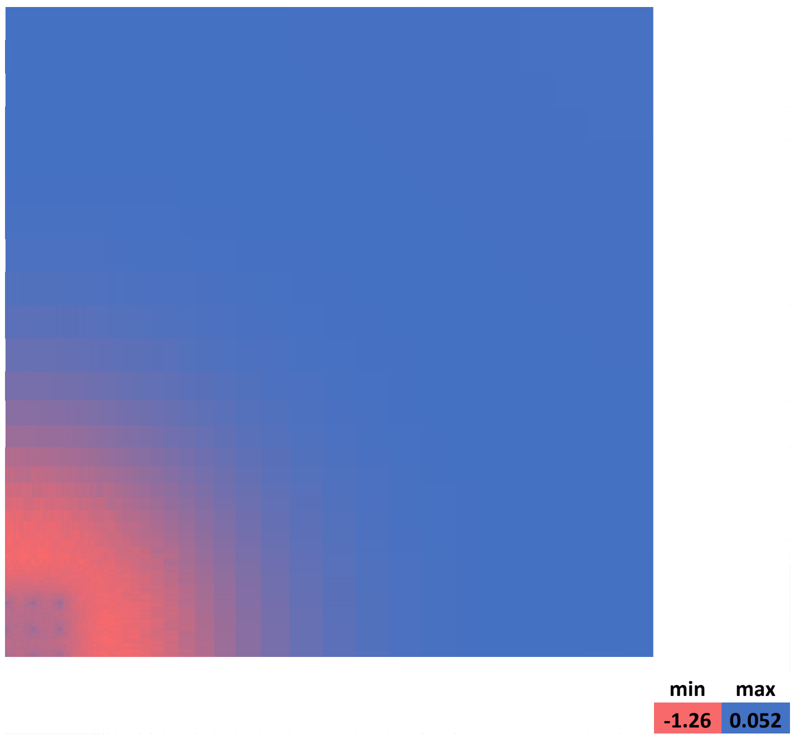

Figure 6-2 Difference in drawdown prediction (in m) between single-phase SIMED and MODFLOW models.

6.1.2 Comparison of MODFLOW single-phase and SIMED dual-phase results

Figure 6-3 presents the difference in drawdown predictions for each model layer, averaged over the entire model layer, between the single-phase MODFLOW and the single and dual-phase SIMED models. The vertical distance between model layers is not represented to scale in this figure.

Results indicate that when comparing the single-phase models (blue line) a maximum error in average drawdown predictions of 1.4 m occurs in layer 4 of the model (the layer overlying the target Bohena Seam), and that with decreasing depth, the difference in drawdown predictions between MODFLOW and SIMED decrease. Overall, the minor differences in predictions of water production and drawdown from the single-phase MODFLOW and SIMED models constituted a sufficient match to then utilise the models for further comparison of dual-phase behaviour.

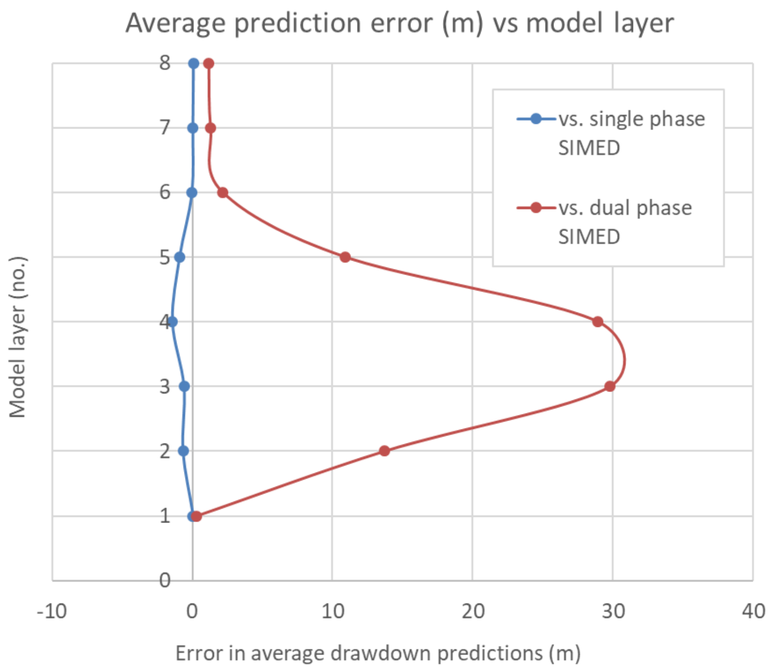

Figure 6-3 Error in model layers for single-phase MODFLOW vs single and dual-phase SIMED drawdown predictions (vertical axis not to scale).

Following verification, the full range of reservoir and production parameters related to dual-phase CSG production were reintroduced into the SIMED model. This included CSG well models where control switches from constant surface rate to constant bottom hole pressure during production, the Shi and Durucan (2006) permeability model which incorporates desorption-induced matrix shrinkage effects, relative permeability models, and Langmuir gas desorption parameters. The output from the fully parameterised SIMED dual-phase model after 20 years of production was compared to the single-phase MODFLOW results (Figure 6-4). Following 20 years production from the target Bohena Seam, differences in drawdown of up to 65 m head (equivalent to 17.3% error) were observed in the regions adjacent to the CSG field, and MODFLOW water production was 22.7% higher than the fully parameterised CSG model. This demonstrated the insufficiency of the single-phase MODFLOW model for capturing the effects of CSG well field influences on groundwater behaviour.

The vertical distribution of prediction error across model layers is also presented in Figure 6-3. This demonstrates the large increase in average error in drawdown predictions when using a single-phase model compared to a dual-phase model. In this case the largest prediction error occurs in the target Bohena Seam, and as with the single-phase model, decreases as distance from the production horizon increases.

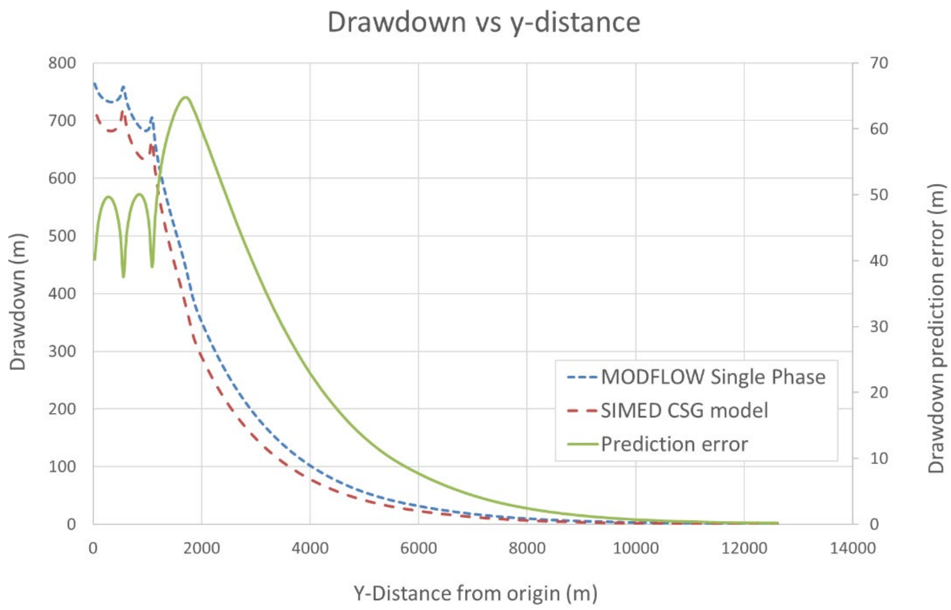

Figure 6-4 Bohena Seam drawdown profiles in horizontal distance from origin for single-phase MODFLOW and dual-phase SIMED.

6.2 Two-phase flow behaviour in MODFLOW-USG

A modified MODFLOW-USG package was supplied to CSIRO by the original software developer of MODFLOW-USG. This modified version allows for the simulation of dual-phase flow through the implementation of the Richards (1931) and van Genuchten (1980) equations for unsaturated flow, and the Brooks and Corey (1964) equation for relative permeability which is applied to model the water relative permeability behaviour only.

In this task the Brooks and Corey exponent for MODFLOW water relative permeability was modelled from the relative permeability data used in the Namoi CSG field model. Comparison of the SIMED curve and the Brooks and Corey model is shown in Figure 6-5. The irreducible water saturation and exponent used in the Brooks and Corey model were 0.84 and 1.626 respectively.

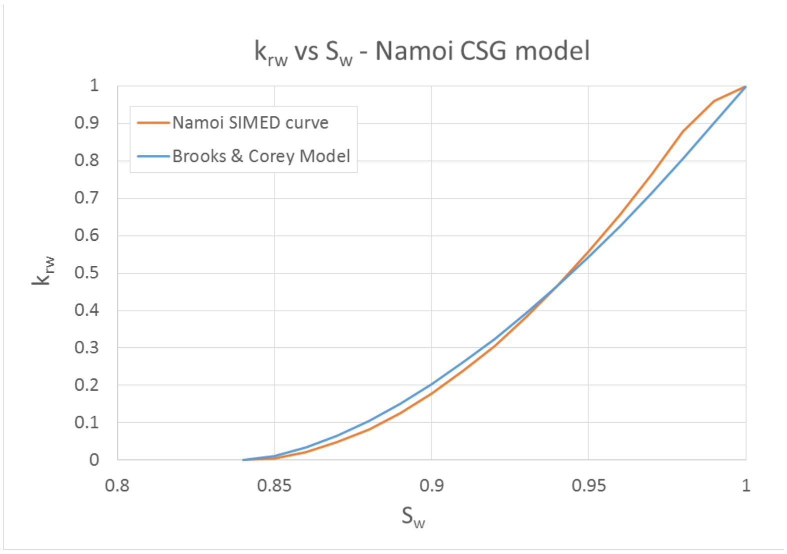

Figure 6-5 Comparison of the SIMED relative permeability data and Brooks and Corey model used in MODFLOW.

The van Genuchten equation, describing the relationship between water saturation and pressure, was used to model the S_w vs P data generated in Chapters 4 and 5 from SIMED production simulations undertaken with the Namoi CSG field symmetry model. The equation is discussed in more detail in Chapter 1 of the report (Equation 1). Three fitting parameters are used to fit the equation to water saturation and pressure data: α, β and h_b. Parameters α and β are fitting parameters which define the S-shaped van Genuchten curve, and h_b represents the bubble point pressure head, which in a CBM context refers to the height of a column of water that corresponds to the desorption pressure of the coal matrix.

As discussed in Chapter 5, the generated S_w vs P data may be interpreted across a range of time periods and spatial regions, from which various averaged relationships can be derived. The S_w vs P data were interpreted to generate a selection of scenarios, including:

- Relationships across a range of production times
- Averaged relationships across the entire target layer in the model domain.
- Relationships within the field boundary, adjacent to, and outside the field boundary.

Figure 6-6 presents the fit of the van Genuchten equation to a selection of S_w vs P curves sampled across a range of production times. The data obtained from the SIMED simulation include S_w vs P relationships from a production time of 5 days through to 20 years. As discussed in Chapter 3, the S_w vs P data did not approach a time-asymptotic relationship, as previously described by Herckenrath et al. (2015) for the Surat Basin CMA. For the Namoi region CSG model, a range of values of S_w that occur throughout the life of the field for a given pressure were averaged (orange data) and used to as the basis for the van Genuchten model fit. The fitting parameters for this model scenario are presented in Table 6-2. As can be observed in Figure 6-6, the model provides a reasonable fit to the average saturation values, but cannot adequately describe the range of saturation and pressure values that occur throughout the life of the field. The van Genuchten model was also used to approximate the S_w vs P relationship derived by averaging the water saturation and pressure across the entire SIMED model target layer throughout the duration of production simulation (Figure 6-7). Similarly, the equation is not able to describe the derived relationship closely.

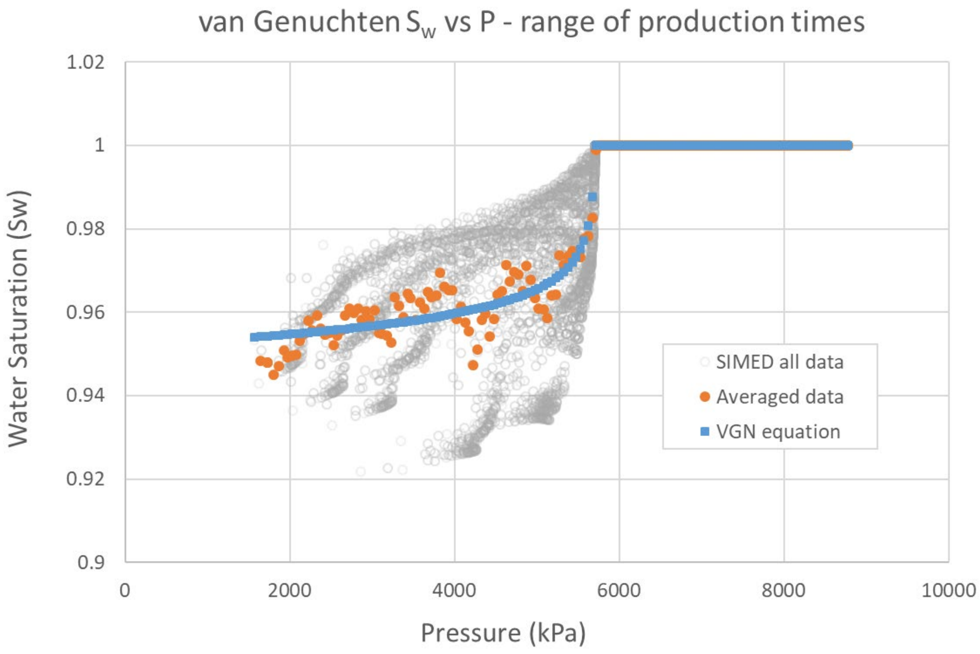

Figure 6-6 van Genuchten equation fit to Namoi CSG field S_W vs P data over a range of production times.

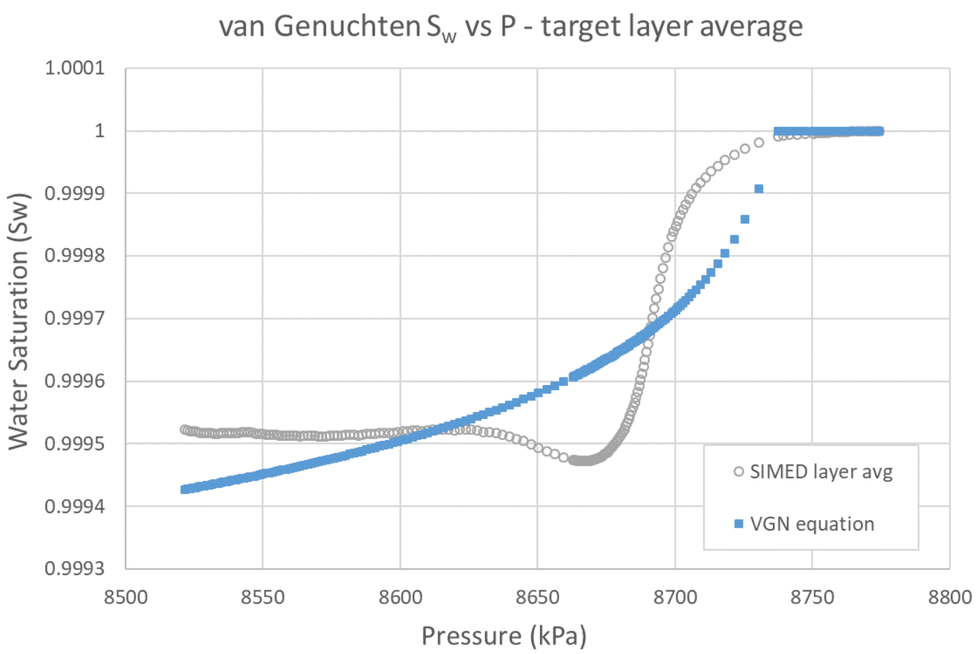

Figure 6-7 van Genuchten equation fit to Namoi CSG field S_W vs P data averaged over the model target layer.

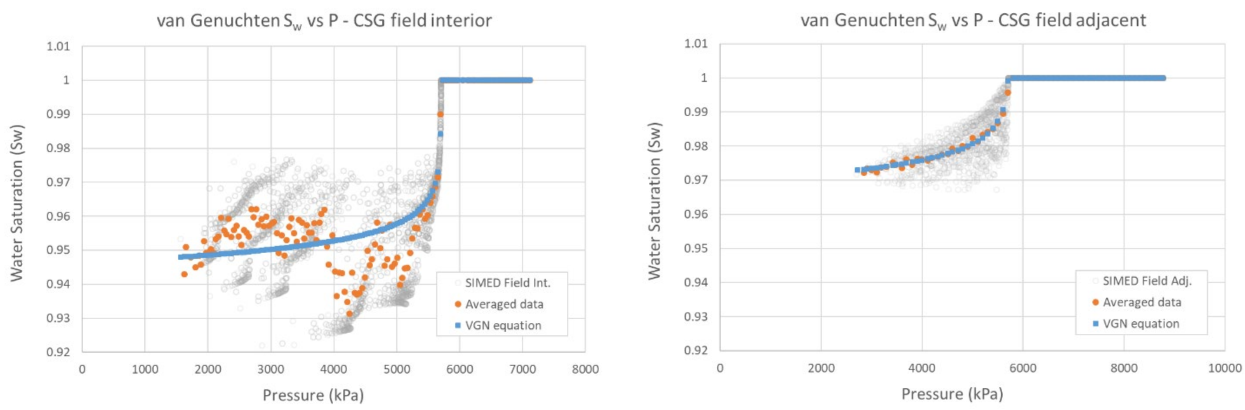

Figure 6-8 van Genuchten equation fit to Namoi CSG field S_W vs P data for the field interior grid blocks (left) and field adjacent grid blocks (right).

Figure 6-8 presents the van Genuchten equation fit for two portions of the Namoi CSG field symmetry model: grid blocks located within the boundaries of the well field, and grid blocks located adjacent or near to the well field. Grid blocks far from the well field do not undergo desaturation and therefore are not suitable for modelling the S_W vs P relationship. For each subsample of grid blocks and production times, the water saturation was averaged across all times for a given pressure (as per Figure 6-6) and this average served as the basis for fitting using the van Genuchten equation. The equation provides a better approximation of the averaged desaturation behaviour in grid blocks adjacent to the CSG field boundary (Figure 6-8, right) as opposed to within the producing CSG field.

Using the three aforementioned parameters to fit the van Genuchten equation to different interpretations of these data will result in different water production and drawdown behaviour once the relationship is implemented in the MODFLOW model. In addition, the grid cells chosen in the MODFLOW model for implementation of the desaturation relationship will affect the drawdown and production behaviour. The fitting parameters for the different interpretations of SIMED Namoi CSG field model S_W vs P data are presented in Table 6-2. For most data sets the van Genuchten equation was fitted using a linear regression, however in the case of the S_W vs P data for the CSG field interior this resulted in parameters which prevented convergence of the MODFLOW model when implemented. To avoid this, the van Genuchten parameters were determined manually to provide adequate fit to the data and stability for the numerical model. The bubble point pressure chosen when modelling the averaged S_W vs P data (see Approach 2, Scenario 2) represents the average pressure across the SIMED model producing layer at the point when averaged water saturation in the layer first drops below 1.

Table 6-2 van Genuchten model fitting parameters for different Namoi CSG field model S_W vs P interpretations.

APPROACH NO.	APPROACH TO MODELLING DESATURATION	alpha	beta	h_b (kPa)
1	Model data across all production times (Figure 6-6)	1.173831	1.054655	5707
2	Model target layer average for S_W and P (Figure 6-7)	1.019564	1.000997	8772
3	Model S_W vs P inside field (Figure 6-8, left)	8	1.049	5707
4	Model S_W vs P outside field (Figure 6-8, right)	0.320141	1.040046	5707
5	Model 20 year production S_W vs P data only	0.001584	1.270822	5707

6.3 Implementation and performance in Namoi MODFLOW model

The dual-phase version of MODFLOW allows users to specify which grid cells will have the capability to model desaturated (and hence dual-phase) flow, and for these grid cells users must specify the Brooks and Corey exponent for water relative permeability, and the van Genuchten equation parameters α, β and h_b. For the implementation of dual-phase flow in this task the desaturated option was specified for cells only within the main target layer, the Bohena Seam of the Maules Creek Formation. Across a number of simulations, a range of implementation scenarios were investigated, wherein different van Genuchten model parameters were assigned to different areas of grid blocks within the target layer. The effect this implementation had on total water production and pressure drawdown profile across the MODFLOW model target layer was determined through comparison with the Namoi CSG field symmetry model. Table 6-3 presents water production data from the different scenarios investigated and compares it to the SIMED Namoi CSG field symmetry model, demonstrating the effect of utilising different desaturation modelling and implementation schemes. Performance of the different modelling and implementation schemes is further discussed in the following sections.

Table 6-3 Selected implementations of van Genuchten equation within MODFLOW and the averaged effects on output compared to Namoi CSG well symmetry model.

SCENARIO NO.	APPROACH TO MODELLING DESATURATION	IMPLEMENTATION IN MODFLOW	WATER PRODUCTION (ML)	DIFFERENCE IN PRODUCTION (%)
1	**Model data across all production times**	Apply to all grid cells in target layer	487.64	+8.5
2	**Model data across all production times**	Apply to grid cells within field boundary only	535.96	+19.2
3	**Model target layer average for S_W and P**	Apply to all grid cells in target layer	549.18	+22.2
4	**Model S_W vs P inside and outside field**	Apply appropriate models to grid cells inside and outside field.	506.88	+12.8
5	**Model 20 year production S_W vs P data**	Apply to all grid cells in target layer	541.12	+20.4

6.3.1 Modelling and implementation Scenario 1

In this scenario the Brooks and Corey relative permeability exponent and the van Genuchten parameters derived using Approach 1 (see Table 6-2) were assigned to all grid blocks located in the target layer of the MODFLOW Namoi groundwater flow model. Figure 6-9 presents heat maps allowing comparison of the magnitude of error in drawdown predictions across the target layer for the single-phase MODFLOW model (left) and the dual-phase MODFLOW model in Scenario 1 (right). The error is defined as the absolute difference in m head for a grid block drawdown prediction between the MODFLOW model and the SIMED Namoi CSG field symmetry model after 20 years production. As Figure 6-9 indicates, the implementation of dual-phase functionality into the MODFLOW model significantly improves drawdown prediction in the region adjacent to the CSG well field. Average drawdown error within the well field boundary is 46.9 m compared to 49.1

m for the single-phase MODFLOW model, and averaged drawdown error outside the well field boundary is 6.3 m compared to 27.1 m for the single-phase MODFLOW model. This represents a 77% reduction in predicted drawdown error beyond the CSG field boundary as a result of dual-phase implementation in MODFLOW. Similarly, error in predictions of water production were reduced by 63%. Notably, the implementation in Scenario 1 resulted in an area of drawdown under-prediction in a triangular area adjacent to the well field (Figure 6-9, right), the implications of which may require consideration if the implementation scheme is utilised in the GISERA GAB flux model. In this scenario, the under-prediction in drawdown was no greater than 4.9% of the total drawdown in the area of interest.

Figure 6-9 Magnitude of drawdown prediction error (in m head) for single-phase MODFLOW (left) and Scenario 1 (right).

The improvements in MODFLOW predictions of groundwater production and drawdown due to the introduction of dual-phase functionality are not limited to the target Bohena Seam only. Figure 6-10 presents the error in averaged drawdown predictions between single and dual-phase MODFLOW models and the fully parameterised SIMED Namoi CSG model after 20 years production. The vertical axis of the plots is not to scale and does not represent the true layer thicknesses. Whole layer averages presented in Figure 6-10 top show reductions in average error of around 20 m in the target Bohena Seam (Layer 3). In shallower layers the improvement due to the implementation of dual-phase functionality is reduced, as the overall influence of CSG production on hydraulic heads diminishes due to the thickness and low permeability of the overlying formations. In the topmost layer of the Namoi CSG model, encompassing all formations from the Trinkey to the Benalabri Formation, the drawdown across this layer after 20 years production ranges from only 7.1 m to negative 0.1 m, with the latter value slightly negative due to model equilibration. The bottom left and right plots in Figure 6-10 also demonstrate how the largest improvement in drawdown prediction occurs in the field exterior, as opposed to the CSG field interior, when implementing the Scenario 1 approach to dual-phase functionality.

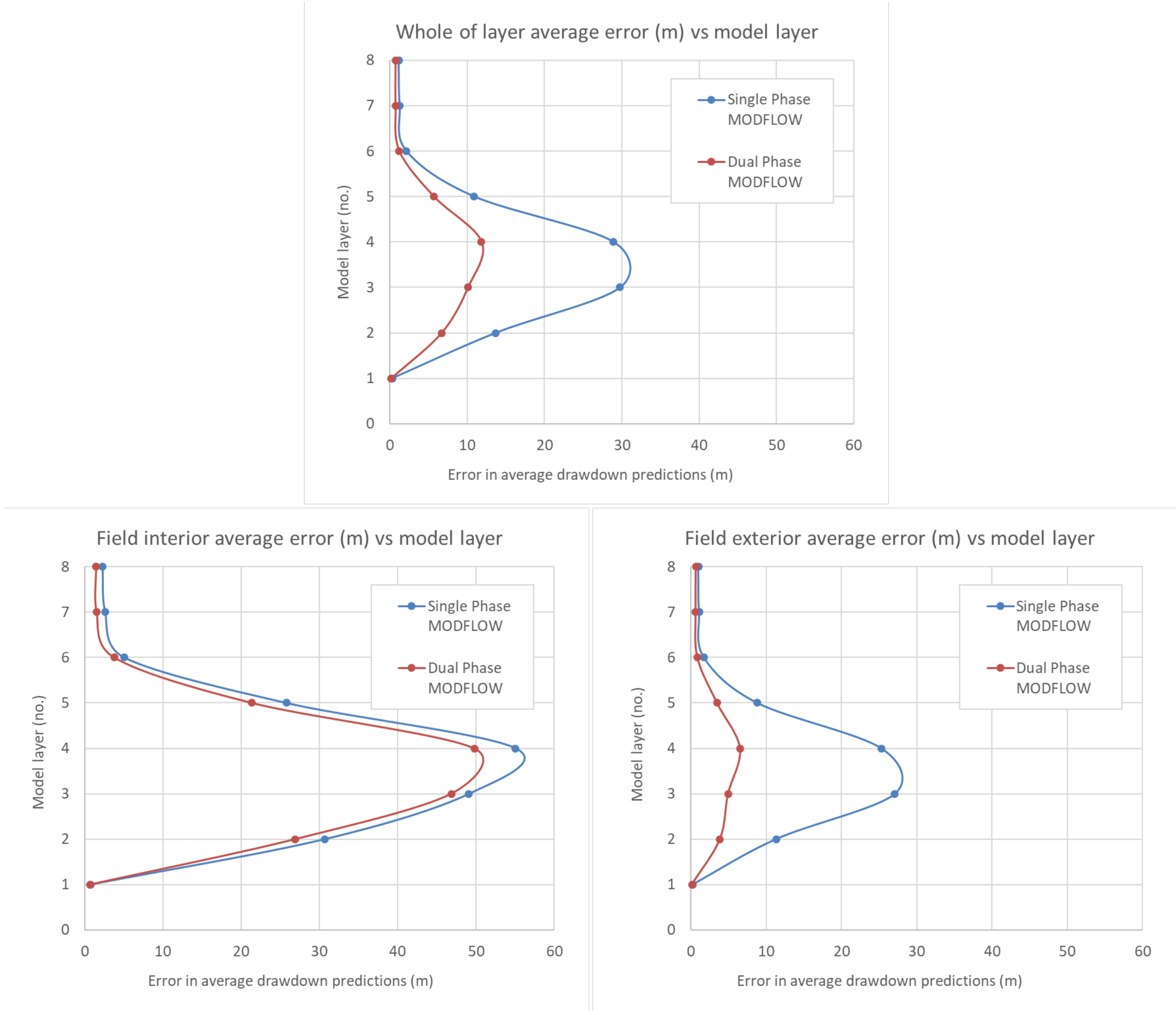

Figure 6-10 Error in model layers compared to dual-phase SIMED drawdown predictions for single-phase and dual-phase MODFLOW models (vertical axis not to scale).

6.3.2 Modelling and implementation Scenario 2

In this scenario the Brooks and Corey relative permeability exponent and the van Genuchten parameters derived using Approach 1 (see Table 6-2) were assigned to grid blocks only located within the boundaries of the well field in the MODFLOW model. No desaturation relationship was assigned to grid blocks beyond the CSG well field boundary. The resulting errors in drawdown predictions are presented in Figure 6-11 and indicate that dual-phase implementation has little effect on predicted drawdown error beyond the CSG field boundary. Average drawdown error within the well field was 35.1 m compared to 49.1 m for the single-phase MODFLOW model, and averaged drawdown error outside the well field boundary was 24.8 m compared to 27.1 m for the single-phase MODFLOW model. The larger reduction of error compared to Scenario 1 for in-field drawdown predictions suggest that production and drawdown behaviour beyond the CSG field boundary will affect predictions within the field. In addition, this means that for more accurate drawdown predictions over a regional scale it will be important to implement some form of dual-phase flow relationship in grid blocks outside any CSG field boundary.

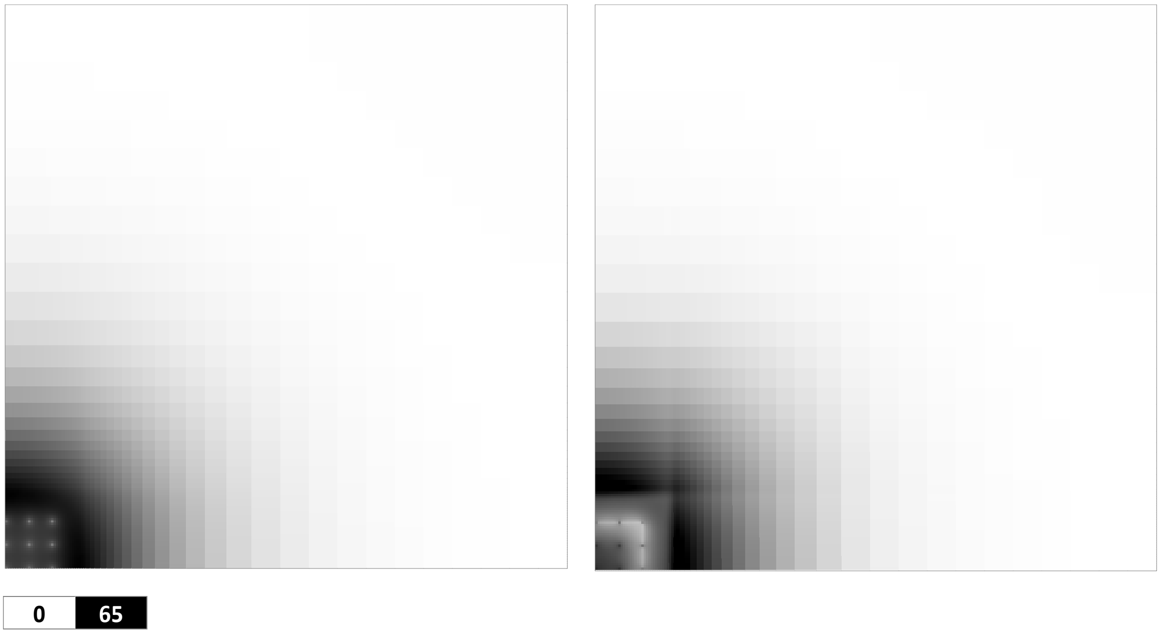

Figure 6-11 Magnitude of drawdown prediction error (in m head) for single-phase MODFLOW (left) and Scenario 2 (right).

6.3.3 Modelling and implementation Scenario 3

In this scenario the Brooks and Corey relative permeability exponent and the van Genuchten parameters derived using Approach 2 (see Table 6-2) were assigned to all grid blocks located in the target layer of the MODFLOW Namoi groundwater flow model. This scenario implemented dual-phase relationships that were derived by averaging over the entire model layer.

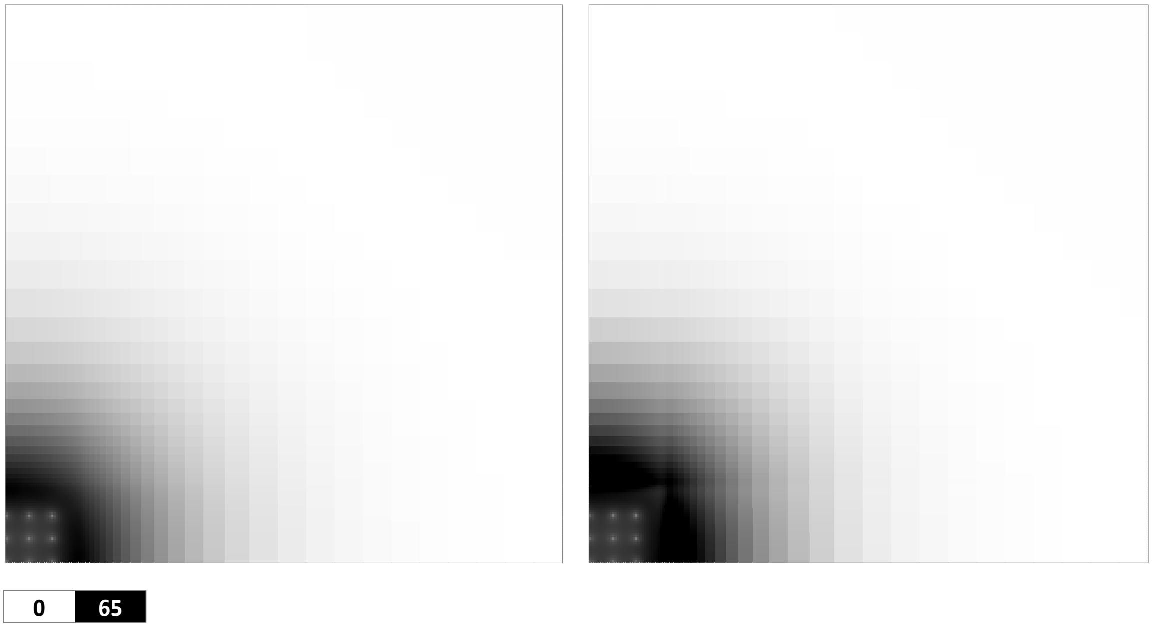

Figure 6-12 Magnitude of drawdown prediction error (in m head) for single-phase MODFLOW (left) and Scenario 3 (right).

A heat map of the drawdown error is presented in Figure 6-12 and shows that the implementation scheme did not have a significant effect on drawdown predictions. No change was observed in average error of drawdown predictions within the CSG field boundary, while the average error in drawdown predictions outside the CSG field boundary at 37.1 m was 10 m greater than the single-phase model. The deleterious effect on drawdown predictions indicates that the effect of spatial scale when implementing dual-phase relationships into the GAB model will need to be considered.

6.3.4 Modelling and implementation Scenario 4

In this scenario the Brooks and Corey relative permeability exponent and the van Genuchten parameters derived using Approach 3 and 4 (see Table 6-2) were assigned to all grid blocks located in the target layer of the MODFLOW Namoi groundwater flow model. As described, two sets of van Genuchten parameters were derived from the S_w vs P relationship across grid blocks inside and outside the CSG well field boundary, and implemented in the corresponding regions of the MODFLOW model. Figure 6-13 presents heat maps of the error in predicted drawdown for Scenario 4. These indicate an improvement in drawdown predictions in the region adjacent to the well field. Average drawdown error within the well field was 38.1 m compared to 49.1 m for the single-phase MODFLOW model, and averaged drawdown error outside the well field boundary was 12.2 m compared to 27.1 m for the single-phase MODFLOW model. The result is superior within the well field but inferior beyond the well field compared to Scenario 1, suggesting either that using a combination of relationships can lead to a more balanced result across an entire model domain, or that it will be necessary to choose an implementation approach based on modelling priorities.

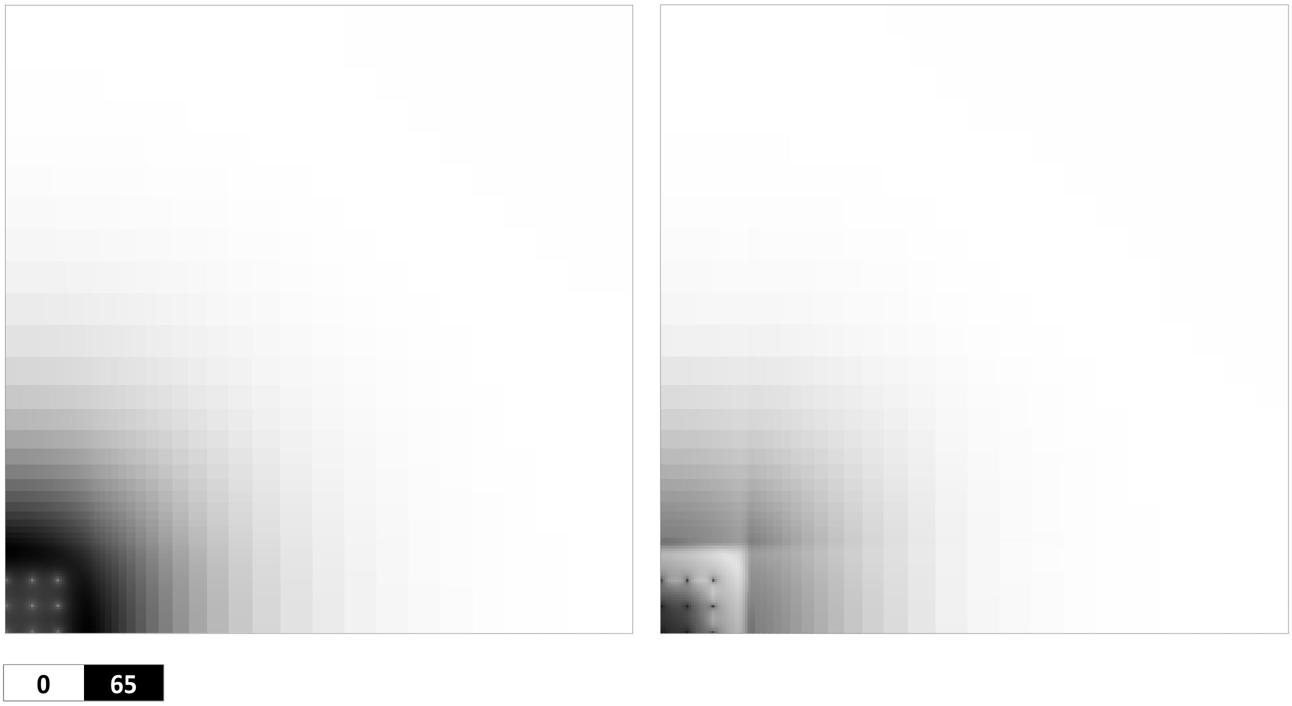

Figure 6-13 Magnitude of drawdown prediction error (in m head) for single-phase MODFLOW (left) and Scenario 4 (right).

6.3.5 Modelling and implementation Scenario 5

In this scenario the Brooks and Corey relative permeability exponent and the van Genuchten parameters derived using Approach 5 (see Table 6-2) were assigned to all grid blocks located in the target layer of the MODFLOW Namoi groundwater flow model. Approach 5 follows that taken by Herckenrath et al. (2015) whereby the 'time-asymptotic' S_w vs P curve that occurs after 20 years of CSG production is modelled using the van Genuchten equation. In reservoir simulations of the Namoi region the time-asymptotic desaturation behaviour was not observed to the same extent as the aforementioned literature, however a relationship suitable for modelling exists. The error in drawdown prediction using the Scenario 5 implementation approach is presented in Figure 6-14. Implementation of this scenario resulted in very little change in average predictions of drawdown. Average drawdown error within the well field was 47.3 m compared to 49.1 m for the single-phase MODFLOW model, and averaged drawdown error outside the well field boundary was 26.9 m compared to 27.1 m for the single-phase MODFLOW model. Despite the similarities in average values the implementation resulted in a larger rate of change in error across grid cells in the vicinity of the field boundary, which may reduce the predictive utility of the model.

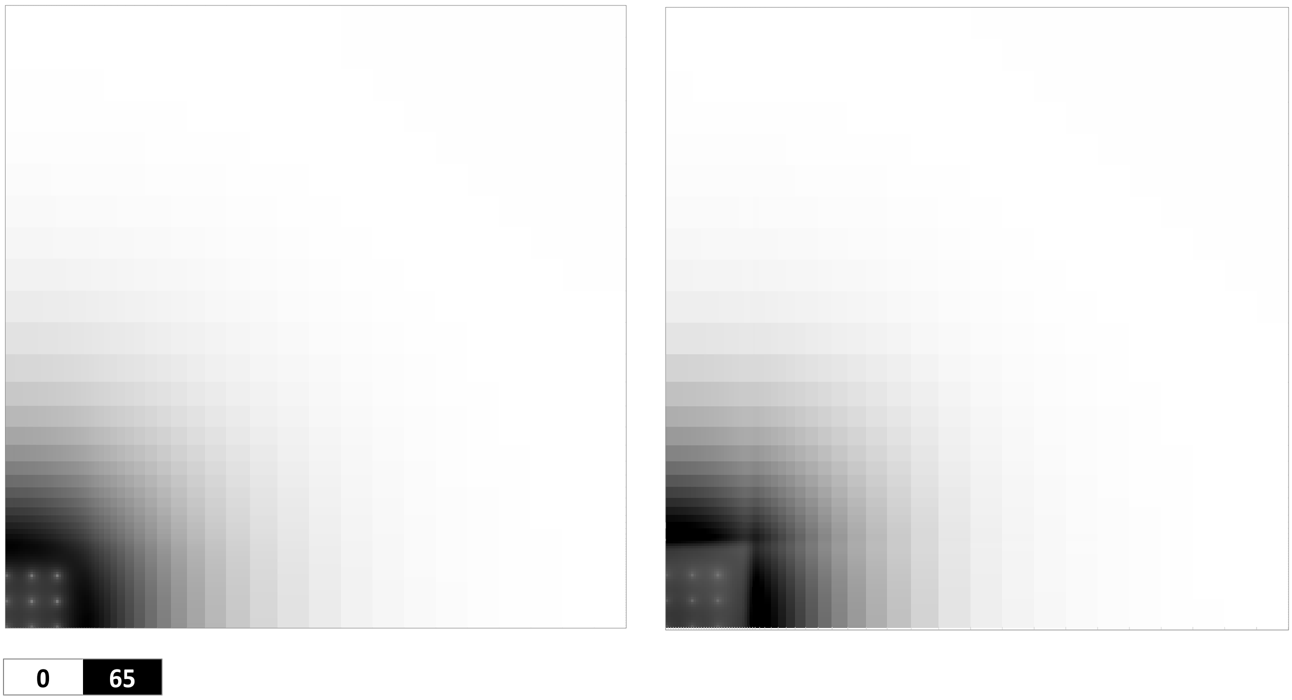

Figure 6-14 Magnitude of drawdown prediction error (in m head) for single-phase MODFLOW (left) and Scenario 5 (right).

6.3.6 Effect of spatial upscaling on implementation

Investigations using the fully parameterised SIMED Namoi CSG model in Chapter 5 established the result of upscaling the S_w vs P relationship derived from simulations conducted using that model. Spatial arithmetic upscaling of the SIMED saturation and pressure output indicated that the relationship would not be altered (Figure 5-10), and that the S_w vs P curve could be modelled using the same values for parameters of the van Genuchten desaturation equation. This suggested that implementation of the desaturation functionality via the van Genuchten equation into larger scale grid blocks utilised in the GAB flux model could utilise the same fitting parameters as derived from the finer scale Namoi CSG model.

To investigate the effect on predicted water production and drawdown of implementing the desaturation functionality into spatially upscaled MODFLOW grid blocks, a number of scenarios are modelled examining different MODFLOW grid block scales. The water production and spatial variation in drawdown within the target Bohena Seam predicted by the MODFLOW models are compared to water production and manually upscaled drawdown results from the 8 layer fully parameterised SIMED Namoi CSG model as described in Section 6.1.1. The scenarios use the same drain conditions, model dimensions, and reservoir parameters, while the grid block size (and consequently number of grid blocks in the model) are varied in the spatial direction. Results from a single-phase MODFLOW model as well as a vertically upscaled 6-layer MODFLOW model (see section 6.3.7) are included for comparison.

Water production results for the five MODFLOW scenarios are presented in Table 6-4. Observing Scenarios 6 to 8, water production increases as grid block size and degree of upscaling increases. This results in an over-prediction in water production that increases from 8.5% in the MODFLOW model with equivalent grid block size to the Namoi CSG model, through to 27.6% in the MODFLOW model utilising larger grid blocks. The over-prediction by MODFLOW will result in a conservative estimation of CSG water production impacts using the groundwater model, however the extent of influence of groundwater model grid block scale can be pronounced. This increased error is likely to be driven by the difference in scale between complex dual-phase reservoir flow processes in the CSG field and the grid block size present in the regional groundwater flow models. The effects of gas production on fluid flow behaviour are more pronounced in the near wellbore region, and these processes are normally captured in CSG reservoir models using fine-scale grid blocks in near wellbore regions. The lack of fine-scale grid blocks (in either the reservoir or groundwater model) limits the accuracy of the model in capturing the effect of these processes, and thus in accurately predicting water production and drawdown. Although Chapter 5 established that the same S_w vs P relationship applies for implementation into MODFLOW even after spatial upscaling of SIMED data, the results of Scenarios 6 to 8 indicate output will differ.

Table 6-4 Effect of MODFLOW grid block size on predicted water production when implementing the van Genuchten equation to spatially upscaled models.

SCENARIO NO.	MODFLOW GRID BLOCK SIZE (M)	MODFLOW MODEL DETAILS	WATER PRODUCTION (ML)	INCREASE COMPARED TO SIMED 8-LAYER (%)
6	**53 - 659**	2 Phase, 8-layer	487.64	8.5
7	**106 - 1318**	2 Phase, 8-layer	516.62	14.9
8	**265 - 3295**	2 Phase, 8-layer	573.65	27.6
9	**265 - 3295**	1 Phase, 8-layer	620.32	38.0
10	**265 - 3295**	2 Phase, 6-layer	555.56	23.6

Figure 6-15 demonstrates the effect of increasing the minimum grid block size on predictions of water production. The sensitivity of the MODFLOW models to increases in the minimum grid block size is greater than observed on the equivalent SIMED model (grey line). As well as being due to the influence of upscaling on representation of near wellbore fluid behaviour as described above, the difference in sensitivity may occur due to the different well models being used by the modelling packages. SIMED CSG reservoir models incorporate the Peaceman (1978) well model whereas the MODFLOW models utilise the drain condition specifying a conductance value that relates changes in grid block head to water production rate.

Despite the differences in sensitivity it can be observed that the implementation into MODFLOW of dual-phase flow via the Richards equation functionality results in an improvement in predictions of water production. In addition, Figure 6-15 suggests that a MODFLOW model that has undergone vertical upscaling to match layering of the GAB flux model (see Section 6.3.7) will provide a closer water prediction to the Namoi CSG model as grid block size increases. In this instance the implementation of dual-phase functionality into a vertically and spatially upscaled MODFLOW model reduced error in predictions of water production by at least 38%.

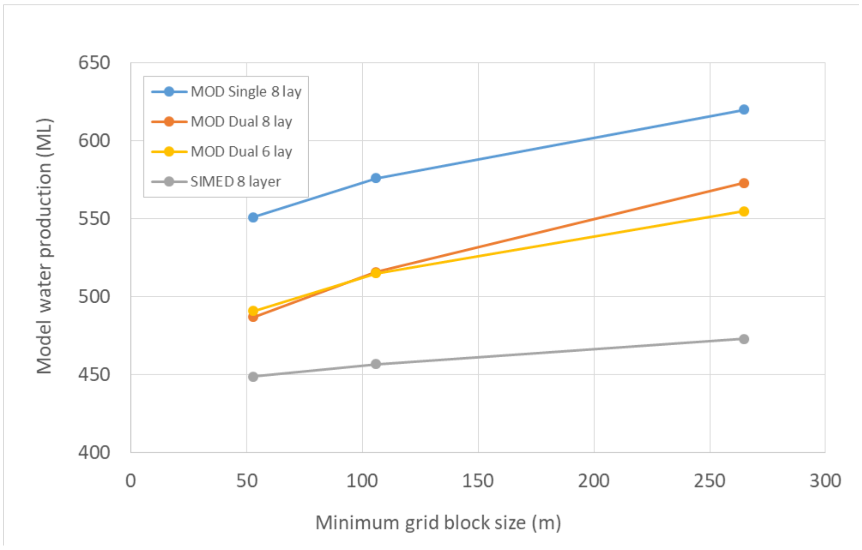

Figure 6-15 Effect of minimum grid block size on predicted water production.

The effect of grid block size can also be observed in predictions of drawdown across the target model layer (Table 6-5). As minimum grid block size was increased through scenario 6 to 8, the average magnitude of drawdown error between the MODFLOW and SIMED CSG models also increased, resulting in greater over-prediction of drawdown both within the CSG field interior and exterior. As with water prediction this represents a more conservative estimate, but again the extent of influence of groundwater model grid block scale can be pronounced. In making drawdown predictions beyond the CSG field boundary, the MODFLOW models that incorporate dual-phase functionality outperform the single-phase models, and in scenario 10, where a degree of vertical upscaling has also been employed, the average magnitude of error in drawdown prediction is reduced by over 70%.

Table 6-5: Effect of minimum grid block size on average magnitude of drawdown error.

SCENARIO NO.	AVERAGE MAGNITUDE OF DRAWDOWN ERROR		
	LAYER TOTAL (m)	FIELD INTERIOR (m)	FIELD EXTERIOR (m)
6	11.3	46.8	6.3
7	21.9	69.8	14.4

8	45.4	110.6	31.8
9	62.8	100.2	54.9
10	17.3	41.6	12.1

6.3.7 Effect of vertical upscaling on implementation

The groundwater flow model produced in MODFLOW for the Namoi subregion Bioregional Assessments uses a total of nine layers to represent Gunnedah Basin hydrostratigraphic units. The Bohena Seam is modelled as part of a layer that combines all geological units of the Maules Creek Formation. These include the Upper Maules Creek Formation, the Rutley, Namoi, Parkes and Bohena Seams and their associated interburden, and the Lower Maules Creek Formation. In the Namoi CSG model constructed in SIMED, the Bohena Seam is modelled as an individual layer, with the upper and lower Maules Creek Formation represented by an additional layer above and below the target seam.

The additional vertical layers in the Namoi CSG model allow for added detail and a more accurate characterisation of coupled reservoir flow processes in the vicinity of the CSG field and target seam. Approaches to modelling these processes and implementing them into an upscaled MODFLOW model with thicker layers were assessed, and the water production and drawdown behaviour of upscaled MODFLOW models compared to the manually upscaled behaviour of the SIMED Namoi CSG model.

In order to directly compare performance to MODFLOW models, the pressure drawdown behaviour of the layers 2, 3 and 4 in the Namoi CSG model were upscaled to an equivalent single layer. As outlined in Chapter 5, the large thicknesses and pore volumes of the overlying and underlying formations adjacent to the Bohena Seam have a significant influence on the vertically upscaled S_w vs P, and relative permeability relationships. Upscaling the output of the Namoi CSG model produces relationships showing only small changes in saturation for large changes in pressure, and large changes in relative permeability for only small changes in saturation. Suitability of these relationships for implementation into a MODFLOW model was assessed.

The spatial variation in pressure drawdown across layers 2, 3 (the target Bohena Seam) and 4 of the Namoi CSG model due to 20 years of simulated CSG production were upscaled to a single layer using a thickness weighted average method. This pressure drawdown profile was used as the basis of comparison to results from other simulations conducted using a MODFLOW model that contained a single layer in place of the original three.

The vertical and horizontal hydraulic conductivity, and the specific storage were calculated for the new MODFLOW layer using thickness-weighted averages of the original values across the three layers. Figure 6-16 presents a heat map detailing the magnitude of error in drawdown prediction for a single-phase upscaled MODFLOW model compared to the upscaled output of the dual-phase Namoi CSG model. The heat map demonstrates that compared to the CSG model, the upscaled single-phase MODFLOW model over-predicts drawdown within the field and adjacent to the boundary, and as distance from the field increases this transitions to an under-prediction of the drawdown which then diminishes with increasing distance.

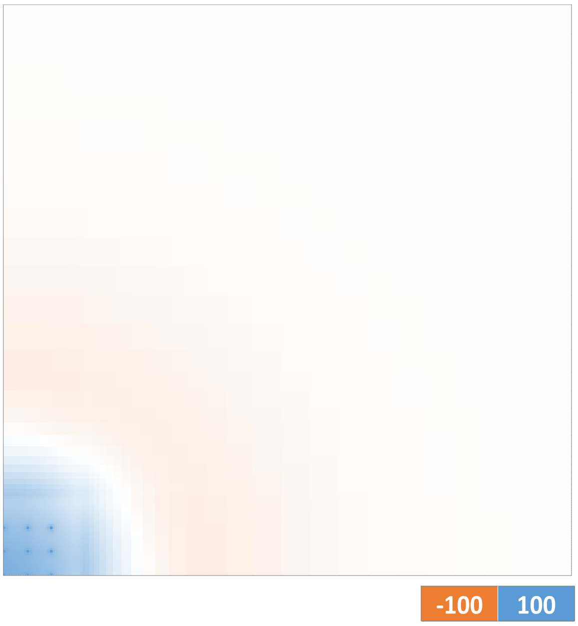

Figure 6-16 Drawdown prediction error (in m head) for the single-phase upscaled MODFLOW model.

The error in prediction of water production compared to the dual-phase Namoi CSG model is presented in Table 6-6.The magnitude of drawdown prediction error inside and outside the field boundary when using the single-phase upscaled MODFLOW model is presented in Table 6-7.

Table 6-6 Difference in water production compared to dual-phase Namoi CSG model for different upscaled MODFLOW scenarios.

SCENARIO NO.	APPROACH TO MODELLING DESATURATION	IMPLEMENTATION IN UPSCALED 6-LAYER MODFLOW MODEL	WATER PRODUCTION (ML)	DIFFERENCE IN PRODUCTION (%)
11	**No desaturation model - water phase only**	No desaturation	469.1	4.37
12	**Upscaled Sw vs P data modelled across all production times**	Apply to entire upscaled layer	467.6	4.03
13	**Bohena Seam data across all production times**	Apply to entire upscaled layer	491.5	9.35
14	**Bohena Seam data across all production times**	Apply to upscaled layer cells within field boundary.	492.1	9.48
15	**Bohena Seam data across all production times**	Apply to upscaled layer cells up to 200m from field boundary	491.3	9.31

Table 6-7 Average magnitude of drawdown prediction error for 6-layer upscaled MODFLOW model.

SCENARIO NO.	AVERAGE OF MAGNITUDE OF DRAWDOWN ERROR		
	LAYER TOTAL (m)	FIELD INTERIOR (m)	FIELD EXTERIOR (m)
11	23.5	68.2	17.3
12	23.3	69.6	16.8
13	10.0	31.5	7.0
14	12.5	38.5	8.9
15	9.7	32.8	6.4

MODFLOW desaturation parameters were also modified to represent the upscaled fluid flow behaviour from layers 2 to 4 of the Namoi CSG model. The effect of using upscaled desaturation parameters was investigated in Scenario 12 (Table 6-6). The Brooks and Corey residual water saturation was determined by thickness weighted upscaling of the irreducible water saturation for each of the SIMED model layers. The value of S_r used in modelling Scenario 12 was 0.98455. The Brooks and Corey exponent was calculated as 1.2975, based on a linear regression of the saturation and water relative permeability data that was derived by upscaling across layers 2 to 4 of the Namoi CSG model.

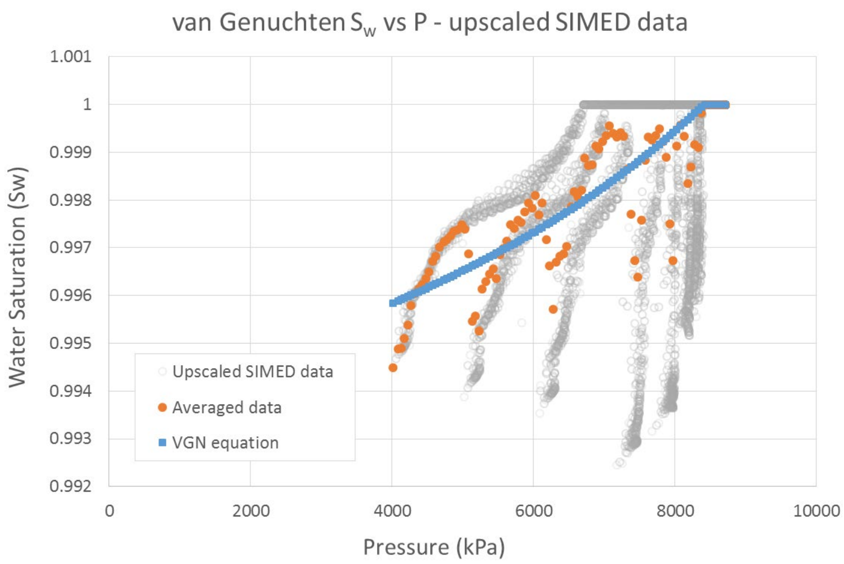

Figure 6-17 van Genuchten equation fit to upscaled Namoi CSG field S_W vs P data over a range of production times.

The saturation pressure relationship within each of the grid blocks in layers 2 to 4 of the Namoi CSG Model was upscaled using thickness-weighted averaging to generate S_w vs P relationships for grid blocks that spanned a thicker single layer. This was equivalent to the producing layer thickness in in the 6-layer MODFLOW model. Upscaling was completed for S_w vs P relationships across different production times, and the averaged data was modelled using the van Genuchten equation (Figure 6-17). The fitting parameters are presented as Approach 1 in Table 6-8, utilised in Scenario 12.

Table 6-8 Different fitting parameters for the van Genuchten equation used in the upscaled MODFLOW model.

APPROACH NO.	APPROACH TO MODELLING DESATURATION	alpha	beta	h_b (kPa)
1	**Model upscaled Sw vs P data across all production times**	0.002555	1.031218	8411.6
2	**Model Bohena Seam data only across all production times**	1.173831	1.054655	5707

In the 8-layer MODFLOW models, the drains are located solely in grid blocks within the target layer. For those scenarios the drain conductance was calculated based on single-phase SIMED Namoi CSG model production data, specifically the well water production rate and the corresponding pressure in the grid block that hosts the well completion (within layer 3, the target Bohena Seam).

Parameters supplied to MODFLOW for the drain condition also contribute to the overall water production, and must be suitably upscaled from reservoir model data to match the layering of the MODFLOW groundwater flow model. Investigation of the effect of drain conductance showed that if this is not undertaken, and drain conductance is calculated from SIMED pressure and water rate data pertaining to the Bohena Seam only, then utilisation of these values in an upscaled MODFLOW layer will result in extremely large over-prediction of water production (>50%). In applying the correct drain condition to the upscaled 6-layer MODFLOW model, the drain conductance used must represent the relationship between well water production rate and the upscaled pressure across not only the host grid block in layer 3, but the adjacent overlying and underlying grid blocks in layer 2 and 4. This value of upscaled host grid block pressure was calculated from the single-phase simulation output data from Namoi CSG model. It was used to calculate appropriate drain conductance to apply to the upscaled producing layer in the 6-layer MODFLOW model.

Implementation of appropriately upscaled dual-phase parameters into the 6-layer MODFLOW model allowed for comparison of the water production and drawdown prediction of a MODFLOW model with the same layering scheme as the GAB flux model, to the dual-phase Namoi CSG model constructed in SIMED. Five different modelling and implementation scenarios were investigated (Table 6-6). Scenario 11 was the single-phase upscaled model as described above.

6.3.7.1 Upscaled implementation Scenario 12

Implementation Scenario 12 utilised modelling Approach 1 (see Table 6-8) where the S_w vs P, relative permeability, and drain conductance relationships generated by SIMED were manually upscaled and modelled prior to implementation in the 6-layer MODFLOW model. The error in drawdown prediction (Figure 6-18) displays a high degree of similarity to the error in drawdown prediction when using a single-phase MODFLOW model such as Scenario 11 (see Figure 6-16). Difference in water production compared to the Namoi CSG model (Table 6-6) and averages of the magnitude in drawdown error presented in Table 6-7 show that no improvement in prediction over single-phase modelling is gained when implementing into MODFLOW desaturation and relative permeability relationships that have been previously vertically upscaled from reservoir simulator data.

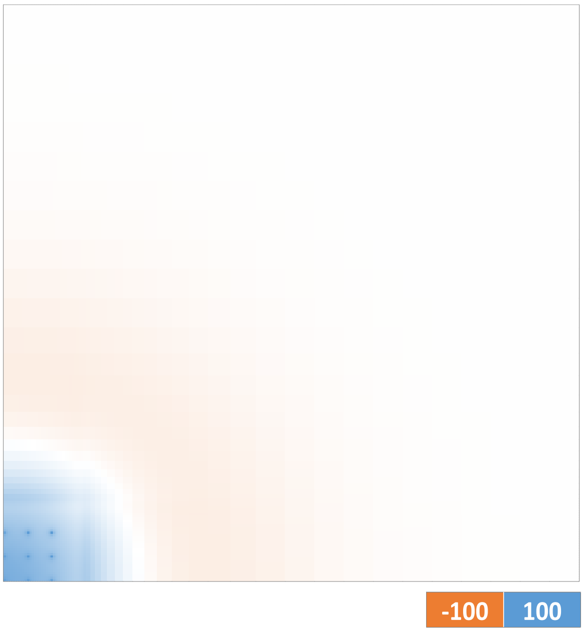

Figure 6-18 Drawdown prediction error (in m head) for Scenario 12 upscaled MODFLOW model.

6.3.7.2 Upscaled implementation Scenarios 13, 14 and 15

Implementation Scenarios 13 to 15 used van Genuchten modelling Approach 2 to represent the saturation vs pressure relationship in the MODFLOW model. This relationship is the same as was employed in Approach 1 of the 8-layer MODFLOW model (Table 6-2), and is based on averages of the S_w vs P behaviour in the Bohena Seam generated in the Namoi CSG model throughout the producing life of the field. For implementation Scenarios 13 to 15, the modelled S_w vs P relationship derived from only the Bohena Seam of the Namoi model (layer 3) was assigned to the entire upscaled layer of the MODFLOW model. As outlined in Table 6-6, Scenario 13 applied the desaturation relationship to every grid block in the upscaled producing layer of the MODFLOW model, Scenario 14 applied the relationship to only grid blocks contained within the field boundary, while Scenario 15 applied the desaturation relationship to grid blocks within the field and up to 200 m from the field boundary.

The resulting water production from each scenario is presented in Table 6-6 and compared to water production from the fully parameterised Namoi CSG model. When utilising the S_w vs P relationship derived from the Bohena Seam only, and applying it to the entire upscaled layer, the predicted water production from the MODFLOW model is approximately 9% higher than water production predicted by the fully parameterised Namoi CSG model.

This compares to an over-prediction of only approximately 4% when using the a single-phase upscaled model, however the single-phase result may reflect the influence of artefacts introduced by upscaling rather than additional accuracy in the single-phase model. By comparison, examining the water production from the 8-layer single-phase MODFLOW model, it was 22.7% greater than the Namoi CSG model, while the upscaled 6-layer single-phase MODFLOW model over-predicted water production by only 4.4%. This lower value is most likely due to the reduced impact in an upscaled layer of any error introduced by neglecting desaturation and dual-phase flow behaviour in the thinner coal seam, and indicated that upscaling has a significant effect on prediction of water production.

The spatial error in drawdown prediction for Scenarios 13 to 15 are presented in Figure 6-19, Figure 6-20, and Figure 6-21. The average magnitude of the drawdown error for the field interior and field exterior is reported in Table 6-7. The average magnitudes of drawdown error across Scenarios 13 to 15 indicate that the implementation into MODFLOW of the S_w vs P relationship derived only from the Bohena Seam, produces a much greater reduction in the drawdown error compared to using an upscaled S_w vs P relationship derived from multiple layers of the SIMED Namoi model (see Scenario 12). This is because in the vicinity of the CSG field significant drawdown occurs in the producing seam relative to the adjacent formations, and it is therefore a large contributor to vertically upscaled drawdown values. The horizontal propagation of pressure drawdown in the producing seam is governed by desaturation relationships in that seam, and thus near the CSG field the spatial propagation of pressure drawdown in the upscaled layer will be predominantly governed by this same seam desaturation behaviour. Therefore implementing the S_w vs P relationship from the target seam only into the upscaled MODFLOW layer provides a more accurate drawdown approximation than implementing an upscaled S_w vs P relationship, as seen in Scenario 12.

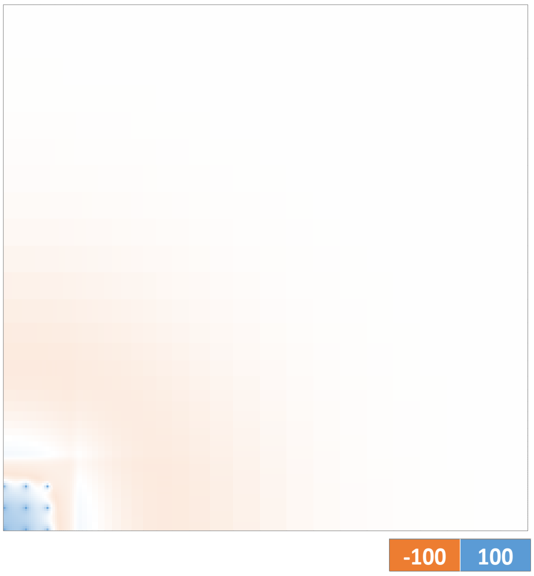

Figure 6-19 Drawdown prediction error (in m head) for Scenario 13 upscaled MODFLOW model.

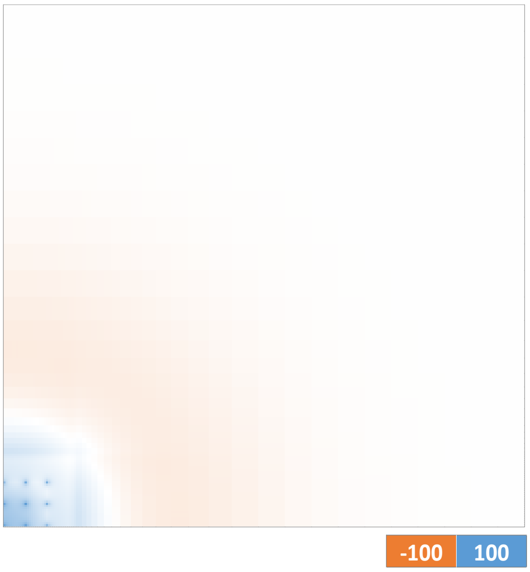

Figure 6-20 Drawdown prediction error (in m head) for Scenario 14 upscaled MODFLOW model.

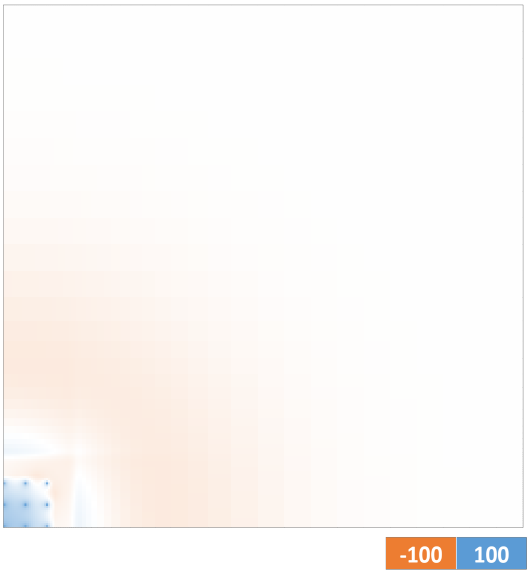

Figure 6-21 Drawdown prediction error (in m head) for Scenario 15 upscaled MODFLOW model.

The heat maps presented in Figure 6-19 to Figure 6-21 indicate the spatial variation of error in drawdown prediction of dual-phase MODFLOW models compared to the Namoi CSG model. Differences in the spatial variation between Scenario 13 (Figure 6-19), where the desaturation functionality is applied to every grid block in the upscaled layer, and Scenario 14 (Figure 6-20,) where it is applied only within the boundaries of the CSG field, highlight the importance of desaturation behaviour beyond the CSG field boundary to drawdown propagation. The importance of these grid blocks was confirmed in Scenario 15 (Figure 6-21) where desaturation functionality was applied to all grid blocks within 200 m of the CSG field boundary. This produce spatial variations in drawdown error similar to Scenario 13, whilst also providing a potential guideline for implementation of the desaturation functionality in regional scale models.

6.3.8 Effect of specific yield

The specific yield is defined as the amount volume of fluid that can be released from pores and fractures per unit area per unit fall in head (OGIA, 2016). The value can be no greater than the effective porosity of the formation. In groundwater modelling it is often used as the key storage parameter assigned to unconfined layers or outcropping grid blocks. The OGIA Surat CMA model also utilised the specific yield parameter in the coal bearing units to describe the release of water from coal layers where the water is displaced by desorbing gas.

In the Namoi groundwater flow model constructed in MODFLOW, the specific yield parameter was applied to all dual-phase grid cells that experience desaturation. In this instance only the coal-bearing layers experience desaturation and the value for specific yield chosen was equal to the coal cleat or fracture porosity (1.3%). During the simulation, grid blocks in coal-bearing layers are initially considered as confined, however once the pressure head in the grid block drops below bubble point head the grid block will convert to unconfined and the specific yield parameter will be included in mass-balance calculations.

A sensitivity study examined predicted water production after 20 years and found that changing the value of specific yield by more than 75% resulted in a change in water production of less than 2%. However this result is in fact sensitive to both the model parameters and simulation length, as the inclusion of specific yield in MODFLOW simulations will modify the water production profile from the model drains.

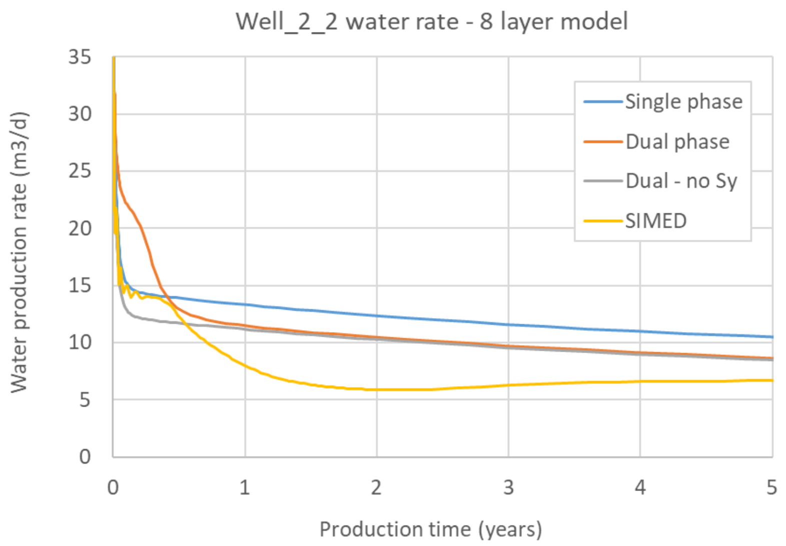

Figure 6-22 Water production rate from a single well or drain in the 8-layer Namoi models.

Figure 6-22 presents the water production rate from one of the 9 SIMED wells or MODFLOW drains in the 8-layer Namoi model. The figure highlights the difference in production rates over the first five years of CSG production depending on inclusion of dual-phase functionality and specific yield. The difference between well rates in SIMED and MODFLOW is clear, and occurs due to the difference in well models and well control functionality, as well as the ability in SIMED to represent complex CSG reservoir flow processes. This results in divergent well rates after gas desorption begins. The implementation of the full dual-phase functionality into MODFLOW (including specific yield) results in a water production rate (orange line) that after 6 months field production is lower than the single-phase water rate (blue line) and closer to the SIMED value. It is this lower water production rate that results in a value for cumulative water production after 20 years that more closely matches SIMED predictions. Interestingly, in the first 6 months of the production simulation, the full dual-phase MODFLOW model produces water from the drain at a higher rate than the single-phase model. After this period the water production rate drops steeply to a lower value. This initial period of sustained higher water production is due to the inclusion of the specific yield parameter, a result confirmed when comparing dual-phase simulation results where the value is set to 1.3% and 0% (Figure 6-22, orange and grey lines respectively).

The effect of specific yield on drain behaviour occurs when pressure head in model grid blocks, beginning with the grid block hosting the MODFLOW drain, is drawn down below the prescribed bubble point head, h_b. Below this value of pressure head the grid block converts to an unconfined cell, and the material balance equation is adapted to include the specific yield storage parameter alongside specific storage. The effect of its inclusion is to:

- Contribute to water flux in the grid block through contribution of water drained from the defined cleat/fracture porosity (in this case 1.3% of the grid block volume).
- Maintenance of a higher pressure head, or reduction in rate of drawdown in the grid block throughout the time that water continues to be produced from the cleat/fracture porosity.

The higher pressure head in the grid block will result in

- A higher rate of water production from any MODFLOW drain located in the grid block, as the rate of water production is proportional to the pressure head.
- Reduced propagation of drawdown in adjacent grid blocks, as the internal transmissivity is lowered by the smaller difference in adjacent pressure heads.

The reduced propagation of drawdown resulting from the inclusion of the specific yield parameter has an important effect on the accuracy of drawdown predictions in the model. Table 6-9 presents the average of magnitude of drawdown error for MODFLOW models compared to SIMED. The inclusion of dual-phase parameters in the 8-layer model results in significant reductions in error for drawdown predictions. Results also indicated that for the 8 layer model, the removal of the specific yield parameter had only a small detrimental effect on the accuracy of drawdown predictions. However, the case is not the same when dual-phase functionality and specific yield are included into an upscaled model layer.

Table 6-9 Effect of specific yield on average magnitude of drawdown prediction error.

SCENARIO	AVERAGE OF MAGNITUDE OF DRAWDOWN ERROR		
	LAYER TOTAL (m)	FIELD INTERIOR (m)	FIELD EXTERIOR (m)
8-layer model - single phase	29.8	49.1	27.1
8-layer model – dual phase	11.3	46.9	6.3
8-layer model – dual phase, no specific yield	11.9	47.9	6.9
Upscaled 6-layer model – single phase	23.5	68.2	17.3
Upscaled 6-layer model – dual phase	10.0	31.5	7.0
Upscaled 6-layer model – dual phase, no specific yield	19.5	83.5	10.6

Figure 6-23 presents the water production rate from MODFLOW drains when the dual-phase functionality has been included in an upscaled groundwater model layer. The inclusion of dual-phase and specific yield results in higher water production than the single-phase MODFLOW model. This is because the value of specific yield is chosen to provide the most accurate representation of drawdown behaviour, in this case through the incorporation of dual-phase parameter values that describe the flow behaviour in the coal seam rather than the entire upscaled layer (see section 6.3.7). The result for water production contains a large contribution due to specific yield. Because the value is assigned to an upscaled grid block and thus accounts for a larger volume of water than would be drained from a thinner coal seam layer, the contribution to overall water production is both larger, and occurs over a more prolonged period.

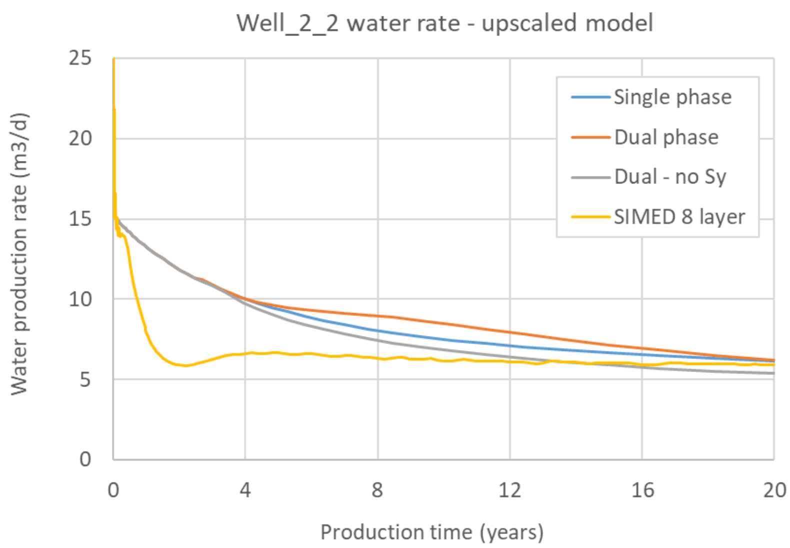

Figure 6-23 Water production rate from a single well in the upscaled 6-layer Namoi models.

This result may suggest that when implementing dual-phase functionality in upscaled layers, the specific yield should be significantly reduced or ignored, in order to maintain lower water production rates that more closely match SIMED predictions. When considering the GAB flux regional model this is not the case however, as the intent and design of the regional model is specifically to predict drawdown impacts from CSG development, and thus the improved accuracy provided by inclusion of dual-phase functionality and the specific yield parameter offers significant advantage. The effect on drawdown predictions in upscaled layers of not including the specific yield value can be seen in Table 6-9, where its removal increases average error in field interior predictions of drawdown by over 150% and in exterior predictions by over 50%.

6.3.9 Implementation of the dual-porosity functionality in an upscaled MODFLOW model.

To address the issue of accurately representing the presence of numerous discontinuous coal seams present in a thick interburden sequence, the OGIA model of the Surat Basin chose to implement MODFLOW dual-porosity functionality, through which the coal seams are represented by a mobile domain, and the interburden by an immobile domain. These two domains remain separate in function but occupy the same model space.

When applying this approach, desaturation and water flow is limited to occur in the mobile domain only, with the flow rate governed by assigned hydraulic conductivity, Brooks and Corey relative permeability parameters, and the van Genuchten saturation versus pressure relationship. Storage parameters, including specific storage and specific yield may also be assigned to the mobile domain. The immobile domain represents the interburden material, and as such is not permitted to desaturate. In order to achieve this, any parameters in the immobile domain governing desaturation are assigned values that will prevent the occurrence of dual-phase fluid behaviour. Lateral water flow is also not permitted to occur in the immobile domain, instead water is transferred into the mobile domain at rate governed by the dual-domain flow transfer rate (DDFTR) parameter, which is calculated from the interburden vertical permeability and average spacing between coal seams using the equation:

$$DDFTR = \frac{4p_c^2}{L_c^2 \sum \frac{p_i}{k_{vi}}}$$

Where p_c is the proportion of coal in a stacked sequence of coals and interburden, L_c is the mean thickness of the coal seams, p_i is the proportion of each non-coal lithology encountered and k_{vi} is the vertical permeability of each non-coal lithology.

The dual-porosity functionality is implemented via the dual-porosity flow (DPF) package in MODFLOW-USG. The other additional parameter assigned to the mobile domain is 'PHIF', the fraction of coal (by thickness) in the upscaled layer. The immobile domain may also be supplied with storage parameters S_s and S_y.

The dual-porosity functionality was applied to the entire producing layer of the 6-layer MODFLOW model to assess for any improved agreement in drawdown and water production predictions compared to the fully parameterised dual-phase SIMED CSG reservoir model. The DDFTR was calculated based on the Bohena Seam target and the adjacent interburden layers, and applied to the equivalent upscaled MODFLOW layer. The vertical permeability used to obtain DDFTR was calculated using upscaled vertical permeability of the associated interburden layers. The storage parameters for the immobile domain were calculated based on thickness-weighted averages of the adjacent interburden storage parameters, and the proportion of coal was calculated from model layer thicknesses. The values assigned to mobile domain parameters (hydraulic conductivity, S_s, S_y, van Genuchten model, Brooks and Corey model) were identical to the values used in Scenario 13 (see Table 6-6) of the upscaled MODFLOW model investigation. Drain head and drain conductance employed in the dual-porosity scenario were identical to the values used in Scenarios 3 to 5 of the single-porosity MODFLOW model.

Simulations conducted using the dual-porosity MODFLOW model resulted in total water production of 424.5 ML, a value approximately 5.6% lower than production from the Namoi CSG model. This value is a closer prediction than achieved using the upscaled single-porosity MODFLOW models that incorporate the desaturation behaviour of the Maules Creek target seam, however it represents a non-conservative estimate of water production behaviour, which may be of significance if the dual-porosity methodology is employed in the GAB regional flux model. Table 6-10 presents the average magnitude of error in drawdown prediction for the dual-porosity MODFLOW model compared to the Namoi CSG model. Implementing the dual-porosity capability in the upscaled MODFLOW layer results in only a small improvement in drawdown prediction accuracy within the CSG field boundary compared to a single-phase MODFLOW model. The average magnitude of error in the predicted drawdown beyond the field boundary is 5.8 m, which is the most accurate prediction compared to the Namoi CSG model of all scenarios investigated.

Table 6-10 Average magnitude of drawdown error when implementing dual porosity MODFLOW functionality.

SCENARIO NO.	AVERAGE OF MAGNITUDE OF DRAWDOWN ERROR		
	LAYER TOTAL (m)	FIELD INTERIOR (m)	FIELD EXTERIOR (m)
Dual porosity	12.5	60.2	5.8

The heat map presented in Figure 6-24 indicated that implementing the dual-porosity functionality using the aforementioned parameters results in an over-prediction of pressure drawdown both within the boundaries of and adjacent to the CSG field when compared to the fully parameterised Namoi CSG model. This over-prediction then transitions to an under-prediction of drawdown moving further away from the field boundary which then gradually decreases with increasing distance. This behaviour is similar to the single-porosity two-phase upscaled MODFLOW models, as well as to the single-phase upscaled MODFLOW model.

These results indicate that when utilising the upscaled MODFLOW model, implementation of desaturation or dual-porosity functionality can result in reduction of drawdown prediction error, but will not result in a uniform over-prediction or under-prediction across the model domain. The potential for areas of possible under-prediction in drawdown (a non-conservative prediction) must be considered when implementing either the desaturation or dual-porosity functionality into the GAB flux model. The dual-porosity functionality as utilised in the above scenario does not provide significant improvements to drawdown predictions beyond the CSG field boundary, whilst at the same time increasing error in predictions with the CSG field boundary. Although the functionality may provide benefits under specific circumstances, the mixed results alongside added complexity suggest it will be a less suitable candidate for implementation into the GAB flux model.

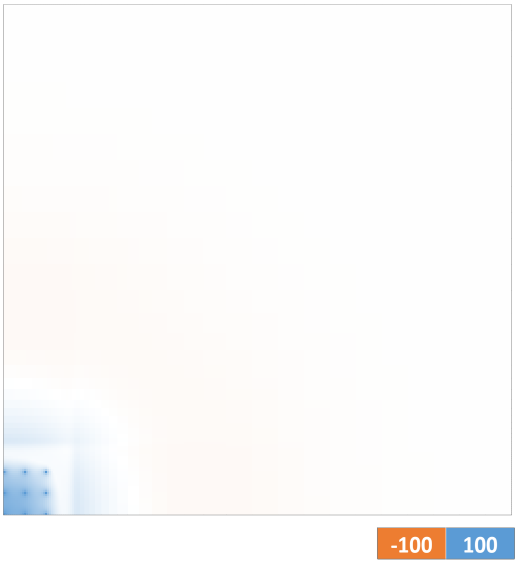

Figure 6-24 Drawdown prediction error (in m head) of layer 5 mobile domain compared to Namoi CSG model.

6.3.10 Modelling and implementation summary

The different approaches to modelling using the van Genuchten equation and deploying these relationships in the MODFLOW Namoi model had a significant effect on the pressure drawdown. The difference in predictions of water production, and of drawdown behaviour both within and adjacent to the modelled CSG producing field as result of applying these different approaches is evident.

The effects of spatial and vertical upscaling, as well as specific yield and the implementation of dual-porosity functionality have been investigated, and in particular indicate that upscaling from the Namoi CSG model grid block scale to the regional groundwater model grid block scale will affect the accuracy of water production and drawdown predictions.

Results comparing 8 layer SIMED and MODFLOW models (Table 6-3) indicated that the implementation of dual-phase behaviour into the MODFLOW Namoi model can reduce over-prediction of water production by up to 63% (Scenario 1). When using that same approach to model and deploy the van Genuchten relationship, the average drawdown error within the well field was 46.9 m compared to 49.1 m for the single-phase MODFLOW model, and averaged drawdown error outside the well field boundary was 6.3 m compared to 27.1 m for the single-phase MODFLOW model. Error in drawdown prediction at the model boundary was also reduced, and was considered negligible. Overall, this represented a significant reduction in error (77%) in predictions of drawdown in the regions adjacent to the CSG well field.

Of the different approaches to generating van Genuchten parameters that were investigated, the curve generated by averaging the S_w vs P relationships derived from a range of production times (Figure 6-6) provides the most promising result for implementation in MODFLOW. When dual-phase functionality is applied to grid cells located only within the CSG field (Scenario 2) the improvement in accuracy of groundwater production and drawdown predictions is reduced. Water drawdown and production behaviour beyond the CSG well field boundary will affect the behaviour within the CSG field. This is to be expected as the region of desaturation extends beyond the field boundary as pressure depletions leads to gas desorption, therefore it is important to include dual-phase functionality in all cells that experience desaturation (i.e. include cells adjacent to the CSG field boundary).

While it is possible to implement a single relationship across all grid blocks and achieve significant improvements in predictions of water production and drawdown (e.g. Scenario 1), the deployment of multiple S_w vs P relationships into the MODFLOW model (e.g. Scenario 4) may lead to a more a balanced reduction in error. Therefore, the approach adopted will depend on modelling priorities. Other methods for generating van Genuchten parameters, such as averaging over model spatial domain (Scenario 3), provided little improvement on single-phase predictions when implemented in MODFLOW. The absence of an obvious time-asymptotic S_w vs P relationship in the late time production data derived from the SIMED model limits the effectiveness of using this data for modelling and deployment in MODFLOW, and improvements in drawdown predictions (Scenario 5) were not observed.

Certain schemes for implementing dual-phase behaviour, whilst more accurate overall, may result in some under-prediction of drawdown in limited areas. The possibility of drawdown under-prediction and its effect on reported results must be considered when implementing dual-phase functionality into the regional model. Implementation into MODFLOW should also consider the effect of grid block scale in the reservoir model, with heavily upscaled relationships derived from SIMED (e.g. target layer average) not providing an improvement to performance of the MODFLOW model when deployed.

Implementing S_w vs P relationships derived from fine-scale CSG reservoir simulations into coarse gridded MODFLOW models can result in a reduction in the improved accuracy of the dual-phase functionality. Scenarios 6 to 8 examined the role of spatial scale and determined that as the grid-block scale of the regional groundwater model diverged from the fine-scale CSG reservoir model, the improvements in water production and drawdown predictions achieved by implementing dual-phase functionality diminished. Despite this, the results still represented an improvement on single-phase groundwater models.

Upscaling in the vertical direction will reduce the overall influence of predictive errors that manifest due to inadequate capture of complex coupled reservoir flow processes in the target layer. This is primarily due to the relatively large thickness of the adjacent formations compared to the Bohena Seam target layer. The impact of implementation of dual-phase functionality into an upscaled MODFLOW model (with layering equivalent to the GAB flux model) was assessed through comparison to upscaled results from the Namoi CSG model. Similar to results observed in the 8-layer model, the implementation of prior-upscaled S_w vs P and relative permeability relationships (Scenario 12, see Figure 6-17) produced no increase in predictive accuracy over the single-phase model.

Scenarios 13 to 15 implement the van Genuchten and relative permeability parameters derived from the fine-scale modelling of the Bohena Seam only, and result in significant improvements in the prediction of drawdown over single-phase MODFLOW models. In the vicinity of the CSG field significant drawdown occurs in the producing seam relative to the adjacent formations, and it is therefore a large contributor to vertically upscaled drawdown values. Horizontal propagation of pressure drawdown in the producing seam is governed by desaturation relationships in that seam, and thus near the CSG field the spatial propagation of pressure drawdown in upscaled layers will be predominantly governed by this behaviour. Predictions of water production are less accurate than the single-phase model, however the relatively good predictive performance of the single-phase model is likely due to the effect of upscaling rather than it being a better approximation of reservoir flow processes.

The importance of including dual-phase functionality into all cells that see desaturation (including beyond the field boundary) is highlighted when comparing Scenarios 13 to 15. The most accurate drawdown predictions are given when dual-phase functionality is extended 200 m beyond the CSG field boundary (Scenario 15). Implementing dual-phase functionality across the entire model domain (Scenario 13) still produces more accurate drawdown predictions compared to limiting to within the CSG field boundary only (Scenario 14). Specifying a distance from the field boundary within which the dual-phase functionality should be implemented will assist in generating more accurate drawdown predictions and reduce risk of possible adverse results generated through the presence of dual-phase functionality in unsuitable model domains.

Investigations demonstrate the importance of specific yield when using dual-phase functionality to derive more accurate predictions of pressure drawdown. The presence of the specific yield parameter in unconfined grid blocks affects rates of drawdown, and the propagation of drawdown into neighbouring grid blocks. Water production from the MODFLOW model is affected by the inclusion of drainage from the cleat/fracture porosity represented by the specific yield value. This may result in higher values of cumulative water production compared to single-phase and SIMED models, depending on a complex interaction of factors such as degree of upscaling, desaturation behaviour and production parameters. Despite uncertainty related to water production rates, the inclusion of specific yield, especially in upscaled layers, is demonstrated to increase the accuracy of MODFLOW drawdown predictions when implementing dual-phase functionality. For models such as the GAB flux model, which are constructed to report impacts on drawdown as opposed to water production, the inclusion of the specific yield parameter will improve accuracy.

The implementation of dual-porosity functionality has a significant effect on predictions of water production, however the predicted values were lower than those calculated by the fully parameterised CSG reservoir model. The resulting non-conservative estimate may limit the suitability of the approach for use in predictive regional groundwater models. The resulting pressure drawdown predictions outside the CSG field boundary were more accurate than other scenarios investigated, indicating the potential for this approach in specific modelling situations.

On the balance of results gained through comparison of a range of implementation approaches, the most suitable approach for incorporation into the regional groundwater model is similar to that investigated in Scenario 15. The use of desaturation parameters derived from the Bohena Seam only, deployed into grid blocks of an upscaled groundwater model layer within a fixed vicinity of the CSG field boundary, produces substantial improvements over single-phase MODFLOW models. Drawdown prediction both inside and outside the CSG field boundary is substantially improved, and a conservative estimate of water production is given that is an improvement over single-phase predictions produced in more detailed models.

While it is demonstrated that improved agreement in drawdown predictions is possible using different modelling and implementation approaches, MODFLOW predictions of production behaviour may continue to differ from SIMED predictions due to other factors, such as differences in well and permeability models. Although it may be possible to quantify the effects of these factors using SIMED, and to supply these data as inputs into the MODFLOW model in order to improve agreement, this is likely to reduce the utility of the MODFLOW model as a predictive tool.

7 Updating of Namoi MODFLOW model predictions

Previous tasks developed a region-specific approach to representation of dual-phase reservoir flow processes into a Namoi sub-region groundwater flow model that uses the MODFLOW-USG code. The approach utilised a fully parameterised Namoi CSG model constructed in SIMED to derive relationships between grid block saturation and pressure, and determined the most appropriate methodology for implementation of these relationships in MODFLOW. The implementation was shown to improve predictions of groundwater pressure drawdown provided by the MODFLOW model. The objective of Chapter 7 is to implement the previously derived approach in the regional groundwater model utilised for GISERA project W7 - Impacts of depressurisation on Great Artesian Basin (GAB) flux. The GAB flux model has been used to predict groundwater impacts in the Namoi sub-region, however there exists potential for over-prediction of drawdown in coal seams and nearby formations, due to the absence of dual-phase flow representation. This may result in overprediction of impacts across a wide range of risk receptors like farmers' bores, groundwater dependent ecosystems, springs etc. The implementation of dual-phase functionality into the regional model assists in improving the accuracy in the prediction of groundwater impacts in the Namoi region.

7.1 Distributions of van Genuchten parameters for groundwater model

The GAB flux model uses a probabilistic approach to predicting possible impacts of CSG development on groundwater production and pressure drawdown. The model undertakes Monte Carlo simulation using a population of 500 realisations of reservoir and production parameters. To successfully integrate the approach to implementing dual-phase functionality with the probabilistic methodology used by the GAB flux model, 500 realisations of appropriate desaturation parameters were required. These realisations were required to take into account any existing relationships between parameters, as well as any physical limits to parameter values imposed by actual reservoir conditions.

Of the model parameters that relate to dual-phase flow processes (i.e. van Genuchten, relative permeability) only the van Genuchten parameters were considered appropriate for furnishing a suite of realisations. Very few measurements exist of the relative permeability behaviour of coal, and often this relationship is used as a fitting variable to calibrate model drawdown and fluid production. Therefore, it is difficult to estimate the Brooks and Corey property values, let alone the statistical properties required for Monte Carlo realisations.

The van Genuchten equation consists of three variables that describe the shape of the saturation versus pressure relationship across the model grid blocks. One of these, the bubble-point head (h_b) corresponds in this context to the desorption pressure of the target coal seam, the pressure below which gas will desorb from the coal surface and migrate as a gas phase alongside water through the coal fracture system. The existence of a set of measurements of the gas content and Langmuir properties of Maules Creek Formation coals allows for the generation of coarse distributions of gas content (Figure 7-1) and Langmuir volume (Figure 7-2) and of the relationship between Langmuir volume and pressure (Figure 7-3). Random values for gas content and Langmuir volume were generated using the probability distributions and used alongside the modelled relationship between Langmuir pressure and volume to generate a distribution of desorption pressure values. This was then converted to a distribution of bubble-point head values that could be utilised for the Monte Carlo simulation.

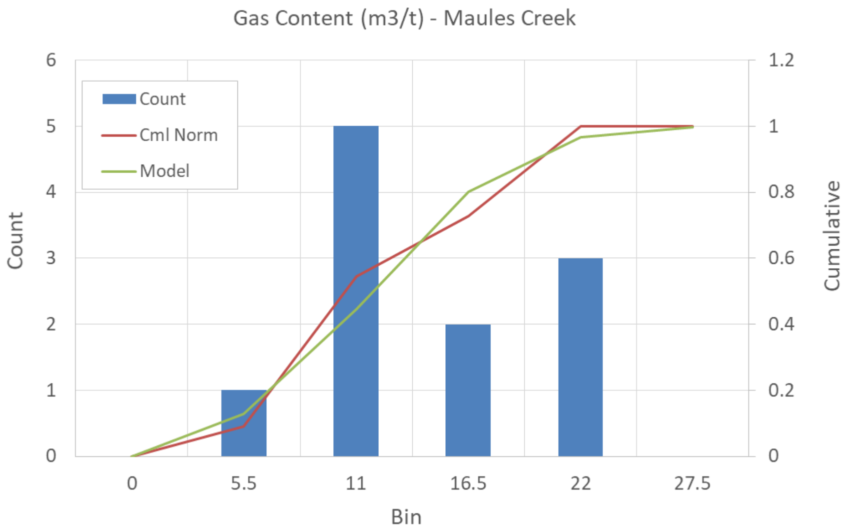

Figure 7-1 Distribution of gas content of Maules Creek coal. Based on measurements reported by Gurba et al. (2009).

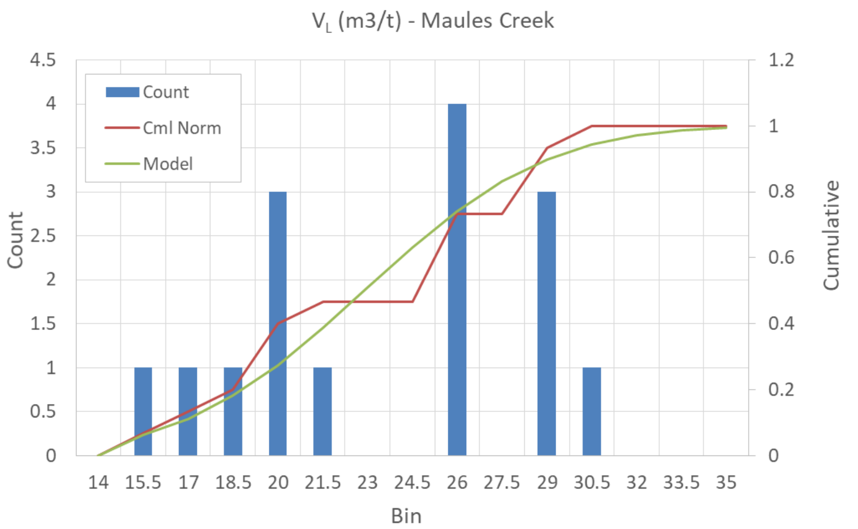

Figure 7-2 Distribution of Langmuir volumes for Maules Creek coal based on measurements reported by Gurba et al. (2009).

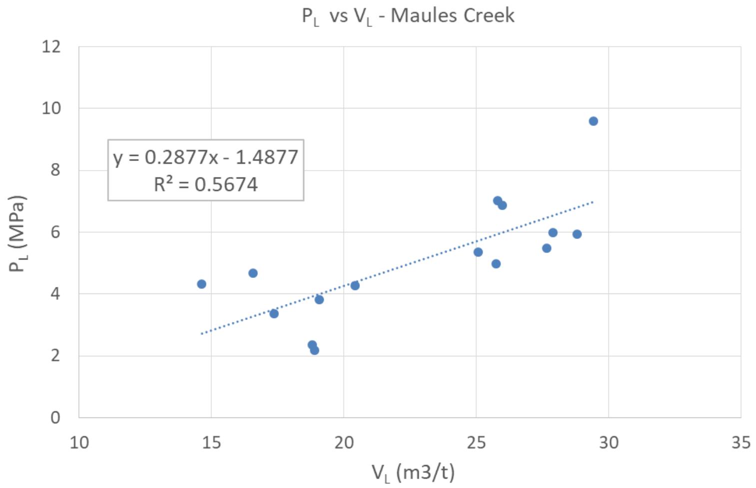

Figure 7-3 Relationship between measured Langmuir volume and pressure for Maules Creek coals. Based on data reported by Gurba et al. (2009).

The values for the other two van Genuchten equation parameters (alpha and beta) are calculated using a least-squares fit of the van Genuchten equation to averaged saturation and pressure data generated by SIMED reservoir simulations using the Namoi CSG model. In order to generate a distribution for these values, a number of reservoir simulations need to be undertaken using the Namoi CSG model, and the van Genuchten equation fitted to the S_w vs P data generated by each of these simulations. Each simulation run on the Namoi CSG model varied the values of parameters related to desaturation. In this case the values of gas content, and the Langmuir properties were varied based on the distributions and relationships outlined in Figure 7-1 to Figure 7-3. The S_w vs P output of the SIMED simulation was then modelled using a least-squares fit of the van Genuchten equation, and the alpha and beta fitting parameters used to generate the probability distribution in Figure 7-4 and the relationship between alpha and beta plotted in Figure 7-5.

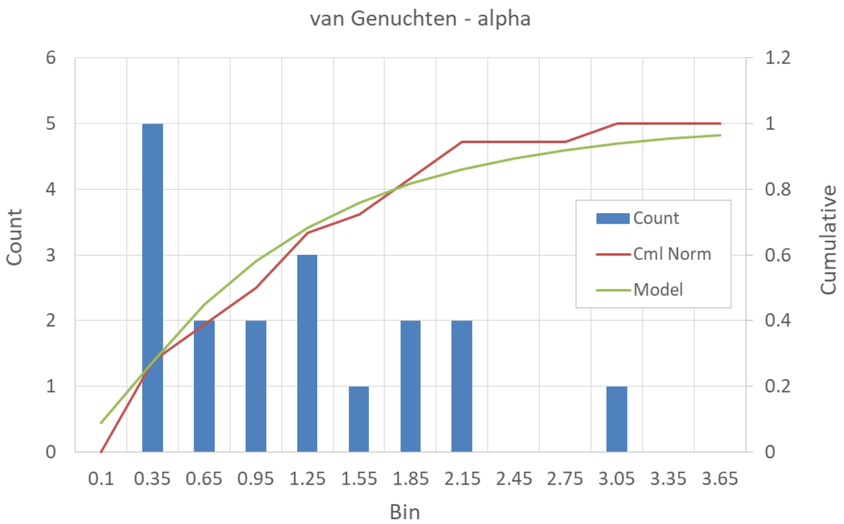

Figure 7-4 Distribution of values of the alpha parameter for the van Genuchten desaturation equation.

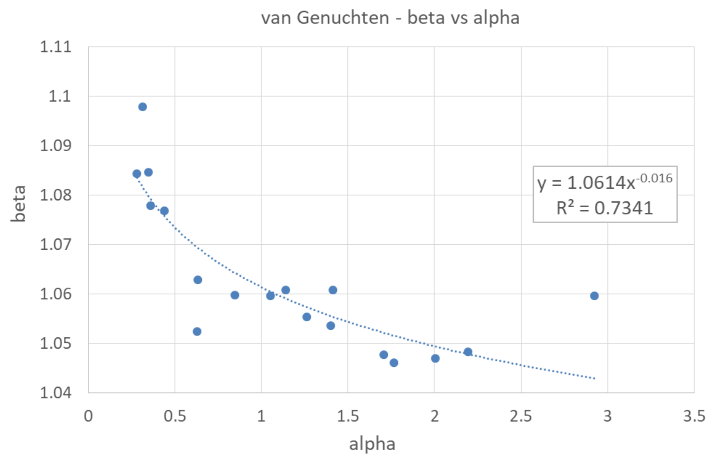

Figure 7-5 Relationship between van Genuchten parameters alpha and beta.

Prior to generating the 500 realisations from the derived probability distributions, the random values generated for bubble-point head were screened to ensure values were not greater than the initial pressure head encountered in grid blocks in the vicinity of the CSG field. This requirement ensured that the grid blocks of the target formation would remain water saturated prior to CSG production, mirroring the condition encountered in the field. Figure 7-6 presents the distributions of the h_b, alpha, and beta values generated in the 500 realisations provided for Monte Carlo simulation.

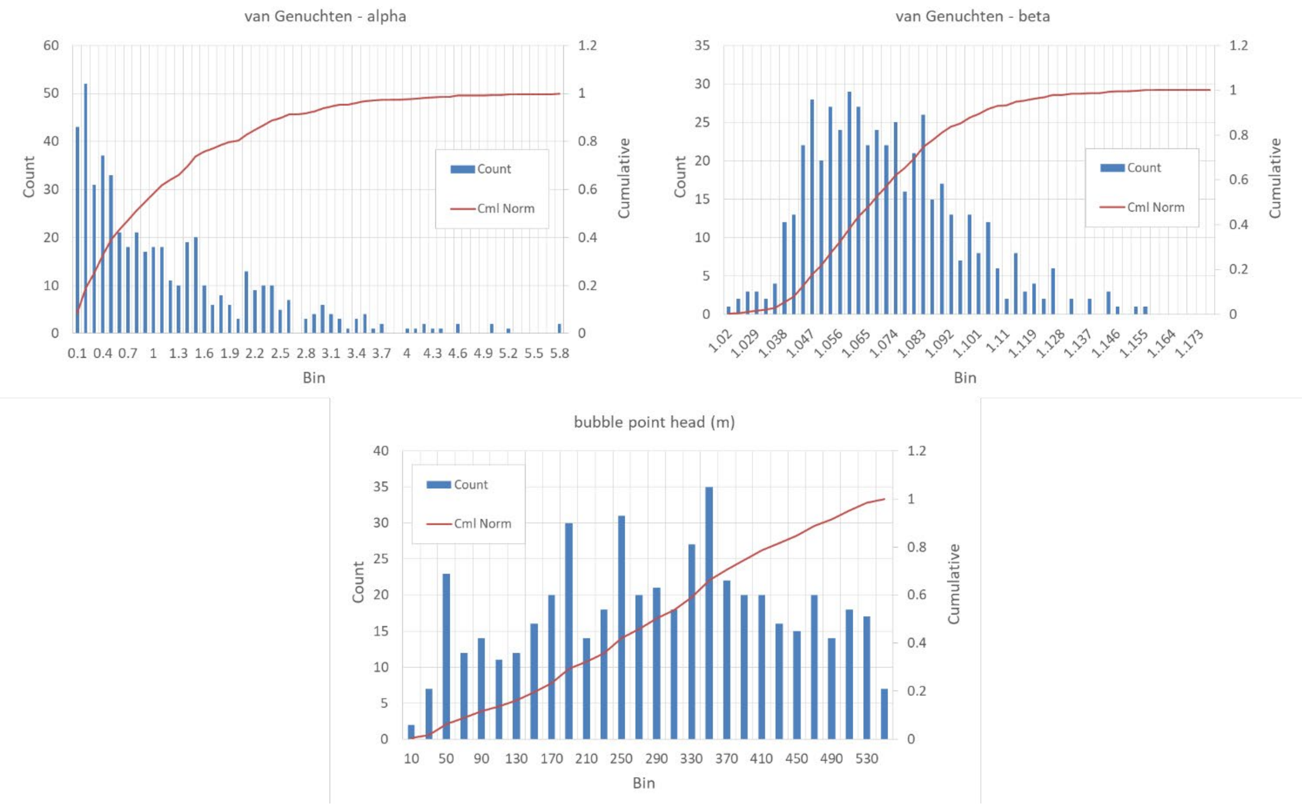

Figure 7-6 Distribution of parameters provided for Monte Carlo simulation.

7.2 The regional groundwater model

The regional groundwater model used in this study for incorporating the dual-phase effects was originally developed as a single-phase MODFLOW model as part of the Bioregional Assessments groundwater modelling study for the Namoi region (Sreekanth et al, 2018). The model was further used in the single-phase mode in the companion GISERA projects to assess groundwater head drawdown and flux changes induced by coal seam gas development from the Gunnedah Basin by the proposed Narrabri Gas Project and to devise monitoring strategies. In the present study we updated the model to account for the dual-phase flow of gas and water in the vicinity of CSG wells and incorporate its effects on the drawdown and flux changes in the GAB aquifer, the Pilliga Sandstone.

The model domain was chosen to include the coal seam gas project area, coal mines in the Gunnedah Basin, parts of the Great Artesian Basin and the Namoi catchment. The model domain was discretised into an unstructured Voronoi mesh with varying cell sizes. A finer resolution of 300 m was used near the CSG wells and farther from the CSG development area cells of 3000 m size were used. The model domain comprising the Gunnedah and Surat Basin formations was discretised into 9 hydrostratigraphic layers as shown in Table 7-1

A no-flow boundary was defined along the northern boundary and eastern boundary of the model that represents the Hunter-Mooki fault. General head boundary conditions were used along all other boundaries of the model. Recharge into the model domain comprises three components – recharge from rainfall, overbank flooding and irrigation. Surface water-groundwater interactions are represented in the model by defining the river reaches within the model domain using the MODFLOW river package. Groundwater extraction from 11,785 bores is also represented using the well package in the model. Coal seam gas water extraction was represented in this model using the MODFLOW drain package. The drain boundary condition is applied to 425 model cells corresponding to the locations of proposed CSG wells.

The model was run using the MODFLOW-USG code. As described in earlier sections and in the companion report (Sreekanth et al., 2018) MODFLOW-USG has several advantages that make it most suitable for this study. As discussed earlier in this report, MODFLOW-USG allowed the updated model to simulate the effects of desaturation, which were traditionally neglected in groundwater flow models. The ability to use unstructured grids also allowed for numerical modelling of pinching out formations.

7.3 Predictive analysis

Thirty seven parameters were considered in the model sensitivity analysis to investigate the effect of recharge, SW-GW interactions, mine and CSG water production, and hydraulic properties on the prediction of head and flux impacts. A detailed description of these parameters is provided in the report from the companion GISERA projects (Sreekanth et al, 2018). In addition to these 37 parameters, 3 additional parameters that influence dual-phase flow characteristics were considered in this work. These correspond to the van Genuchten alpha, van Genuchten beta and bubble-point head of the van Genuchten equation described in Section 2.2. These parameters were sampled from the corresponding distributions shown in Section 7.1 to do a Monte Carlo simulation of head and flux impacts. A total of 500 parameter combinations were sampled from their distributions. Forward model runs were undertaken to generate the predictive distribution of CSG-induced drawdown and flux changes accounting for the dual-phase flow effects. Out of the 500 parameter combinations sampled, 391 resulted in successful completion of the MODFLOW-USG model runs.

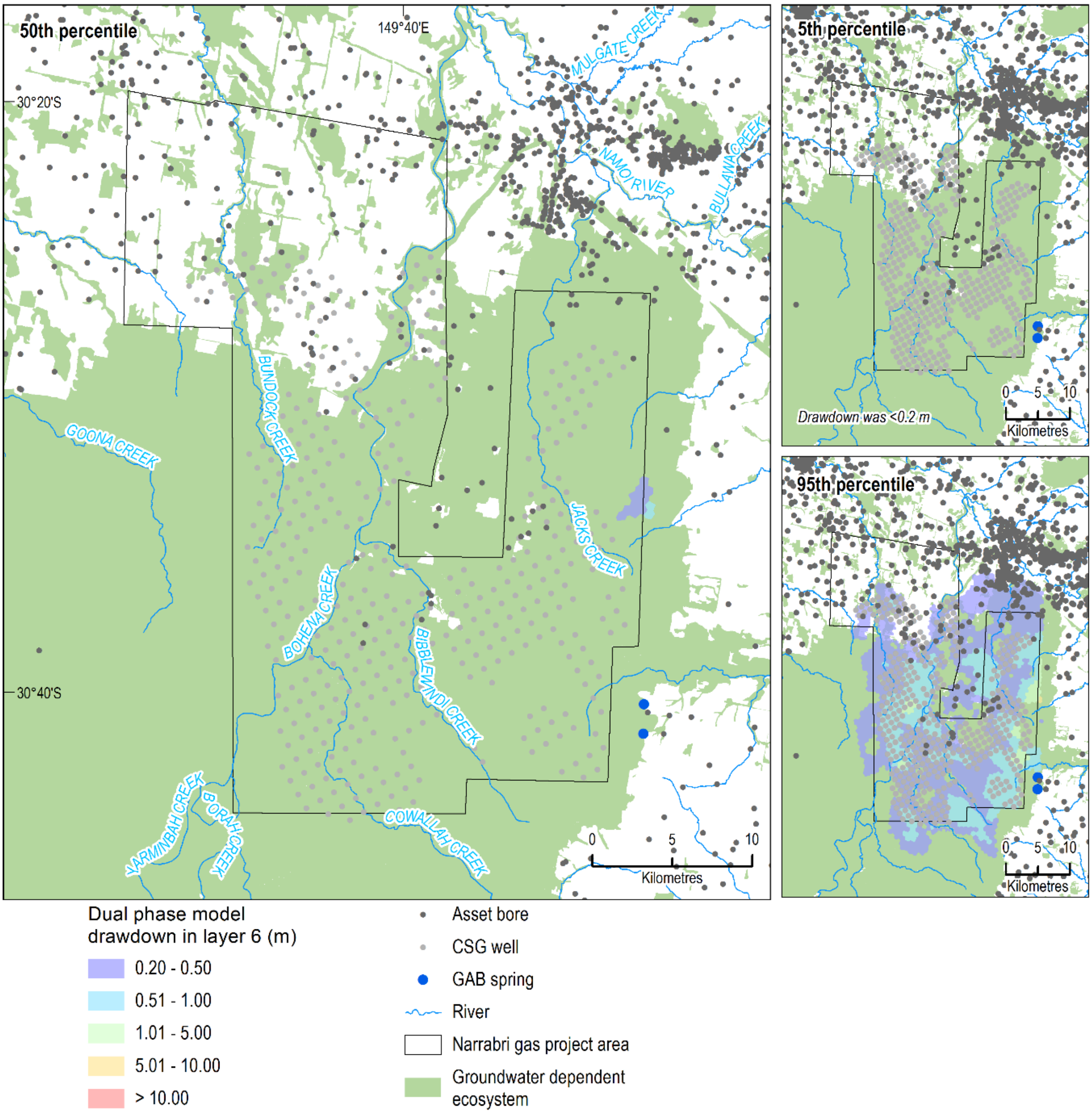

Figure 7-8 5th, 50th and 95th percentile groundwater head drawdown contours for model layer 6 corresponding to the Pilliga Sandstone aquifer.

7.3.1 Pilliga Sandstone

The 5th, 50th and 95th percentile of predicted drawdown in model layer 6 corresponding to the Pilliga Sandstone is shown in Figure 7-8. This figure indicates that in the median case produced in the Monte Carlo simulation the Pilliga Sandstone aquifer sees approximately 0.2 to 1 m drawdown in a small area at the eastern boundary of the CSG development. The 5th percentile case shows no drawdown above 0.2 m in the Pilliga Sandstone aquifer in the vicinity of the Narrabri CSG project extent, while the 95th percentile sees drawdowns of at least 0.2 m across the majority of CSG project area.

Comparison of these drawdown percentiles with the single-phase model outputs (Sreekanth et al, 2018) indicates that prediction of drawdown in the aquifer formation is not significantly affected by the dual-phase flow effect. As evident from the scenario analysis reported in section 5, the effect of dual-phase flow on drawdown is prominent close to the CSG wells and decreases at distances farther from the wells in the horizontal direction. Meanwhile in the vertical direction, the propagation of drawdown and dual-phase flow effects is less evident. This is potentially due to the fact that the aquifer of interest, the Pilliga Sandstone, is situated well above the coal seams and separated by multiple layers of aquitard formations. Any altered drawdown characteristics due to implementation of dual-phase functionality in the Maules Creek layer will not propagate through to the shallower aquifer layers. Reduced propagation of drawdown in the vertical direction was also observed in the SIMED model of the Namoi sub-region stratigraphy (see Section 6.3) due to low permeability layers acting as aquitards between the deeper CSG target layer and the Pilliga Sandstone.

To further confirm that the representation of dual-phase flow in the coal-bearing layers of the GAB flux model would not produce effects that were observable in the shallower aquifers of interest, dual-phase functionality was included in the Hoskissons Coal Member as well as the primary Maules Creek target. Although the Hoskissons seam is only a secondary CSG target, expected to be responsible for approximately 6% of the total water production from the CSG development (CDM Smith, 2014), its shallower location closer to the overlying aquifers means that any altered drawdown in the layer could have a greater influence on Pilliga Sandstone drawdown predictions. It is important to note that the values for dual-phase parameters derived in earlier chapters relate specifically to reservoir flow behaviour in the Bohena Seam primary CSG target. As such, their implementation in the Hoskissons coal layer is likely to not provide the optimum representation of reservoir dual-phase reservoir flow processes occurring during production from that target seam. However, for the purposes of investigating any impact of dual-phase implementation on shallower layers it provides a valuable indication; and it has been observed in the literature that dual-phase modifications to drawdown behaviour are relatively insensitive to the van Genuchten parameters chosen (Herckenrath et al., 2015). Even with the implementation of dual-phase functionality in the Hoskissons seam the drawdown percentiles from the Pilliga Sandstone aquifer do not differ significantly from the single-phase model outputs, indicating limited effect on the aquifer of interest from their inclusion.

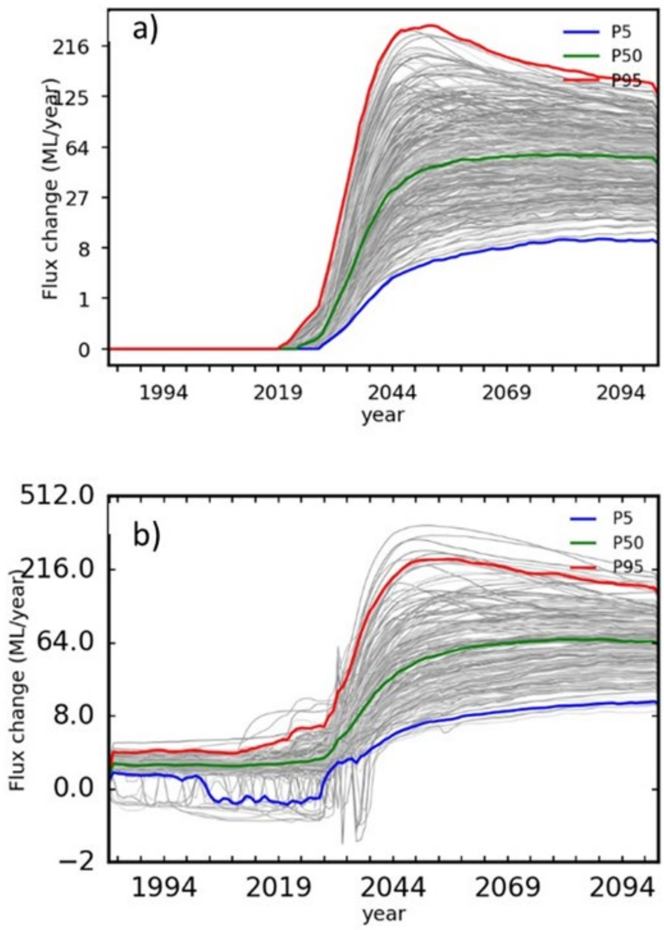

Figure 7-9 CSG-induced additional flux losses from the Pilliga Sandstone aquifer to the Gunnedah Basin Formations corresponding to a) single-phase MODFLOW-USG runs and b) dual-phase MODFLOW-USG runs.

The comparison between the flux changes induced by coal seam gas development predicted using single-phase MODFLOW-USG and dual-phase MODFLOW-USG models is shown in Figure 7-9. In addition, the values for the 5th, 50th and 95th percentiles of maximum flux change induced by CSG development simulated by the single-phase and dual-phase models are compared in Table 7-2. These results are based on 287 model runs comparable between the single and dual-phase configuration of the model. In this present analysis, with the updated regional scale MODFLOW-USG model, we investigated whether the representation of dual-phase flow of gas and water around the CSG wells, which was not accounted in the previous study, has any significant effects on the prediction of flux losses.

Similar to results reported in the final report of the GISERA companion project on “Impact of CSG depressurization on the Great Artesian Basin flux” (Sreekanth et al, 2018), predicted CSG flux impacts to the Pilliga Sandstone aquifer when using the dual-phase MODFLOW-USG model are small. Figure 7-9 indicates that the implementation of dual-phase functionality also influenced the prediction of flux change prior to the commencement of CSG production in the model. It is possible this may occur as result of the large areal extent over which the dual-phase functionality was implemented, covering model areas beyond the CSG field boundary where pressure head may drop lower than the bubble point head prescribed for the Monte Carlo realisation. Areas of the GAB flux model simulate water production that occurs prior to the commencement of CSG production (e.g. mine dewatering). The area of dual-phase functionality overlaps one these abstraction zones, therefore it is possible that dual-phase flow affects modelled flux change prior to the start of CSG production. The median value for flux change prior to CSG production remains close to zero, and final flux change results suggest that the minor alteration to initial conditions had little effect on predictions that result from CSG production.

Table 7-2 Comparison of maximum CSG induced flux losses (ML/year) from Pilliga Sandstone predicted by the single and dual-phase models.

MODEL	5TH PERCENTILE (ML/YEAR)	50TH PERCENTILE (ML/YEAR)	95TH PERCENTILE (ML/YEAR)
Single phase	11	59	242
Dual phase	14	69	249

Between the single and dual-phase flow model runs, a small increase in the maximum value of flux change in the dual-phase model run is observed. The larger flux change in the dual-phase model may occur as a result of increased water production from the Maules Creek target layer, itself a result of the influence of the specific yield parameter on mass balance equations and the MODFLOW drain model. As discussed in Section 6.3.8, the inclusion of this parameter is important for enabling more accurate predictions of drawdown, particularly in upscaled layers. The effect on flux change may propagate through to shallower layers of the GAB flux model, such as the Pilliga Sandstone aquifer. It was observed that the flux loss induced by the single-phase model is slightly greater until its peak, after which the dual-phase flow model simulates slightly higher amount of flux loss (Figure 7-10).

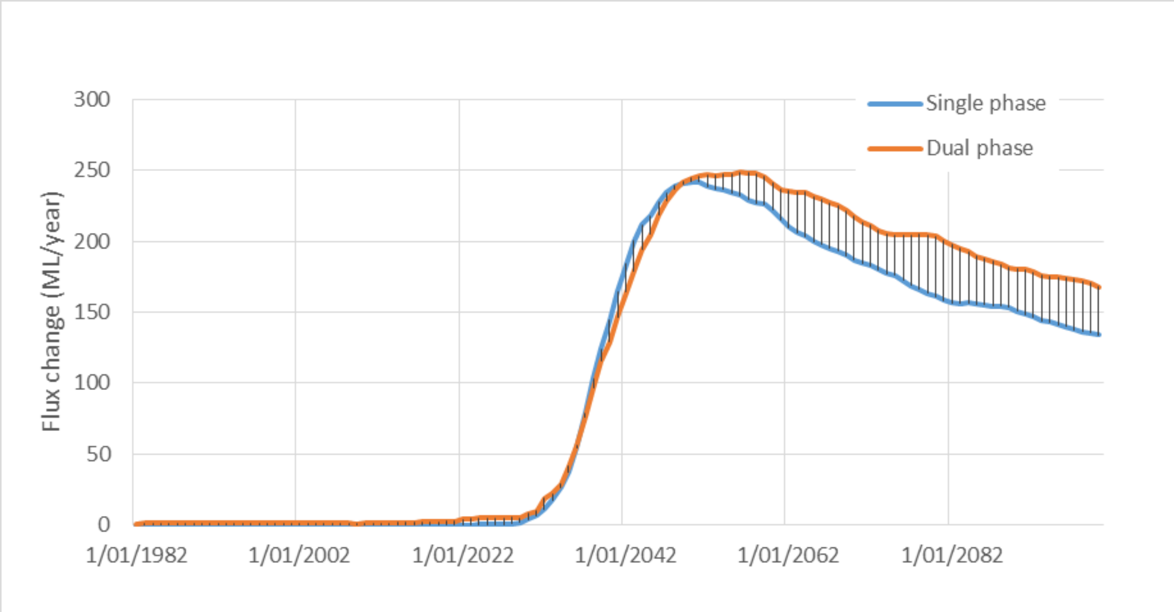

Figure 7-10 95th percentile of CSG-induced flux losses from the Pilliga Sandstone aquifer simulated by the single-phase and dual-phase models.

The small difference in the 5th, 50th and 95th percentile maximum values of flux change (Table 7-2) is insignificant in the scale of the predictive interest of the regional model. For example, the 50th percentiles of 59 and 69 ML/year by the single-phase and dual-phase models, respectively, compare to 0.19 and 0.23% of the long-term annual average extraction limit set for the GAB groundwater source in the area of the Narrabri Gas Project.

It is noteworthy that the small alterations to flux change predictions could be because of the vertical separation of the Pilliga Sandstone layer from the coal seams by several aquitard layers. This would imply that, as with predictions of drawdown, the dual-phase flow effect does not have significant effect of the prediction of flux losses from the overlying aquifers that are separated by thick layers of aquitards.

7.3.2 Maules Creek Formation

More pronounced effects of dual-phase flow are evident in the drawdown predicted for the model Layer 14, representing Maules Creek Formation in the groundwater model. The contours of CSG-induced drawdown in the Maules Creek Formation predicted by the single-phase and dual-phase MODFLOW model runs are shown in Figure 7-11. The contours correspond to the median of the maximum predicted drawdown at each point within the Narrabri Gas Project area. The contour plot indicates that there was a difference of up to 184 m in the drawdown simulated by the dual-phase and single-phase models.

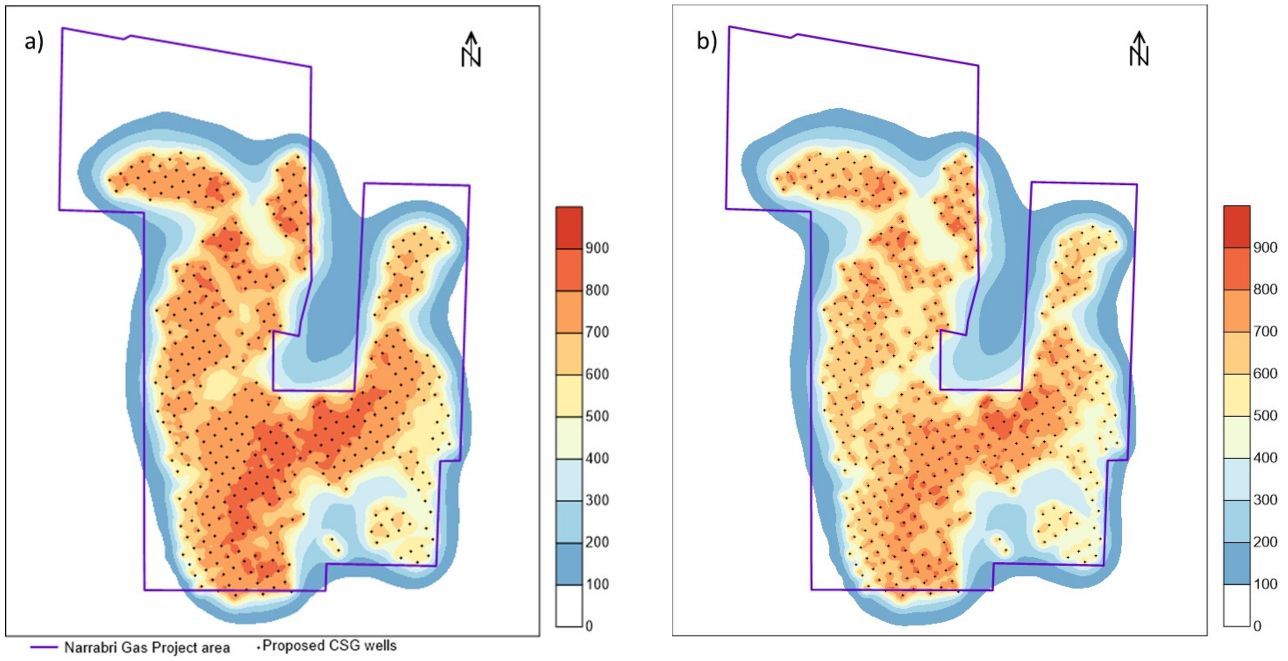

Figure 7-11 Comparison of median of head drawdown in the Maules Creek Formation between a) single-phase MODFLOW and b) dual-phase MODFLOW model runs.

The scatter plot of median drawdown predicted by single and dual-phase model runs is shown in Figure 7-12. Overall, the dual-phase model runs produce lower values of drawdown than the single-phase runs. It is noteworthy that when drawdown is higher (closer to wells) the drawdown simulated by the dual-phase model is less than the corresponding values from the single-phase model. This result agrees with comparisons between SIMED and single-phase MODFLOW simulations described in Chapter 6.

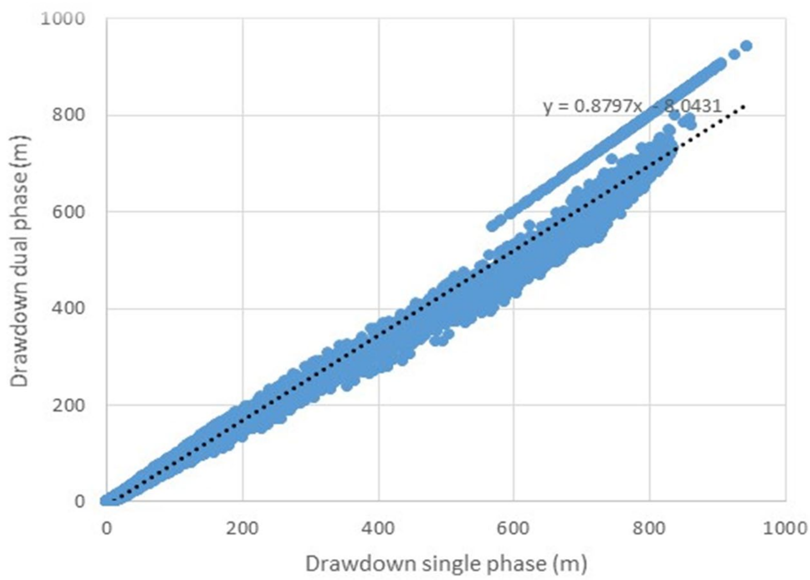

Figure 7-12 Comparison of median drawdown by single and dual-phase model runs in corresponding cells of the Maules Creek Formation.

It is observable from the two contour plots that single-phase model runs overestimate the maximum drawdown around the CSG wells. In the close vicinity of the CSG wells this over estimation is up to 184 m. Interference of drawdown from different wells is also less prominent in the case of dual-phase model runs. For example, maximum drawdown of over 700 m is confined to small areas around each well in the north and west of the well field in the case of dual-phase flow model runs, whereas it extends over considerable areas in the case of single-phase model runs. However, farther from the CSG wells there is no significant difference between the predictions of single and dual-phase model runs. The 5th and 95th percentile of predicted maximum drawdown from the Monte Carlo analysis for the single-phase and dual-phase model runs are given in Figure 7-13 and Figure 7-14. Similar to the median drawdown plots, both the 5th and the 95th percentile drawdown comparison also indicate that the single-phase model slightly overestimates the drawdown around the CSG wells. Further from the wells, there is no significant difference between the single and dual-phase model runs.

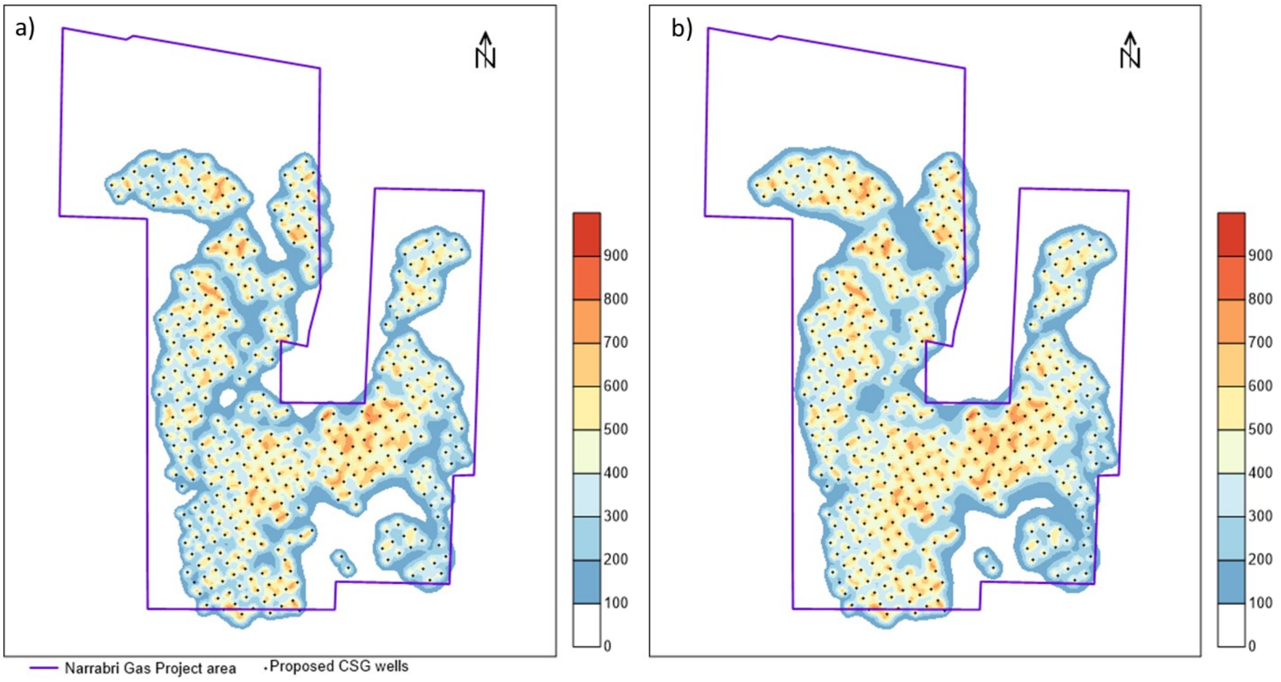

Figure 7-13 Comparison of 5th percentile maximum head drawdown in the Maules Creek Formation between a) single-phase MODFLOW and b) dual-phase MODFLOW model runs.

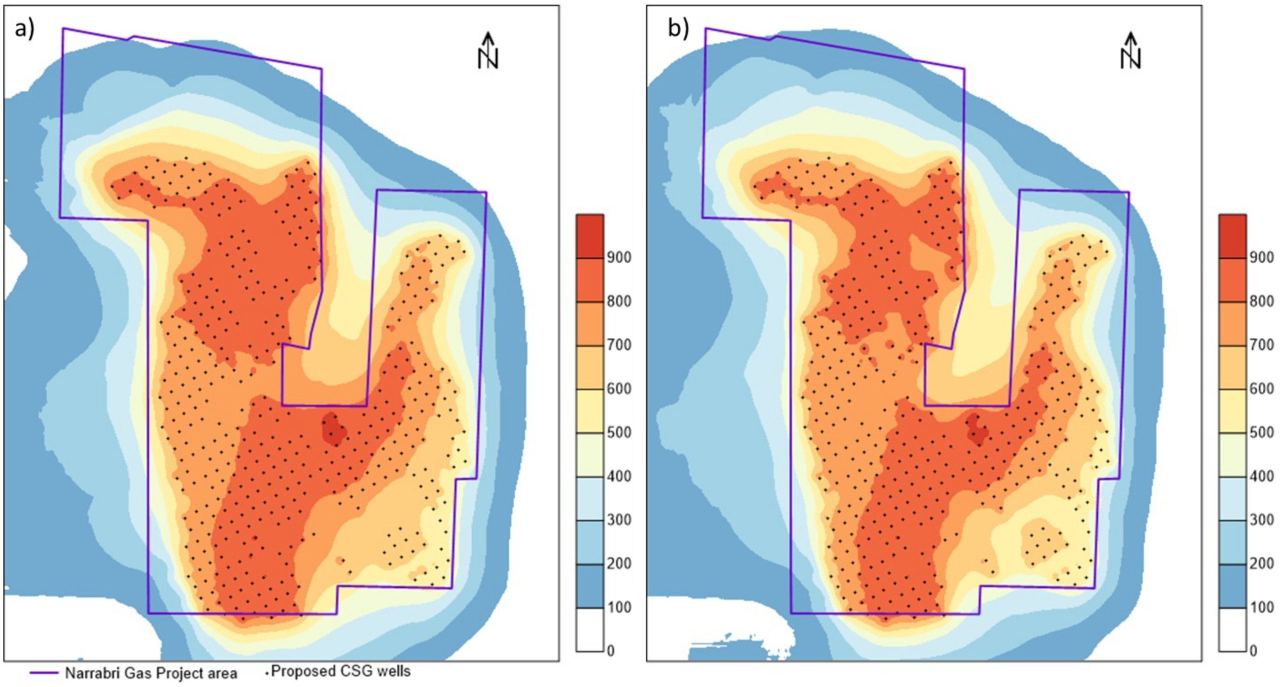

Figure 7-14 Comparison of 95th percentile maximum head drawdown in the Maules Creek Formation between a) single-phase MODFLOW and b) dual-phase MODFLOW model runs.

7.4 Summary of updated Namoi MODFLOW predictions

The methodology investigated in this report using the Richard's equation to represent dual-phase flow effects in the MODFLOW-USG model, was implemented in the regional scale groundwater flow model developed and used in the companion GISERA project (Sreekanth et al., 2018). The effects of dual-phase flow on CSG-induced flux and drawdown impacts on the Pilliga Sandstone aquifer and drawdown effects in the CSG target, the Maules Creek Formation, were compared. The comparison demonstrated that there is no significant effect of dual-phase flow on the flux and drawdown changes in the Pilliga Sandstone formation, which is separated from the CSG target by means of thick aquitard formations. For the regional scale groundwater flow model developed for the Namoi region, the prediction of CSG impacts on the GAB aquifers using a single-phase MODFLOW-USG model is justified. However, the comparisons indicated that drawdown and flux changes in the close vicinity of the CSG wells would require accounting of the dual-phase flow effects. This is important for studying the CSG water production and pressure differences. The regional scale MODFLOW-USG model applied in this study is not intended, nor used for making these predictions.

Table 7-1 Hydrostratigraphic, numerical and geological layers of the regional groundwater flow model.

Layer name	Hydrostratigraphic layer	Numerical model layers	Geological units
Alluvium 1	1	1	Narrabri Formation
Alluvium 2	2	2	Gunnedah Formation Cubbaroo Formation
Interburden 1	3	3,4,5	Warrumbungle Volcanics Liverpool Range Volcanics Rolling Downs Group
Pilliga Sandstone	4	6	Pilliga Sandstone
Interburden 2	5	7,8,9	Purlawaugh Formation Garrawilla Volcanics Napperby and Deriah Formations Black Jack Group – Coogal and Nea subgroups
Hoskissons Coal	6	10	Hoskissons Coal
Interburden 3	7	11,12,13	Black Jack Group – Brothers subgroup Watermark Formation Porcupine Formation
Maules Creek Formation	8	14	Maules Creek Formation
Basement	9	15	Boggabri Volcanics

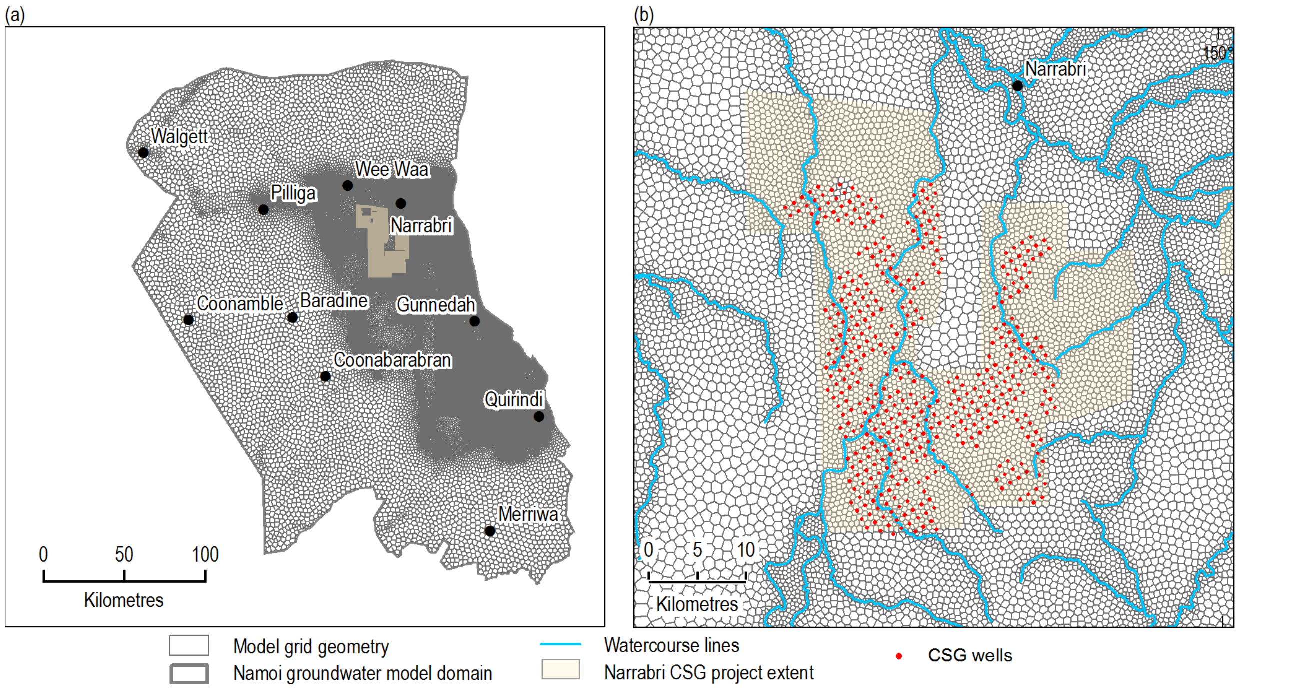

Figure 7-7 Plan view of the model grid and refinement of the grid within the Narrabri Gas Project area (Sreekanth et al, 2018).

A no-flow boundary was defined along the northern boundary and eastern boundary of the model that represents the Hunter-Mooki fault. General head boundary conditions were used along all other boundaries of the model. Recharge into the model domain comprises three components – recharge from rainfall, overbank flooding and irrigation. Surface water-groundwater interactions are represented in the model by defining the river reaches within the model domain using the MODFLOW river package. Groundwater extraction from 11,785 bores is also represented using the well package in the model. Coal seam gas water extraction was represented in this model using the MODFLOW drain package. The drain boundary condition is applied to 425 model cells corresponding to the locations of proposed CSG wells.

The model was run using the MODFLOW-USG code. As described in earlier sections and in the companion report (Sreekanth et al., 2018) MODFLOW-USG has several advantages that make it most suitable for this study. As discussed earlier in this report, MODFLOW-USG allowed the updated model to simulate the effects of desaturation, which were traditionally neglected in groundwater flow models. The ability to use unstructured grids also allowed for numerical modelling of pinching out formations.

7.5 Predictive analysis

Thirty seven parameters were considered in the model sensitivity analysis to investigate the effect of recharge, SW-GW interactions, mine and CSG water production, and hydraulic properties on the prediction of head and flux impacts. A detailed description of these parameters is provided in the report from the companion GISERA projects (Sreekanth et al, 2018). In addition to these 37 parameters, 3 additional parameters that influence dual-phase flow characteristics were considered in this work. These correspond to the van Genuchten alpha, van Genuchten beta and bubble-point head of the van Genuchten equation described in Section 2.2. These parameters were sampled from the corresponding distributions shown in Section 7.1 to do a Monte Carlo simulation of head and flux impacts. A total of 500 parameter combinations were sampled from their distributions. Forward model runs were undertaken to generate the predictive distribution of CSG-induced drawdown and flux changes accounting for the dual-phase flow effects. Out of the 500 parameter combinations sampled, 391 resulted in successful completion of the MODFLOW-USG model runs.

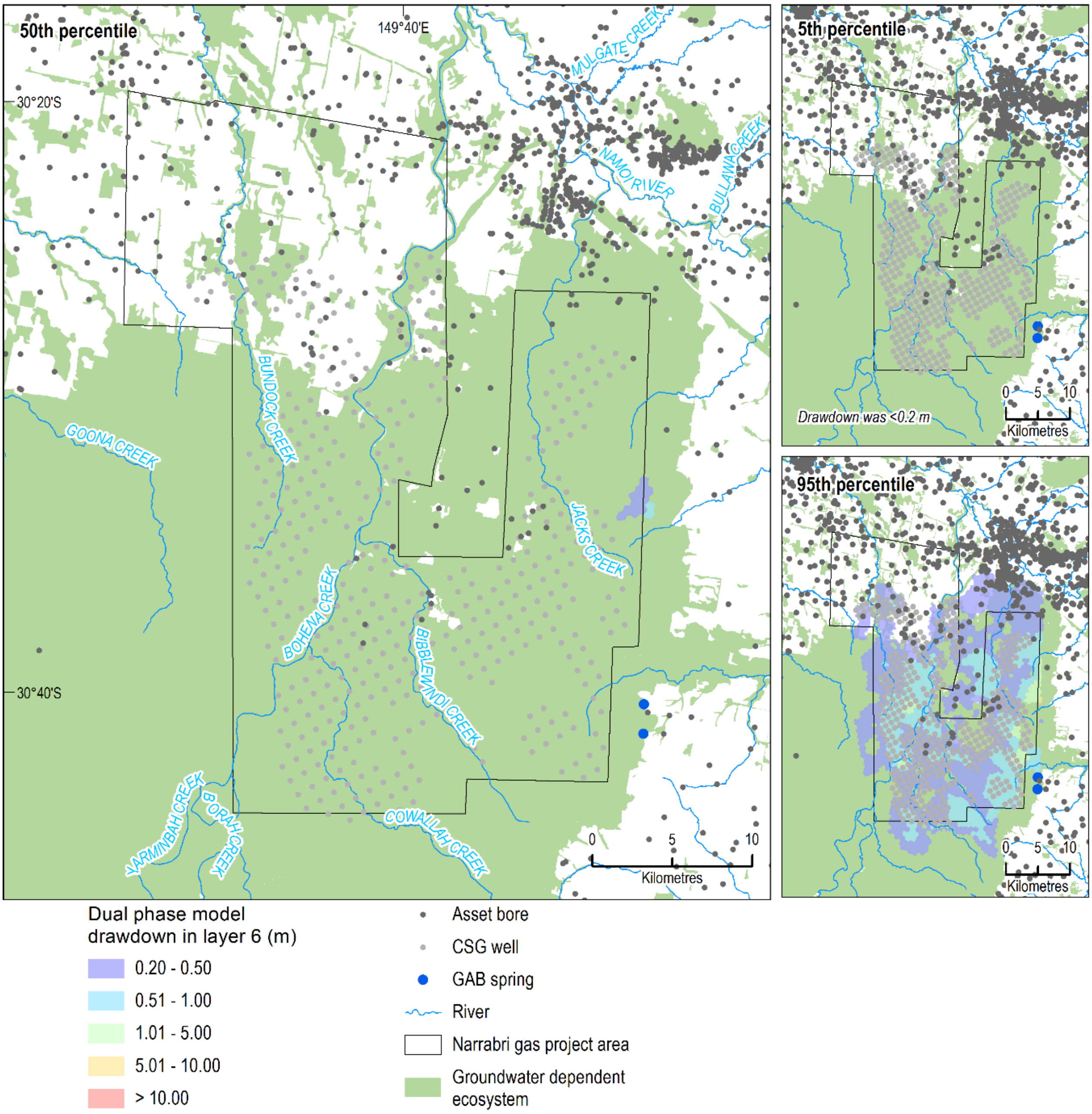

Figure 7-8 5th, 50th and 95th percentile groundwater head drawdown contours for model layer 6 corresponding to the Pilliga Sandstone aquifer.

7.5.1 Pilliga Sandstone

The 5th, 50th and 95th percentile of predicted drawdown in model layer 6 corresponding to the Pilliga Sandstone is shown in Figure 7-8. This figure indicates that in the median case produced in the Monte Carlo simulation the Pilliga Sandstone aquifer sees approximately 0.2 to 1 m drawdown in a small area at the eastern boundary of the CSG development. The 5th percentile case shows no drawdown above 0.2 m in the Pilliga Sandstone aquifer in the vicinity of the Narrabri CSG project extent, while the 95th percentile sees drawdowns of at least 0.2 m across the majority of CSG project area.

Comparison of these drawdown percentiles with the single-phase model outputs (Sreekanth et al, 2018) indicates that prediction of drawdown in the aquifer formation is not significantly affected by the dual-phase flow effect. As evident from the scenario analysis reported in section 5, the effect of dual-phase flow on drawdown is prominent close to the CSG wells and decreases at distances farther from the wells in the horizontal direction. Meanwhile in the vertical direction, the propagation of drawdown and dual-phase flow effects is less evident. This is potentially due to the fact that the aquifer of interest, the Pilliga Sandstone, is situated well above the coal seams and separated by multiple layers of aquitard formations. Any altered drawdown characteristics due to implementation of dual-phase functionality in the Maules Creek layer will not propagate through to the shallower aquifer layers. Reduced propagation of drawdown in the vertical direction was also observed in the SIMED model of the Namoi sub-region stratigraphy (see Section 6.3) due to low permeability layers acting as aquitards between the deeper CSG target layer and the Pilliga Sandstone.

To further confirm that the representation of dual-phase flow in the coal-bearing layers of the GAB flux model would not produce effects that were observable in the shallower aquifers of interest, dual-phase functionality was included in the Hoskissons Coal Member as well as the primary Maules Creek target. Although the Hoskissons seam is only a secondary CSG target, expected to be responsible for approximately 6% of the total water production from the CSG development (CDM Smith, 2014), its shallower location closer to the overlying aquifers means that any altered drawdown in the layer could have a greater influence on Pilliga Sandstone drawdown predictions. It is important to note that the values for dual-phase parameters derived in earlier chapters relate specifically to reservoir flow behaviour in the Bohena Seam primary CSG target. As such, their implementation in the Hoskissons coal layer is likely to not provide the optimum representation of reservoir dual-phase reservoir flow processes occurring during production from that target seam. However, for the purposes of investigating any impact of dual-phase implementation on shallower layers it provides a valuable indication; and it has been observed in the literature that dual-phase modifications to drawdown behaviour are relatively insensitive to the van Genuchten parameters chosen (Herckenrath et al., 2015). Even with the implementation of dual-phase functionality in the Hoskissons seam the drawdown percentiles from the Pilliga Sandstone aquifer do not differ significantly from the single-phase model outputs, indicating limited effect on the aquifer of interest from their inclusion.

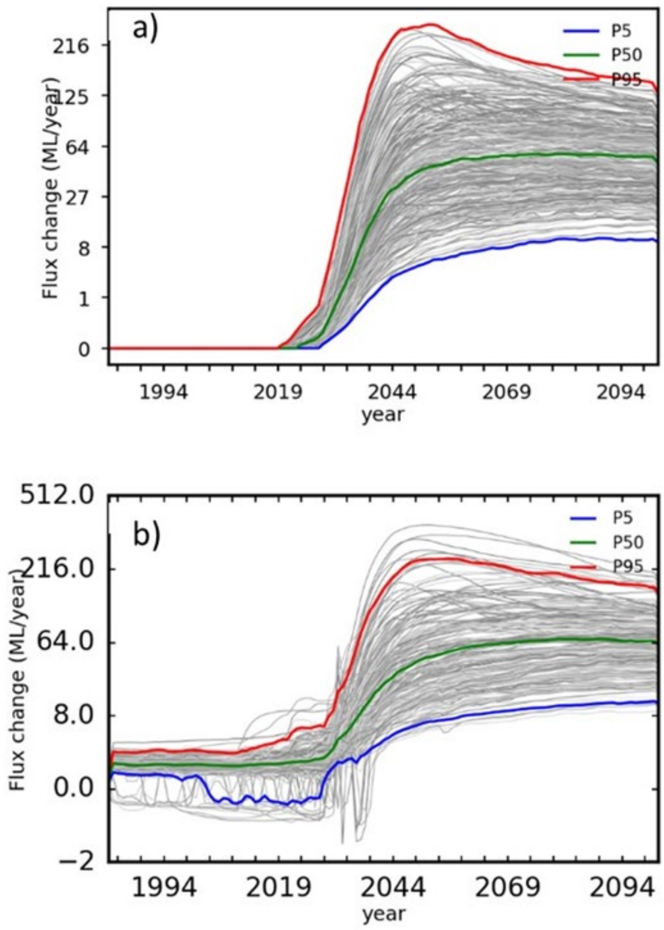

Figure 7-9 CSG-induced additional flux losses from the Pilliga Sandstone aquifer to the Gunnedah Basin Formations corresponding to a) single-phase MODFLOW-USG runs and b) dual-phase MODFLOW-USG runs.

The comparison between the flux changes induced by coal seam gas development predicted using single-phase MODFLOW-USG and dual-phase MODFLOW-USG models is shown in Figure 7-9. In addition, the values for the 5th, 50th and 95th percentiles of maximum flux change induced by CSG development simulated by the single-phase and dual-phase models are compared in Table 7-2. These results are based on 287 model runs comparable between the single and dual-phase configuration of the model. In this present analysis, with the updated regional scale MODFLOW-USG model, we investigated whether the representation of dual-phase flow of gas and water around the CSG wells, which was not accounted in the previous study, has any significant effects on the prediction of flux losses.

Similar to results reported in the final report of the GISERA companion project on “Impact of CSG depressurization on the Great Artesian Basin flux” (Sreekanth et al, 2018), predicted CSG flux impacts to the Pilliga Sandstone aquifer when using the dual-phase MODFLOW-USG model are small. Figure 7-9 indicates that the implementation of dual-phase functionality also influenced the prediction of flux change prior to the commencement of CSG production in the model. It is possible this may occur as result of the large areal extent over which the dual-phase functionality was implemented, covering model areas beyond the CSG field boundary where pressure head may drop lower than the bubble point head prescribed for the Monte Carlo realisation. Areas of the GAB flux model simulate water production that occurs prior to the commencement of CSG production (e.g. mine dewatering). The area of dual-phase functionality overlaps one these abstraction zones, therefore it is possible that dual-phase flow affects modelled flux change prior to the start of CSG production. The median value for flux change prior to CSG production remains close to zero, and final flux change results suggest that the minor alteration to initial conditions had little effect on predictions that result from CSG production.

Table 7-2 Comparison of maximum CSG induced flux losses (ML/year) from Pilliga Sandstone predicted by the single and dual-phase models.

MODEL	5TH PERCENTILE (ML/YEAR)	50TH PERCENTILE (ML/YEAR)	95TH PERCENTILE (ML/YEAR)
Single phase	11	59	242
Dual phase	14	69	249

Between the single and dual-phase flow model runs, a small increase in the maximum value of flux change in the dual-phase model run is observed. The larger flux change in the dual-phase model may occur as a result of increased water production from the Maules Creek target layer, itself a result of the influence of the specific yield parameter on mass balance equations and the MODFLOW drain model. As discussed in Section 6.3.8, the inclusion of this parameter is important for enabling more accurate predictions of drawdown, particularly in upscaled layers. The effect on flux change may propagate through to shallower layers of the GAB flux model, such as the Pilliga Sandstone aquifer. It was observed that the flux loss induced by the single-phase model is slightly greater until its peak, after which the dual-phase flow model simulates slightly higher amount of flux loss (Figure 7-10).

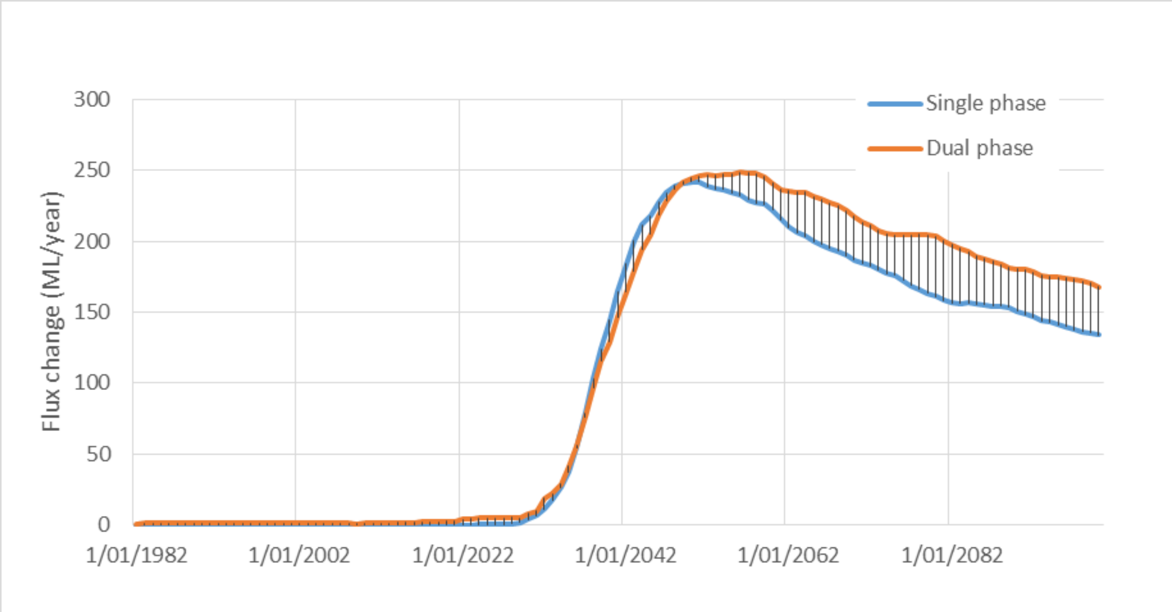

Figure 7-10 95th percentile of CSG-induced flux losses from the Pilliga Sandstone aquifer simulated by the single-phase and dual-phase models.

The small difference in the 5th, 50th and 95th percentile maximum values of flux change (Table 7-2) is insignificant in the scale of the predictive interest of the regional model. For example, the 50th percentiles of 59 and 69 ML/year by the single-phase and dual-phase models, respectively, compare to 0.19 and 0.23% of the long-term annual average extraction limit set for the GAB groundwater source in the area of the Narrabri Gas Project.

It is noteworthy that the small alterations to flux change predictions could be because of the vertical separation of the Pilliga Sandstone layer from the coal seams by several aquitard layers. This would imply that, as with predictions of drawdown, the dual-phase flow effect does not have significant effect of the prediction of flux losses from the overlying aquifers that are separated by thick layers of aquitards.

7.5.2 Maules Creek Formation

More pronounced effects of dual-phase flow are evident in the drawdown predicted for the model Layer 14, representing Maules Creek Formation in the groundwater model. The contours of CSG-induced drawdown in the Maules Creek Formation predicted by the single-phase and dual-phase MODFLOW model runs are shown in Figure 7-11. The contours correspond to the median of the maximum predicted drawdown at each point within the Narrabri Gas Project area. The contour plot indicates that there was a difference of up to 184 m in the drawdown simulated by the dual-phase and single-phase models.

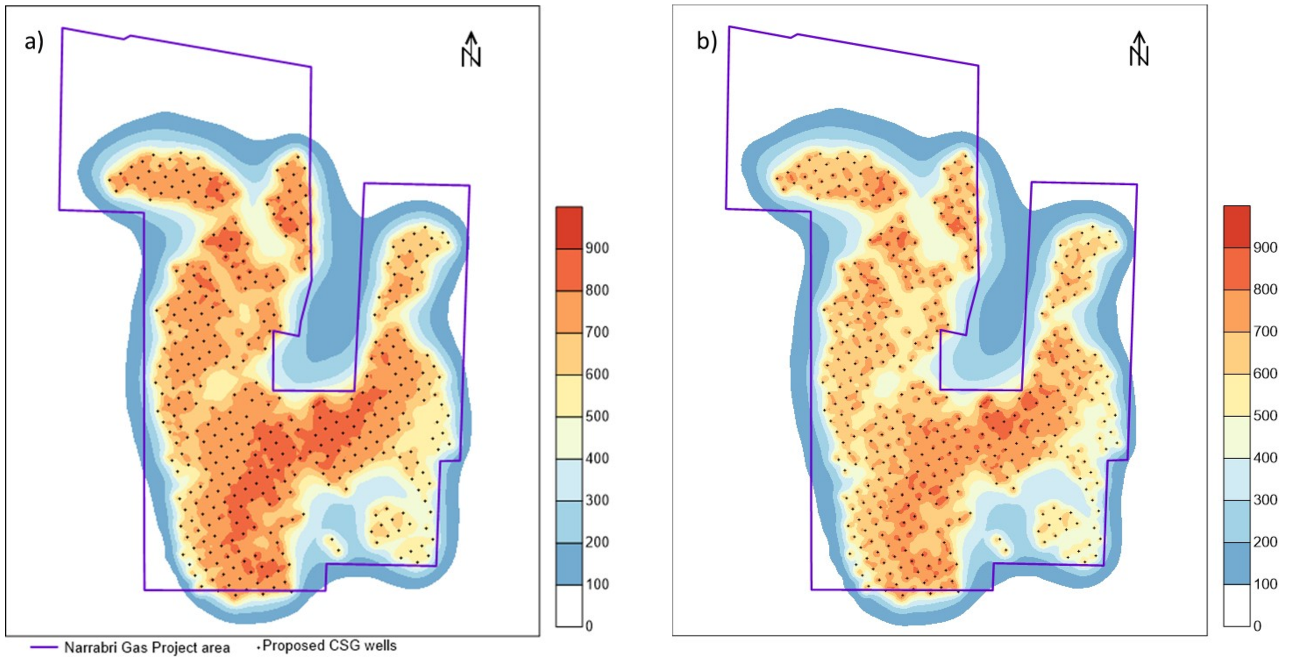

Figure 7-11 Comparison of median of head drawdown in the Maules Creek Formation between a) single-phase MODFLOW and b) dual-phase MODFLOW model runs.

The scatter plot of median drawdown predicted by single and dual-phase model runs is shown in Figure 7-12. Overall, the dual-phase model runs produce lower values of drawdown than the single-phase runs. It is noteworthy that when drawdown is higher (closer to wells) the drawdown simulated by the dual-phase model is less than the corresponding values from the single-phase model. This result agrees with comparisons between SIMED and single-phase MODFLOW simulations described in Chapter 6.

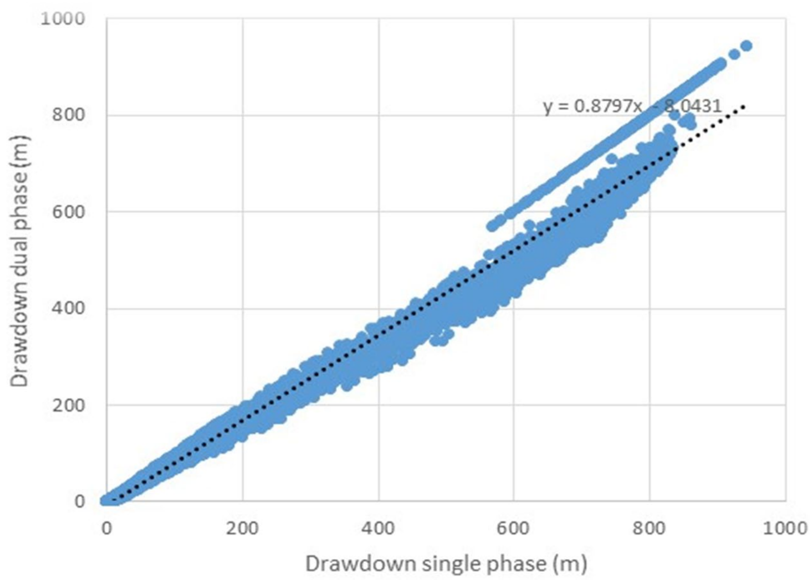

Figure 7-12 Comparison of median drawdown by single and dual-phase model runs in corresponding cells of the Maules Creek Formation.

It is observable from the two contour plots that single-phase model runs overestimate the maximum drawdown around the CSG wells. In the close vicinity of the CSG wells this over estimation is up to 184 m. Interference of drawdown from different wells is also less prominent in the case of dual-phase model runs. For example, maximum drawdown of over 700 m is confined to small areas around each well in the north and west of the well field in the case of dual-phase flow model runs, whereas it extends over considerable areas in the case of single-phase model runs. However, farther from the CSG wells there is no significant difference between the predictions of single and dual-phase model runs. The 5th and 95th percentile of predicted maximum drawdown from the Monte Carlo analysis for the single-phase and dual-phase model runs are given in Figure 7-13 and Figure 7-14. Similar to the median drawdown plots, both the 5th and the 95th percentile drawdown comparison also indicate that the single-phase model slightly overestimates the drawdown around the CSG wells. Further from the wells, there is no significant difference between the single and dual-phase model runs.

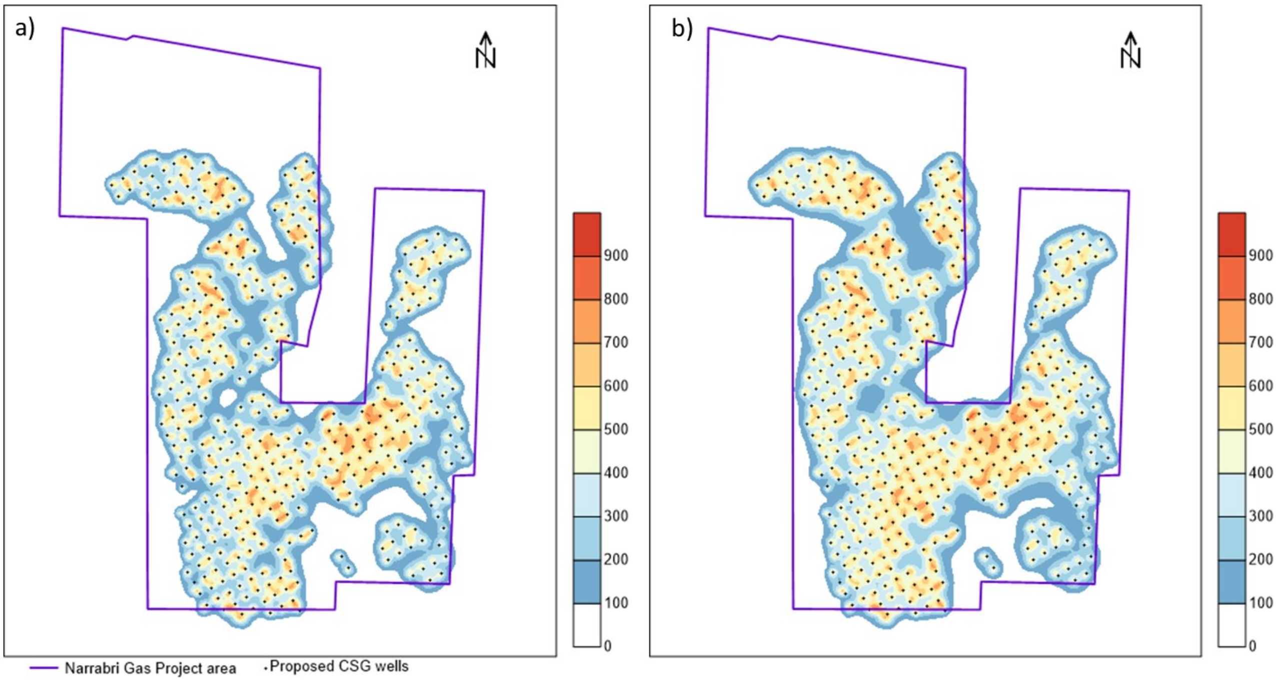

Figure 7-13 Comparison of 5th percentile maximum head drawdown in the Maules Creek Formation between a) single-phase MODFLOW and b) dual-phase MODFLOW model runs.

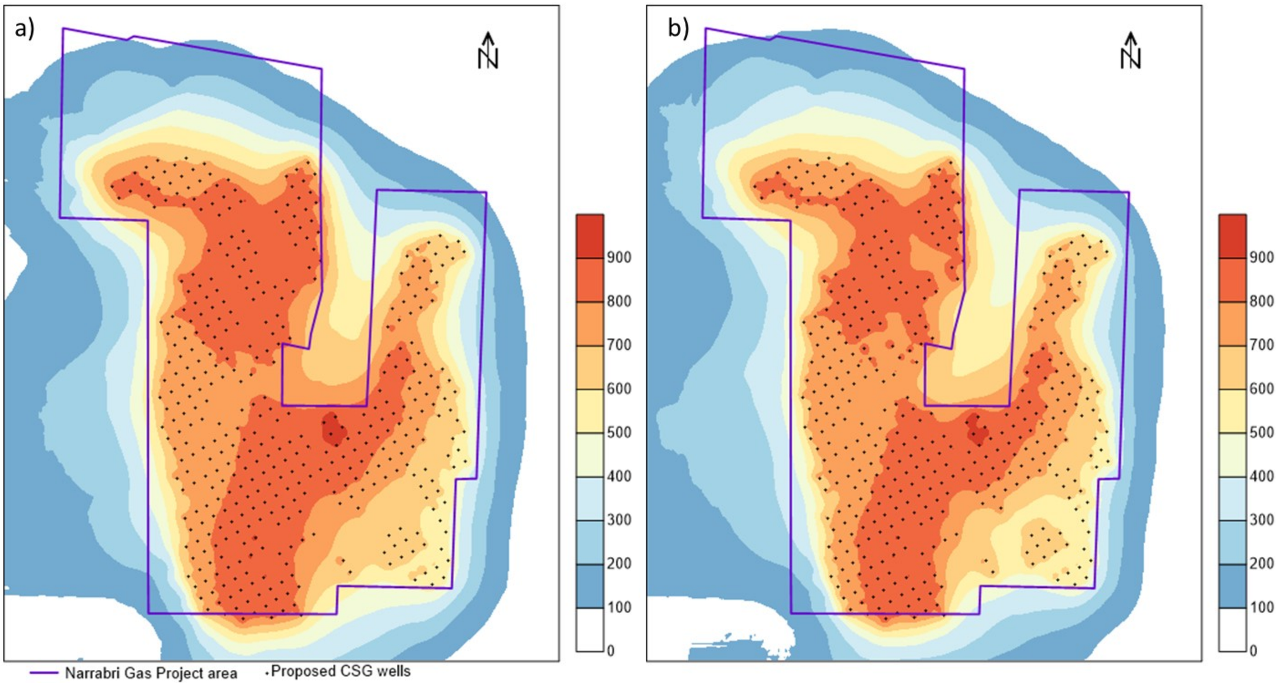

Figure 7-14 Comparison of 95th percentile maximum head drawdown in the Maules Creek Formation between a) single-phase MODFLOW and b) dual-phase MODFLOW model runs.

7.6 Summary of updated Namoi MODFLOW predictions

The methodology investigated in this report using the Richard's equation to represent dual-phase flow effects in the MODFLOW-USG model, was implemented in the regional scale groundwater flow model developed and used in the companion GISERA project (Sreekanth et al., 2018). The effects of dual-phase flow on CSG-induced flux and drawdown impacts on the Pilliga Sandstone aquifer and drawdown effects in the CSG target, the Maules Creek Formation, were compared. The comparison demonstrated that there is no significant effect of dual-phase flow on the flux and drawdown changes in the Pilliga Sandstone formation, which is separated from the CSG target by means of thick aquitard formations. For the regional scale groundwater flow model developed for the Namoi region, the prediction of CSG impacts on the GAB aquifers using a single-phase MODFLOW-USG model is justified. However, the comparisons indicated that drawdown and flux changes in the close vicinity of the CSG wells would require accounting of the dual-phase flow effects. This is important for studying the CSG water production and pressure differences. The regional scale MODFLOW-USG model applied in this study is not intended, nor used for making these predictions.

8 Conclusions

Complex coupled reservoir flow processes that govern rates of gas production from coal seams will also influence the rate of water production. These processes include dual-phase flow and gas desorption and operate at small scales around producing CSG wells, making them difficult to represent in large-scale single-phase regional groundwater models used to assess water production and drawdown impacts of CSG production. The inability to represent these detailed flow processes has potential to significantly impact the accuracy of CSG groundwater assessments (Commonwealth of Australia, 2014; Moore et al., 2015; Herckenrath et al., 2015). Existing models rely on either simplified relationships or CSG water production estimates, and the conservative assumptions made in order to compensate for these inaccuracies can lead to over-estimation of the impacts of CSG water extraction. Similarly, assigning dual-phase simulator derived water production rates to a single-phase model still results in over-prediction of pressure drawdown, and further relationships governing two-phase flow in coal seams must be included.

The methodology described by Herckenrath et al. (2015) and applied to CSG related regional groundwater modelling of the Surat Basin provides an approach to representing dual-phase flow processes in regional models. Implementation of this approach requires site-specific reservoir modelling to determine relationships between water saturation and pressure, which are then modelled using the van Genuchten water content vs capillary pressure relationship. Use of the SIMED reservoir simulator to model CSG production scenarios specific to the geology, reservoir properties, and development strategies of the Namoi sub-region allows for investigation of these region specific relationships. The SIMED reservoir model included parameters specific to CSG production that are not modelled in other reservoir simulators, such as the relationship between coal permeability and effective stress, and the influence on permeability of matrix shrinkage. This improved representation allowed for more detailed investigation of complex coupled reservoir flow processes, and of their potential for implementation into a Namoi regional model.

Geological, hydraulic, mechanical and CSG-specific properties were derived for the representative CSG model of the Namoi sub-region constructed in SIMED. Values for production parameters, including well type, well spacing and production rates were also derived. Sources included previous groundwater flow models of the Namoi sub-region, environmental impact statements (EIS), well completion reports, well test results, and commissioned reports related to regional groundwater and resources. A suite of SIMED Namoi models were used to assess reservoir flow processes inside the CSG field (well-symmetry model), in the vicinity of the field boundary (field model), and to assess the impact of model layering (upscaled model). The relationships between coal seam reservoir properties, likely development scenarios, and groundwater flow and drawdown were examined. Models were calibrated against predictions of future field development and water production given in the EIS produced by Santos, the Namoi field operator.

Simulations undertaken on the Namoi CSG single well-symmetry model explored relationships between key driving variables (e.g. pressure, saturation) specific to the portion of the producing reservoir contained within the boundary of the CSG well field. Here, pressure interference between adjacent producing wells results in higher levels of pressure drawdown and gas desorption than at the field boundary. Results showed maximum drawdown occurring in the target Bohena Seam, diminishing with vertical distance from the target interval. Examination of intra-grid block relationships, such as grid block saturation versus pressure indicated that time-asymptotic pseudo-steady state behaviour does not occur in a subset of grid blocks contained entirely within the boundaries of the CSG well field. Significant differences also exist between relationships based on the distribution of intra-grid block data, and relationships based on spatial averaging. In the case of relationships between reservoir variables and well production rate, the influence of adjacent wells and proximity to field boundary needs to be considered.

The Namoi CSG field model included multiple wells and an extended model boundary to investigate the key driving variables of CSG production in the vicinity of the field boundary, and further from the production area. At field scale, the influence of the adjacent formation beyond the field boundary resulted in different relationships compared to the single? well symmetry model. Any spatial averaging of reservoir relationships was strongly influenced by conditions and reservoir properties beyond the field boundary. This reduced the suitability of implementing spatially averaged relationships, or those that operate as a function of production data into the regional groundwater model. Based on these considerations the intra-grid block S_w vs P relationship was considered most appropriate for development as an input to the regional model.

The field scale S_w vs P relationship in the Namoi region does not approach a time-asymptotic pseudo steady state to the same extent as observed by Herckenrath et al. (2015) in the Surat Basin. It was also shown that the grid block size used in SIMED affects determination of the S_w vs P relationship, with larger grid blocks not sufficiently capturing the near-wellbore dual-phase flow processes and resulting in a poorly defined curve. The 300 m minimum grid block size used in regional groundwater modelling would provide insufficient detail if used in a CSG model to determine these relationships. Instead, spatial upscaling of the saturation and pressure data derived from fine-scale CSG simulations produced S_w vs P curves that match those derived from fine-scale data. However, this does not ensure that implementation of these relationships into upscaled grid blocks leads to the same drawdown and water production results. Vertical upscaling of CSG simulation saturation and pressure outputs to incorporate overlying and underlying saturated strata resulted in altered S_w vs P curves that exhibited strong influence on saturation from the adjacent formations. Implementation of these upscaled relationships into the regional groundwater models requires appropriate relative permeability curves to be derived.

Implementation of the saturation and pressure relationships into regional groundwater flow models required a version of MODFLOW-USG with dual-phase functionality via the Richards equation and van Genuchten formulations. Identical Namoi field models created in SIMED and MODFLOW were verified for matching single-phase predictions, then used to assess modelling and implementation approaches for representing dual-phase flow in MODFLOW. Without implementing dual-phase functionality, errors of up to 65 m head were observed in MODFLOW predictions after 20 years production, and water production was 22.7% higher than SIMED predictions. The error in single-phase MODFLOW drawdown predictions was observed to decrease with increasing vertical distance from the target formation. Numerous approaches were investigated for both processing and modelling the S_w vs P data using the van Genuchten equation, and for deploying the equation into the MODFLOW grid. In nearly all cases, deploying dual-phase functionality resulted in improved predictions of water production and pressure drawdown from

MODFLOW, but the different approaches tested provided notably different predictions. Inclusion of specific yield in the MODFLOW dual-phase deployment results in more accurate drawdown prediction, but cumulative water production values are sensitive to the effect the parameter has on water production rate from MODFLOW drains, especially in upscaled layers.

Averaging Bohena target seam S_w vs P curves across a range of production times to produce a set of van Genuchten parameters provided the best combination of improved accuracy and ease of deployment into the regional model. Deployment in MODFLOW reduced error in water production predictions by 63%, and error in average drawdown prediction adjacent to the CSG field by 77% (in the target formation). Results also indicated that it is important to include dual-phase functionality in all cells of the regional model that may experience desaturation (i.e. include cells beyond the CSG well field boundary). Other approaches, such as the deployment of different van Genuchten equation parameters across different model areas, may be appropriate depending on regional modelling priorities. However, the possibility of localised drawdown under-prediction and its effect on reported results must be considered when implementing dual-phase functionality into the regional model.

Implementing S_w vs P relationships derived from fine-scale CSG reservoir simulations into spatially coarse MODFLOW models reduces the improved accuracy due to dual-phase functionality. Implementation into vertically upscaled regional models that amalgamate overlying and underlying strata reduces the influence of predictive errors that manifest due to inadequate capture of complex coupled reservoir flow processes in the target layer. It was demonstrated that implementation into an upscaled regional model of van Genuchten and relative permeability parameters derived from CSG modelling of the Bohena target seam only, provides the greatest improvements in predictive accuracy. Even when deploying into upscaled layers, it is important to extend dual-phase functionality to all cells in the target layer that may see desaturation (including beyond the CSG field boundary).

The Richards equation dual-phase functionality was deployed in the regional scale groundwater flow model developed and used in the companion GISERA project W7 - Impacts of depressurisation on Great Artesian Basin (GAB) flux. A set of realisations of van Genuchten equation parameters were generated for use in Monte Carlo simulation completed using the MODFLOW model. Results indicated horizontal and vertical separation from CSG producing wells reduces the impact of modelling dual-phase flow on drawdown predictions.

Drawdown predictions in the GAB aquifer of interest, the Pilliga Sandstone, remained similar to predictions made using the single-phase model. Flux change predictions in the Pilliga Sandstone displayed a small increase, insignificant compared to the scale of the long-term annual average extraction limit set for the GAB groundwater source in the area of the Narrabri Gas Project. The presence of thick aquitard layers between the CSG target and the Pilliga Sandstone aquifer reduced the impact on the aquifer of dual-phase drawdown and flux predictions in the CSG target. This result suggests that for the regional scale groundwater flow model developed for the Namoi sub-region, the prediction of CSG impacts on the GAB aquifers using a single-phase MODFLOW-USG model is justified.

Dual-phase flow predictions of drawdown offer an improvement over single-phase predictions in the Maules Creek layer, with the latter overestimating the maximum drawdown by up to 184 m in the vicinity of the CSG well field. The dual-phase model also presents a more precise estimation of drawdown interference from multiple wells compared to the single-phase model, with areas of high drawdown more localised to around CSG wells as opposed to distributed over larger areas. For the Namoi GAB flux model, the effects of modelling dual-phase flow are largely confined to the vicinity of the CSG well field, while farther from the CSG wells there is no significant difference between the predictions of single and dual-phase model runs.

Implementation of the Richards equation dual-phase functionality developed in this GISERA project into the GAB flux MODFLOW model successfully demonstrated the ability to improve accuracy of drawdown predictions using this approach. The geologic conditions and presence of aquitard layers in the modelled region resulted in no significant change to drawdown and flux predictions in the overlying aquifer of interest, the Pilliga Sandstone aquifer. However, demonstrated improvements to the accuracy of drawdown predictions in the CSG target layers establish the importance of utilising this approach in regions where geological conditions may imply greater communication between underlying and overlying strata.

9 References

Aryal, S.K., Northey, J., Slatter, E., Ivkovic, K., Crosbie, R., Janardhanan, S., Peña-Arancibia, J. & Bell, J. (2017a). Observations analysis, statistical analysis and interpolation for the Namoi subregion. Product 2.1-2.2 for the Namoi subregion from the Northern Inland Catchments Bioregional Assessment. Department of the Environment and Energy, Bureau of Meteorology, CSIRO and Geoscience Australia, Australia.

Aryal, S.K., Northey, J., Slatter, E., Ivkovic, K., Crosbie, R., Janardhanan, S., Peña-Arancibia, J. & Bell, J. (2017b). Observations analysis, statistical analysis and interpolation for the Namoi subregion. Product 2.1-2.2 for the Namoi subregion from the Northern Inland Catchments Bioregional Assessment. Department of the Environment and Energy, Bureau of Meteorology, CSIRO and Geoscience Australia, Australia.

Barnett, B., Townley, L. R., Post, V., Evans, R. E., Hunt, R. J., Peeters, L., ... & Boronkay, A. (2012). Australian groundwater modelling guidelines. National Water Commission, Canberra.

Barrett, C. (2012). Upper Namoi groundwater source – status report 2011. NSW Department of Primary Industries, Office of Water, Sydney.

Brooks, R., & Corey, T. (1964). Hydraulic Properties Of Porous Media. Hydrology Papers, Colorado State University.

CDM Smith, (2014). Santos Narrabri Gas Project Groundwater Modelling Report. CDM Smith Australia Pty Ltd, Subiaco, Australia. October 2016.

CDM Smith, (2016). Santos Narrabri Gas Project Groundwater Impact Assessment. CDM Smith Australia Pty Ltd, Subiaco, Australia. 28 October 2014.

Commonwealth of Australia (2014). Coal Seam Gas Extraction: Modelling Groundwater Impacts, Prepared by: Coffey Geotechnics for the Department of the Environment, Commonwealth of Australia, Rep.

Crosdale, P. J., Beamish, B. B., & Valix, M. (1998). Coalbed methane sorption related to coal composition. International Journal of Coal Geology, 35(1-4), 147-158.

CSIRO (2012) Water resource assessment for the Surat region. A report to the Australian Government from the CSIRO Great Artesian Basin Water Resource Assessment. CSIRO Water for a Healthy Country Flagship, Australia.

De Vertuil, D., Howell, S., Campbell, L., Guiton, S., & Ryan, D. (2013). Introducing dual phase to integrated regional groundwater numerical modelling of large scale coal seam gas development. IAH Congress, Perth, 2013.

Decker, D. (1999) Discovery and geology of Narrabri gas fields. Symposium Abstracts, Oil and Gas in South-East Australia. New Ideas, New Data, New Interpretations, New Production and Markets, The University of Sydney, Sydney.

Eastern Star (2007). Petroleum Exploration Licence 238 Gas Utilisation Project, New South Wales Major Projects Application Preliminary Assessment Report. https://narrabrigasproject.com.

au/uploads/2015/06/NSW_CSG_Narrabri_02_Preliminary_Assessment_Report.pdf. Accessed Nov, 2017.

Eastern Star (2011). Eastern Star Gas Quarterly Report – June 2011. https://hotcopper.com.au/threads/ann-quarterly-reports-june-2011.1512950/#.WioDMGcy68g. Accessed Nov, 2017.

Gastar (2006). Gastar Exploration Provides Update on Australian Activities-Pel 238 Drilling Program. http://www.marketwired.com/press-release/gastar-exploration-provides-update-on-australian-activities-pel-238-drilling-program-amex-gst-583614.htm. Accessed Nov, 2017.

Giambastiani, B.M.S., McCallum, A.M., Andersen, M.S., Kelly, B.F.J. & Acworth, R.I. (2012). Understanding groundwater processes by representing aquifer heterogeneity in the Maules Creek Catchment, Namoi Valley (New South Wales, Australia). Hydrogeology Journal 20, 1027–1044.

Green, P., Carmichael, D., Brain, T., Murray, C., McKellar, J., Beeston., J & Gray, A. (1997). "Lithostratigraphic units in the Bowen and Surat Basins, Queensland" in *The Surat and Bowen basins of south-east Queensland*, ed. P. Green, Queensland Minerals and Energy Review Series edn, Queensland Department of Mines and Energy, Brisbane, pp. 41-108.

Gurba, L., Golab, A., Jaworska, J., Douglass, J. & Hyland, K., (2009). CO2 Geological Storage Opportunities in the Gunnedah Basin, and the Southern Bowen Basin, NSW. Cooperative Research Centre for Greenhouse Gas Technologies, Canberra, Australia, CO2CRC Publication Number RPT09-1456. 125pp.

Hamilton, S.K., Esterle, J.S. & Sliwa, R. (2014). Stratigraphic and depositional framework of the Walloon Subgroup, eastern Surat Basin, Queensland. Australian Journal of Earth Sciences, vol. 61, no. 8, pp. 1061-1080.

Herckenrath, D., Doherty, J., & Panday, S. (2015). Incorporating the effect of gas in modelling the impact of CBM extraction on regional groundwater systems. Journal of Hydrology, 523, 587-601.

Herckenrath, D., Doherty, J., & Moore, C. (2013). Simulation of regional CSG groundwater impacts—errors upscaling & multi-phase flow. In 22nd National Conference of the Australian Society for Operations Research, Adelaide, Australia (pp. 1-6)

Herczeg, A.L. (2008). Background report on the Great Artesian Basin, a report to the Australian government from the CSIRO Murray-Darling Basin Sustainable Yields Project. CSIRO, Australia.

Laxminarayana, C., & Crosdale, P. J. (1999). Role of coal type and rank on methane sorption characteristics of Bowen Basin, Australia coals. International Journal of Coal Geology, 40(4), 309-325.

Meaney, K., & Paterson, L. (1996). Relative permeability in coal. In SPE Asia Pacific Oil and Gas Conference. Society of Petroleum Engineers.

Merrick N (2001) Report on Lower Namoi groundwater flow model. Department of Land & Water Conservation.

Moore, C. R., Doherty, J., Howell, S., & Erriah, L. (2015). Some challenges posed by coal bed methane regional assessment modeling. Groundwater, 53(5), 737-747.

Moore, C. R., Doherty, J., Cui, T., Howell, S., & Erriah, L. (2013). Challenges for up-scaling hydraulic properties and processes in the coal seam gas context.

Northey, J., Pinetown, K. & Sander, R. (2014). Coal and coal seam gas resource assessment for the Namoi subregion. Product 1.2 for the Namoi subregion from the Northern Inland Catchments Bioregional Assessment. Department of the Environment, Bureau of Meteorology, CSIRO and Geoscience Australia, Australia.

OGIA (2016a). Groundwater modelling report for the Surat Cumulative Management Area, September 2016. The Office of Groundwater Impact Assessment, Department of Natural Resources and Mines, Queensland, 2016.

OGIA (2016b). Hydrogeological conceptualisation report for the Surat Cumulative Management Area, August 2016. The Office of Groundwater Impact Assessment, Department of Natural Resources and Mines, Queensland, 2016.

OGIA (2016c). Underground Water Impact Report for the Surat Cumulative Management Area, 2016. The Office of Groundwater Impact Assessment, Department of Natural Resources and Mines, Queensland, 2016.

Peaceman, D. W. (1978). Interpretation of well-block pressures in numerical reservoir simulation. SPE Journal, 18(3), 183-194.

Radke, B.M., Ferguson, J., Cresswell, R.G., Ransley, T.R., Habermehl, M.A. (2000) Hydrochemistry and implied hydrodynamics of the Cadna-owie – Hooray Aquifer, Great Artesian Basin. Bureau of Rural Sciences, Canberra.

Reiss, L. H. (1980). The reservoir engineering aspects of fractured formations (Vol. 3). Editions Technip.

Richards, L. A. (1931). Capillary conduction of liquids through porous mediums. Physics, 1(5), 318-333.

Ryan, D., Hall, A., Erriah, L. & Wilson, P. (2012). The Walloon coal seam gas play, Surat Basin, Queensland, APPEA Journal, vol. 52, pp. 273-289.

Santos (2016). Narrabri Gas Project Environmental Impact Statement, Chapter 11: Groundwater and Geology. Santos, Sydney, Australia.

Seidle, J. P., Jeansonne, D. J. and Erickson, D. J. (1992) Application of matchstick geometry to stress dependent permeability in coals, paper SPE 24361 presented at SPE Rocky Mountain Regional Meeting, Casper, Wyoming, 18–21 May, pp. 433–444.

Seidle, J. (2011). Fundamentals of coalbed methane reservoir engineering. PennWell Books.

Shi, J. Q., & Durucan, S. (2004). Drawdown induced changes in permeability of coalbeds: a new interpretation of the reservoir response to primary recovery. Transport in porous media, 56(1), 1-16.

Sreekanth et al. (2018). Impacts of depressurisation on Great Artesian Basin (GAB) flux. August 2018. CSIRO, Canberra.

SWS (2012). Namoi Catchment Water Study Independent Expert Phase 3 Report. Schlumberger Water Services (Australia) Pty Ltd. Perth, Australia. April, 2012.

Tadros, N.Z., (1993). The Gunnedah Basin, New South Wales, Memoir 12. Geological Survey of New South Wales, Sydney.

Tadros, N.Z. (1995) Gunnedah Basin. C.R. Ward, H.J. Harrington, C.W. Mallett, J.W Beeston (Eds.), Geology of Australian Coal Basins, Geological Society of Australia Coal Geology Group, Special Publication, vol. 1 (1995), pp. 247-298

U.S. National Research Council. (2010). Management and effects of coalbed methane produced water in the Western United States. National Academies Press.

Van Genuchten, M. T. (1980). A closed-form equation for predicting the hydraulic conductivity of unsaturated soils. Soil science society of America journal, 44(5), 892-898

Welsh, W., Hodgkinson, J., Strand, J., Northey, J., Aryal, S., O'Grady, A., Slatter, E., Herron, N., Pinetown, K., Carey, H., Yates, G., Raisbeck-Brown, N. & Lewis, S. (2014). Context statement for the Namoi subregion. Product 1.1 from the Northern Inland Catchments Bioregional Assessment. Department of the Environment, Bureau of Meteorology, CSIRO and Geoscience Australia, Australia.

Contact us

Paul Cunningham
Phone: +61 7 3838 5924
Email: gisera@gisera.csiro.au
gisera.csiro.au